Mitochondrial dysfunction in rabies virus infection of neurons

By

Thamir Abdulaziz A Alandijany

A Thesis submitted to the Faculty of Graduate Studies of

The University of Manitoba

in partial fulfillment of the requirements of the degree of

Master of Science

Department of Medical Microbiology

University of Manitoba

Winnipeg, Manitoba, Canada

Contributions

Dr. Wafa Kammouni performed the western blotting analysis of 4-HNE expression in PC12 cells shown in Figure 9. She also dissected, cultured, infected, and harvested the dorsal root ganglion neurons used in the measurement of Krebs cycle enzyme and electron transport chain Complex activities. Dr. Subir Roy Chowdhury prepared the stock solutions of reduced cytochrome c and malate used in Complex IV activity assay and respiration assay, respectively.

Dedication

I would like to dedicate this work to my parents (Aisha, and Abdulaziz), my brothers (Basem and Majed), sisters (Tahani, Shahad, and Lina) son (Moath), and parents-in-law (Nihad and Ali).

From the bottom of my heart, I dedicate this work mostly to my wife (Arwa). Without her patience and love, I would have not been able to accomplish this.

Acknowledgements

I would like to show gratitude to my supervisor Dr. Alan Jackson, who has granted me this position in his lab. It was an honor for me to have the opportunity to benefit from his knowledge and experience.

I would like to thank my research committee members, Drs. Paul Fernyhough and Kevin Coombs for their time, guidance, and feedback on my research.

I would like to thank Drs. Wafa Kammouni and Subir Roy Chowdhury for technical assistance.

I would like also to show gratitude to King Abdul Aziz University for their financial support.

Abstract

Infection with challenge virus standard-11 (CVS) strain, a laboratory fixed rabies virus strain, induces neuronal process degeneration in both *in vivo* and *in vitro* models. CVS-induced axonal swellings of primary rodent dorsal root ganglion neurons are associated with 4-hydroxy-2-nonenal staining indicating a critical role of oxidative stress. Mitochondrial dysfunction is one of the most important causes of oxidative stress. We hypothesized that CVS infection induces mitochondrial dysfunction leading to oxidative stress. We investigated the effects of CVS infection on several mitochondrial parameters in different cell types. CVS infection increased electron transport chain capacity, Complex I and IV activities, but did not affect Complex II-III, citrate synthase, and malate dehydrogenase activities. CVS maintained normal oxidative phosphorylation capacity and proton leak, indicating a tight mitochondrial coupling. Possibly as a result of enhanced Complex activity and efficient coupling, a high mitochondrial membrane potential was generated. CVS infection reduced the intracellular ATP level and altered the cellular redox state as indicated by high NADH/NAD+ ratio. CVS infection was associated with a higher rate of hydrogen peroxide production. We conclude that CVS infection induces mitochondrial dysfunction leading to ROS overgeneration, oxidative stress and neuronal process degeneration.

Tables of contents:

List of Figures:

List of copyrighted materials:

Figures 1, 2, 3, and 6 (page 6, 7, 11, and 29, respectively) with permission obtained from Nature Publishing Group.

Figures 4 and 5 (page 17 and 25, respectively) with permission obtained from American Society for Microbiology.

List of abbreviations:

AA: antimycin A

Acetyl-CoA: acetyl coenzyme A

ADP: Adenosine diphosphate

AIF: apoptosis inducing factor

AMPK: adenine monophosphate-activated protein kinase

ANT: adenine nucleotide translocator

Asc: ascorbate

BALF: bronchi alveolar lavage fluid

BHK-S13: baby hamster kidney clone-S13

BSA: bovine serum albumin

CMV: cytomegalovirus

CNS: Central nervous system

Cu-Zn SOD: copper zinc superoxide dismutase

CSF: cerebrospinal fluid

CVS: challenge virus standard-11

Dig: digitonin

DRG: dorsal root ganglion

DTNB: 5,5′-Dithiobis(2-nitrobenzoic acid)

ERK: extracellular signal regulated kinase

FCCP: Carbonylcyanide p-trifluoromethoxyphenylhydrazone

FMN: flavin mononucleotide

HBV: hepatitis B virus

HeLa: human epithelial carcinoma

HIV: human immunodeficiency virus

HIV soluble viral protein: HIV-Vpr

4-HNE: 4-hydroxy-2-nonenal

IL-1: interlukin-1

iNOS: induced nitric oxide synthase

KCL: potassium chloride

KCN: potassium cyanide

KOH: potassium hydroxide

Mal: malate

MNA: Mouse neuroblastoma

Mn-SOD: manganese superoxide dismutase

MOI: multiplicity of infection

MPT: mitochondrial permeability transition

MTT: tetrazolium dye

nAChR: nicotinic acetylcholine receptor

NADH: β-Nicotinamide adenine dinucleotide

NCAM: neuronal cell adhesion molecule

NCS: neonatal calf serum

NF-KB: nuclear factor kappa B

NGF: nerve growth factor

Olig: oligomycin

Pyr: pyruvate

P75 NTR: low affinity neurotrophin receptor

RIG-I: retinoic acid-inducible gene I

ROS: reactive oxygen species

SIRT: sirtuin

STAT-1: signal transducers and activators of transcription-1

TLR-3: toll-like receptor 3

TMPD: N,N,N′,N′-Tetramethyl-p-phenylenediamine dihydrochloride

TMRE: tetramethylrhodamine ethyl ester

TNB: 5-thio-2-nitrobenzoic acid

TNF: tumor necrosis factor

VSV: vesicular stomatitis virus

1. Introduction:

Rabies is a fatal viral infection caused by rabies virus. The virus targets the nervous system and induces acute encephalitis in the infected hosts leading eventually to death (Jackson and Wunner, 2007). The disease is considered as preventable, in part, due to the use of highly effective vaccines. Yet, rabies continues to be a serious issue worldwide. World Health Organization indicates that rabies virus infection leads to 35,000 to 50,000 deaths each year (WHO, 1999). This number is believed to be an underestimate related to inadequate or perhaps lack of laboratory facilities and confirmatory tests (Knobel *et al.,* 2005). Currently, there is no effective therapeutic approach against rabies probably due to our limited current knowledge about rabies pathogenesis (Jackson, 2011). A better understanding of the viral pathogenesis and the viral-host interactions would be of a great importance in order to develop an effective therapy for rabies.

1.1 Epidemiology:

The majority of rabies cases take place in Asia and Africa (Knobel *et al,* 2005). The main route of transmission in these two continents is exposure to bites from rabid dogs (Knobel *et al*., 2005). As dogs are considered the main reservoirs for rabies virus, the incidence of human rabies in a particular population usually correlates with the incidence of canine rabies (Childs and Real, 2007). In the USA, 236 human rabies cases were identified from 1946 to 1965 (Held *et al.,* 1967). Most of the cases were due to exposure to infected dogs (Held *et al.,* 1967). Nowadays, human rabies is very rarely seen in North America and Europe. Vaccination of dogs and availability of effective human

vaccines have led to the remarkable reduction of human rabies cases in these two continents (Centres for Disease Control and Prevention, 2005 and Advisory Committee on Immunization Practice, 1999). Based on the information obtained from the history of the patients and the molecular characteristics of the virus, several cases of human rabies in the USA and European countries have acquired the infection outside of these countries (Noah *et al.,* 1998). Reporting "imported" human rabies is expected to continue until the infection is controlled in countries where rabies is endemic (Childs and Real, 2007). In Canada and the USA, most recent human rabies cases acquired in the two countries are acquired from bats (Krebs *et al.,* 2003 and Public Health Agency of Canada, 2003). Human rabies cases reported in the USA are mostly associated with silver haired, tricolored, and, to a lesser extent, Brazilian free-tailed bats. Skunks, foxes, and racoons are also common rabies virus reservoirs in the USA (Blanton *et al.,* 2011).

Animal bites are responsible for most rabies virus transmission. Direct contact of mucosal membranes with infectious particles is another less common route for viral transmission (World Health Organization 2004). In Ethiopia, two human-to-human cases have been reported (Fekadu *et al.*, 1996). A case of congenital, mother-to-child, rabies virus infection has been reported (Sipahioglu and Alpaut 1985). In addition to natural routes of transmission, iatrogenic routes also contribute to spreading human rabies infection. The USA (Houff *et al.*, 1979), France (Centres for Disease Control and Prevention, 1980), and three other Asian countries (Centres for Disease Control and Prevention 1981, Gode

and Bhide 1988, World Health Organization 1994) have reported rabies cases acquired from corneal transplantation. In the USA, transplantation of a liver, kidneys, and a vascular segment from a single rabies virus–infected donor resulted in four human rabies cases in 2004 (Srinivasan *et al.,* 2005). One year later, Germany also reported rabies in three organ transplant recipients (Maier *et al.,* 2010).

1.2 Overview of the viral life cycle:

The rabies virus life cycle starts when a rabid animal bites a human or another animal. The infectious virus is inoculated subcutaneously or intramuscularly in the new host (Jackson, 2010). The incubation period is very variable from host to host ranging between 30 and 90 days in most cases (Smith *et al.,* 1991). Molecular investigation conducted on skunks that were infected with street rabies virus strain indicated that the virus remains at the inoculation area during most of the incubation period (Charlton *et al*., 1997). The viral RNA was detected using reverse transcriptase polymerase chain reaction assay in the muscles at the site of inoculation at 2 months post-infection (Charlton *et al.,* 1997). This finding was further supported by immunohistochemistry staining where rabies virus-infected muscle fibers were detected at or near the site of infection (Charlton *et al*., 1997). On the other hand, the viral genome was absent in the spinal cord and the spinal ganglia (Charlton *et al*., 1997). The virus spreads to the central nervous system (CNS) in axons of peripheral nerves by retrograde fast axonal transport. The virus transports within the CNS via the axons (Klingen, *et al*., 2008, Kucera *et al*., 1985, Tsiang *et al.,* 1991). This

axonal transport is quite fast reaching up to 250 and 400 mm per day in retrograde and anterograde direction, respectively (Kucera *et al.,* 1985, Tsiang *et al.,* 1989, Tsiang *et al.,* 1991). It is believed that both motor and sensory neurons are involved in this process (Kucera *et al.,* 1985, Tsiang *et al.,* 1991). The virus can transfer from one neuron to another along neuroanatomical connections (Jackson, 2010). Parasympathetic nervous system may play an important role in delivering the virus from the CNS to various organs such as salivary glands. The infectious viral particles are secreted in the saliva of the infected host and the cycle continues.

1.3 The viral genome and proteins:

Rabies virus is classified within the lyssavirus genus in which the genome is comprised of single RNA strand with negative sense (Jackson and Wunner 2007, Tordo *et al.,* 2005). The rabies virus genome is approximately 12 kb in size and is composed of five different genes responsible for encoding the five viral proteins: nucleoprotein, phosphoprotein, matrix protein, glycoprotein, and large protein (Le Mercier *et al.,* 1997, and Marston *et al.,* 2007). Each coding region (gene) is located between two non-coding ones (intergenic regions). The transcription is initiated by transcription initiation signals at the beginning of each gene, and is terminated by transcription termination polyadenylation signals at the end of this gene (Tordo *et al.,* 1986b, Tordo *and* Poch. 1988a). With the exception of the intergenic region located between glycoprotein and large protein sequences, the non-coding sequences are relatively short in length in most of the lyssaviruses (Tordo *et al.,* 1986b). In addition to the intergenic regions located

between the five genes, there are another two non-coding regions located at both genome termini (Tordo *et al.,* 1986a, Tordo and Poch. 1988b). The leader is a 58 nucleotide region and is located at the 3' end of the viral genome. This region is believed to be critical in initiating the transcription process (Tordo *et al.,* 1986a). On the 5' end, approximately 70 nucleotides form the trailer, a non-coding region is responsible for terminating the genome transcription (Bourhy *et al*., 1989, Conzelmann and Schnell, 1994, Tordo and Poch. 1988b). Figure 1 and 2a shows the viral structural proteins and genomic structure, respectively. The viral nucleoprotein is composed of 450 amino acids, and it encapsidates the viral genome leading to nucleocapsid formation (Iseni *et al.,* 1998, Thomas *et al*., 1985). Then, the phosphoprotein (297 amino acids) is linked to both nucleocapsid and large proteins (2130 amino acids) to form ribonucleoprotein (Mavrakis *et al*., 2003, 2006, and Chenik *et al.,* 1998). Matrix protein is comprised of 202 amino acids and is associated with the inner side of the viral membrane linking the viral nucleocapsid to the glycoprotein (505 amino acids) on the viral surface (Mebatsion *et al.,* 1999). Upon completion of transcription and translation processes, rabies virus forms a bullet-like structure that has a conical and a flat end (Matsumoto *et al.,* 1962, Tordo and Poch, 1988b). While the virion is 75 nm in diameter, the length is different among different strains and it ranges from 100 to 300 nm (Matsumoto *et al.,* 1962, Tordo and Poch, 1988b).

1.4 The viral replication cycle:

Figure 2b explains the sequential steps of the rabies virus replication cycle.

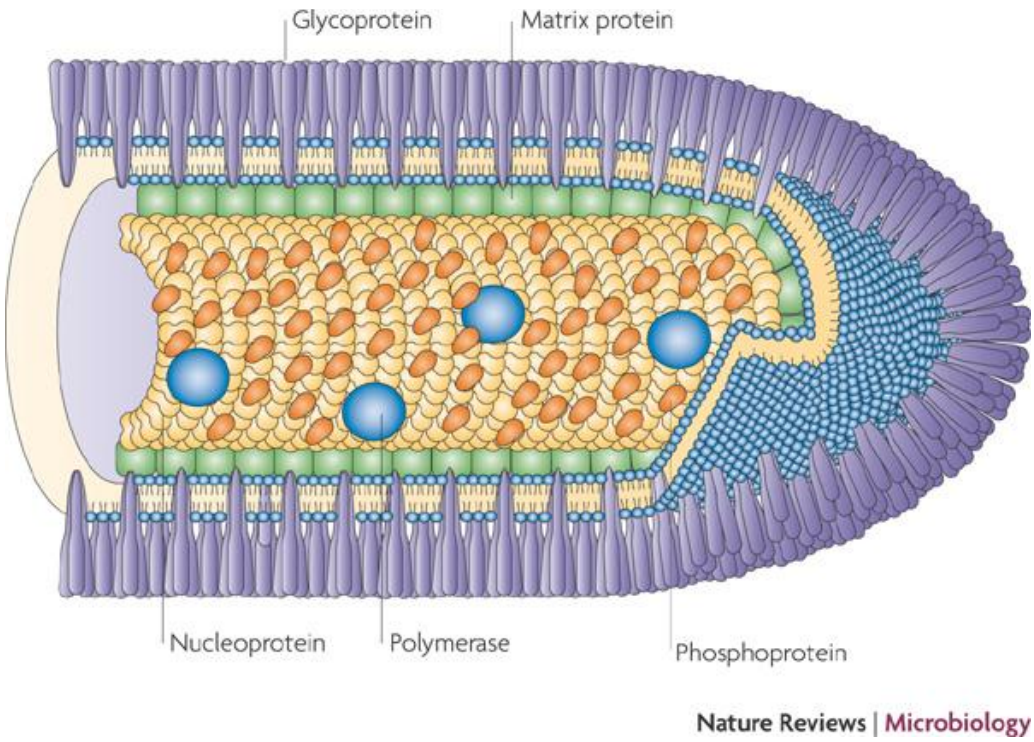

Figure 1: Rabies virus structure. It is composed of five different proteins (nucleoprotein, phosphoprotein, polymerase or large protein, matrix protein, and glycoprotein) arranged in bullet-like structure (reproduced from Schnell *et al,* 2010 with permission from Nature Publishing Group www.nature.com).

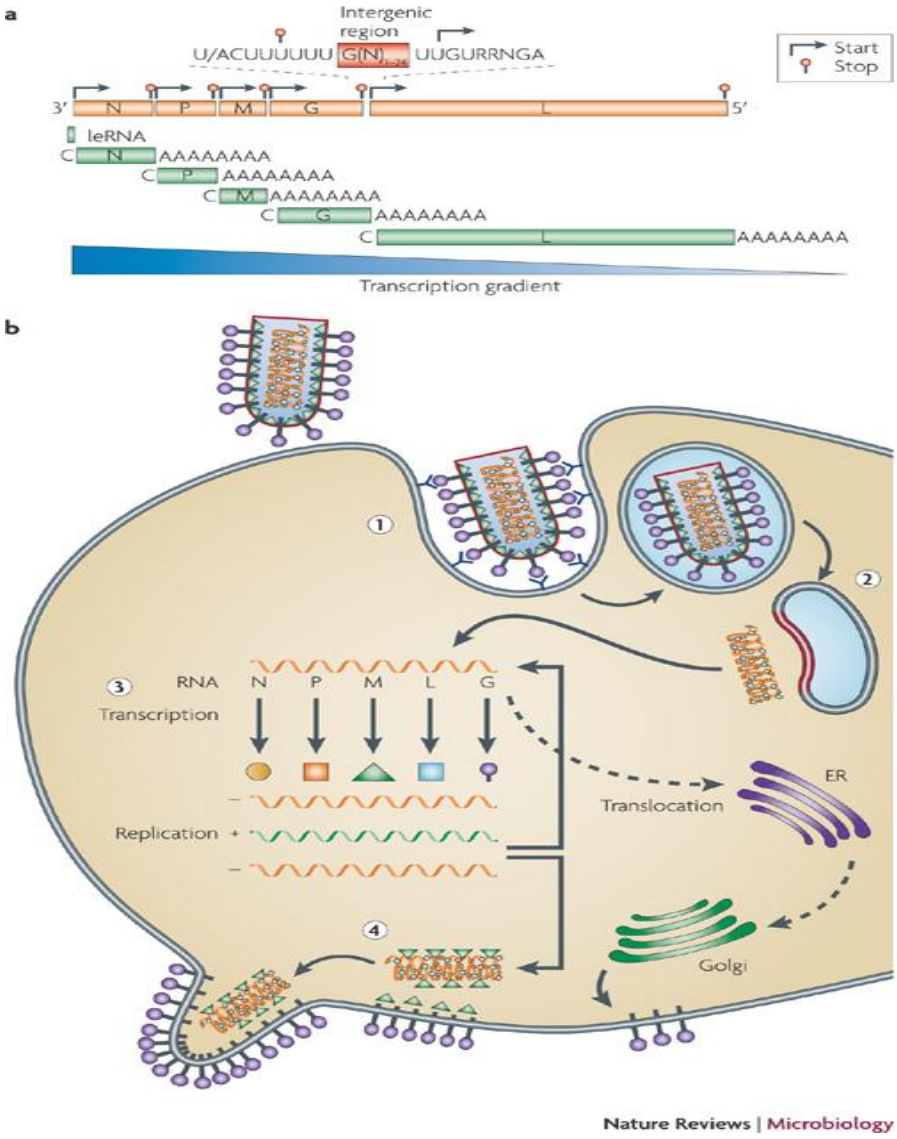

Figure 2: a) rabies virus genomic structure. Negative sense single stranded RNA composed of 5 genes (N, P, M, G, and L) and 6 non-coding regions (exist between the genes and at both genome termini. **b) rabies virus replication cycle.** The cycle starts with viral attachment and internalization. The viral genome is uncoated to initate transcription and translation processes followed by the viral replication. Then, the viral budding occurs at the plasma membrane and the cycle continues (reproduced from Schnell *et al,* 2010 with permission from Nature Publishing Group www.nature.com).

1.4.1 Attachment and host receptors:

Glycoprotein, in particular the amino acid at position 333, is critical for viral attachment to the receptors of the targeted cells (Tuffereau *et al.,* 1989, Etessami *et al.,*. 2000). Several membrane molecules have been reported as receptors for rabies virus. For instance, Lentz and his colleagues indicated that rabies virus interacts with nicotinic acetylcholine receptor (nAChR) in order to bind mouse diaphragm (Lentz *et al.,* 1982). A few years later, the same research group identified amino acids located between 173 and 204 in the rabies virus glycoprotein as critical sites for this viral-host interaction (Lentz *et al.*, 1987). Pre-treatment of dorsal root ganglion primary neurons with monoclonal antibodies raised against α-subunit of nAChR partially reduced their susceptibility to rabies virus infection (Castellanos *et al.,* 1997). The neuronal cell adhesion molecule (NCAM) is another cellular component that is believed to play a significant role for rabies virus internalization (Thoulouze *et al.,* 1998). Rabies virus-susceptible cell lines usually express NCAM on their surfaces. On the other hand, rabies virus-resistant cell lines lack NCAM (Thoulouze *et al.,* 1998). Pre-treatment of PC12 cells, cell lines originated from rat adrenal medulla, with nerve growth factor enhances the expression of NCAM. The infectivity of rabies virus in NGF-treated PC12 cells is approximately 3 times higher versus untreated PC12 cells (Thoulouze *et al.*, 1998). Moreover, treatment of rabies virus-susceptible cells with either anti-NCAM antibodies or NCAM ligands drastically suppresses the infection (Thoulouze *et al.,* 1998). Primary cortical neurons derived from NCAM-

deficient mice are less susceptible to rabies virus infection than those derived from wild type mice (Thoulouze *et al.,* 1998). In vivo experiments conducted on NCAM-deficient mice revealed that the reduction of NCAM expression remarkably impairs the neuroinvasion by rabies virus (Thoulouze *et al.*, 1998). Other host molecules such as the low affinity neurotrophin receptor (p75NTR) (Tuffereau *et al.,* 1998, Langevin *et al.,* 2002) and gangliosides, especially highly sialylated gangliosides (Superti F *et al.,* 1986), are also believed to largely participate in the viral attachment to the host cells.

1.4.2 The viral fusion and internalization:

The virus induces endosome formation in order to internalize the host cells (Superti *et al.,* 1984). The virus was detected by electron microscopy in both coated and uncoated vesicles. Due to low pH of the endosome, the viral glycoprotein is fused with the cellular membrane resulting in ribonucleocapsid release, a process called “uncoating” (Superti *et al.,* 1984). The viral glycoprotein plays a critical role in membrane fusion as the fusion is impaired when rabies virus glycoprotein is replaced with human immunodeficiency virus-1 (HIV-1)-glycoprotein 160 (McGettigan *et al.,* 2001).

1.4.3 Transcription and translation:

Rabies virus enters the neurons at axon locations which do not provide the suitable environment for transcription, translation and replication (Schnell *et al.,* 2010 and Malgaroli *et al.,* 2006). Therefore, the whole virus or only the viral capsid needs to be transported to the cell bodies in order to initiate protein synthesis (Klingen, *et al.,* 2008, Jacob *et al.,* 2000, and Raux *et al.,* 2000). Figure

3 shows how rabies virus enters the neurons at axons and how it is transported to the cell bodies. Once the virus reaches the cell body, the RNA polymerase is activated and, thereby, initiates the genome transcription. Recently, it was proposed that the viral transcription and replication take place in the Negri bodies (Lahaye *et al.,* 2009). The first transcript produced by the polymerase complex is the leader RNA. This uncapped transcript which lacks ploy A tail is relatively short, 55 to 58 bp (Colonno and Banerjee 1978, Leppert *et al.,* 1979). After the transcription of the leader RNA, the nucleoprotein', phosphoprotein', matrix protein', glycoprotein', and large protein' mRNAs are transcribed (Tordo *et al.,* 1986b). Upon transcribing a given mRNA, the transcription stops at the next intergenic region prior to restarting the transcription of the next mRNA. This stop-start fashion is important for mediating the viral gene expression. Unlike the leader RNA, all the other viral mRNAs have caps and poly A tails (Ogino and Banerjee, 2007). In the presence of an adequate amount of nucleoprotein, transcription switches to replication: A complete complementary positive sense RNA is produced which serves as a template for the progeny genome (Liu *et al.,* 2004). When the new nucleoprotein is synthesized, it specifically binds to the viral RNA via a phosphoprotein-regulated mechanism (Masters and Banerjee, 1988). Phosphorylation of the Ser 389 in nucleoprotein enhances phosphoprotein and nucleoprotein-RNA complex interaction (Toriumi and Kawai, 2004). Indeed, viral replication and transcription were impaired when the phosphorylation site was mutated (Wu *et al.,* 2002). Matrix protein is also believed to be important in

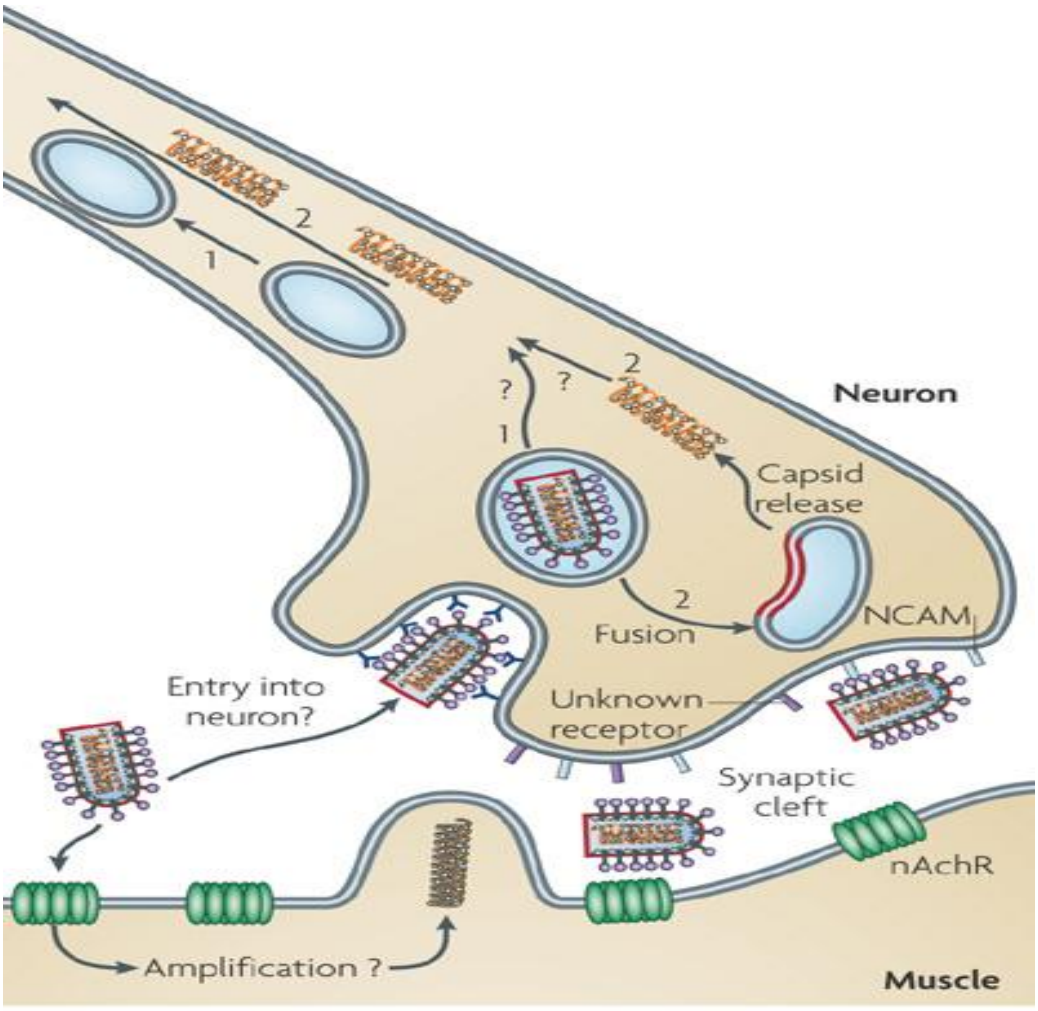

Figure 3: The viral entry and transportation within neurons. Rabies virus enters axons at neuromuscular junctions, and, then, either the whole virus or the viral capsid is transported to the cell body in order to initiate the transcription of the viral genome (reproduced from Schnell *et al,* 2010 with permission from Nature Publishing Group www.nature.com).

mediating the transcription rate (Finke *et al.,* 2003). Figure 2a shows an overview of the transcription of the viral genome.

1.4.4 Budding:

Budding and release of the progeny virions can be regarded as the last step in the viral life cycle. It takes place at the plasma membrane although it is unknown how the virions transfer to the budding site. It is believed that both glycoprotein and matrix protein play a significant role in this process (Mebatsion *et al.,* 1996, Mebatsion *et al.,* 1999). Indeed, the viral yield was suppressed by 500,000-fold and 30-fold in the absence of matrix protein and glycoprotein, respectively (Mebatsion *et al.,* 1999, Mebatsion *et al.,* 1996). When the progeny virions are released, they infect the neighbor cells and the cycle continues.

1.5 Host Immune response:

Rabies virus enhances its gene expression in order to produce an adequate amount of viral components. However, in order to complete the replication cycle, this amount must be below the level that triggers cell death and the host immune response (Schnell *et al,* 2010). Alternatively, the virus can employ a tactic to escape immune response when it is triggered (Schnell *et al,* 2010). It was shown that factors of the innate immune response are activated in response to rabies virus infection. For instance, retinoic acid-inducible gene I (RIG-I) is overexpressed during rabies virus infection (Hornung *et al.,* 2006). The overexpression of RIG-I, in turn, induces type I interferon (e.g. IFN-β) which drastically suppresses the viral pathogenesis (Faul *et al.,* 2008). The virus has evolved a mechanism to evade such an immune response by upregulating the

production of its phosphoprotein (Brzozka *et al.,* 2005). The viral phosphoprotein blocks the phosphorylation of some IFN-β-mediated factors (e.g. IFN regulatory factor 3) and, thereby, impairs IFN-β activation (Brzozka *et al.,* 2005). Toll-like receptor-3 (TLR-3) also plays a role in the secretion of type I IFN, and it was found to be upregulated during rabies virus-induced encephalitis (Jackson, *et al.* 2006). Recently, a role of TLR-3 in the formation of rabies virus-induced Negri bodies has been identified (Menager *et al.,* 2009). Rabies virus also interferes with IFN-signal transduction pathways (Vidy *et al.,* 2005). Indeed, interaction between the viral phosphoprotein and Signal Transducers and Activators of Transcription-1 (STAT1) in the cytosolic compartment blocks the nuclear translocation of STAT1. This prevents the activation of the downstream nuclear process required for viral clearance (Vidy *et al.,* 2005). Pathogenic rabies virus strains evade the immune system in the brain by impairing the trafficking of the immune cells through the blood brain barrier (Hooper *et al.,* 2007). It was shown that pathogenic silver haired bat rabies strain, but not an attenuated strain, is associated with intact blood brain barrier (Hooper *et al.,* 2007). As a consequence, the immune effector cells are unable to enter the CNS (Hooper *et al.,* 2007). The host immune system induces apoptosis as a defense mechanism against several viral infections (Isamu *et al.,* 2004). It is likely that only attenuated strains induce apoptosis. CVS strain, pathogenic rabies strain, induces apoptosis neither in mouse nor human lymphocytes (Thoulouze *et al.,* 1997). In contrast, ERA strain, attenuated strain, induces apoptosis in both types of lymphocytes (Thoulouze *et al.,* 1997). Whereas intracerebral inoculation of CVS induced

neuronal cell death in the infected mice (Jackson *et al.,* 1997 and Theerasurakarn *et al.,* 1998), peripheral inoculation did not induce apoptosis of neurons indicating the importance of the route of infection in apoptosis induction (Scott *et al.,* 2008). No evidence of apoptosis has been observed in postmortem brain tissues from fatal human rabies cases (Jackson *et al.,* 2008). Proteomic analysis indicated that only attenuated strains stimulate the expression of pro-apoptotic proteins; proteins that play a critical role in inducing apoptosis (Dhingra *et al.,* 2007). It is believed that the expression level of viral glycoprotein is a critical factor for inducing apoptosis as attenuated strains produce a greater amount of glycoprotein in comparison with pathogenic strains (Faber *et al.,* 2002 and Prehaud *et al.,* 2003). Although some exceptions apply, pathogenic rabies virus strains are likely to evade apoptosis and, thereby, enhance their pathogenicity.

1.6 The viral pathogenesis:

Studies conducted on experimental animals have greatly improved our current understanding about rabies pathogenesis (Jackson *et al.*, 2007). However, these studies do not mimic the natural infection in several aspects such as the strain of the virus and the route of inoculation. Indeed, laboratory fixed rabies virus strains rather than wild type strains are widely used in these studies (Jackson *et al.*, 2007). An in vitro study indicated that the virus enters the neurons at neuromuscular junctions via interacting with nicotinic acetylcholine receptors (Lentz *et al.*, 1982). Subsequently, the virus travels among the axons via retrograde axonal transport (Tang *et al.*, 1999, Kelly and Strick, 2000). After

the infection is developed, rabies virus spreads widely in the central nervous system. Accumulating data suggest that the neuropathogenesis of rabies is due to impairment of neuronal functions rather than induction of neuronal death (Iwasaki and Tobita, 2002 and Jackson and Wunner, 2007). Both in vivo and in vitro studies revealed that rabies virus infection induces alterations in the neuronal functions (Jackson *et al.,* 2007). It was shown that rabies virus infection affects the functions of neurotransmission components such as α-amino-n-butryic acid (Ladogana *et al.,* 1994), opioid (Munzel and Koschel, 1981), serotonin (Ceccaldi *et al.,* 1993) and acetylcholine (Tsiang, 1982). Although some alterations were observed, none of them had enough significance to explain rabies-virus induced neuronal dysfunction (Jackson *et al.,* 2007). Iwata and his colleagues studied the effect of rabies virus infection on membrane ion channels (Iwata *et al.,* 1999). Ion channels of plasma membrane play a significant role in the neurons response to neurotransmitters. Abnormalities in ion channels, in particular voltage-dependent Na+ current and inward rectifier K+ current, functions were observed in rabies virus-infected mouse neuroblastoma cell line (Iwata *et al.,* 1999). The viral infection also resulted in depolarization of resting membrane potential (Iwata *et al.,* 1999). Rabies virus-induced nitric oxide is another potential explanation for the neuronal dysfunction (Hooper *et al.,*. 1995). Nitric oxide serves as an intermediate component in neuronal signal transmission. However, overproduction of nitric oxide may lead to free radical formation (e.g., peroxynitrite) and cellular damage. It was shown that laboratory fixed strain induces nitric oxide generation by upregulating nitric oxide synthase

activity (Hooper *et al.,* 1995). Wild type rabies street strain remarkably enhanced the mRNA expression level of induced nitric oxide synthase (iNOS) (Hooper *et al.,* 1995). In comparison with expression level of genes in normal brain, the expression level of approximately 90% of the genes is suppressed in the infected brain (Prosniak *et al.,* 2001). Of note, some genes involved in cell metabolism were overexpressed in the rabies virus-infected brain (Prosniak *et al.,* 2001).

1.7 Rabies virus-induced neurodegeneration:

Severe degeneration in neuronal processes associated with mild pathological alteration in cell bodies was observed in the brain of rabies virus N2C-infected mice after intracerebral inoculation (Li *et al.,* 2005). Disappearance of intracellular organelles and synaptic structures was evident in the infected brain (Li *et al.,* 2005). Similar findings were observed in rabies virus N2C-infected primary neurons at 5 days post-infection (Li *et al.,* 2005). Attenuated rabies virus strain (SN-10) induced neither of these pathological changes in mice nor in primary neurons (Li *et al.,* 2005).

In the transgenic mice model that express yellow fluorescent protein, peripheral inoculation of rabies virus was associated with only mild inflammatory and histopathological alterations within the CNS (Scott *et al.,* 2008). Similarly, evidence of apoptosis was very limited (Scott *et al.,* 2008). Severe degeneration in the axons and dendrites of various neuronal cell types such as layer V cortical pyramidal neurons and inferior cerebral peduncle, and mossy fibers was observed at 6 days post-infection (Scott *et al.,* 2008). These

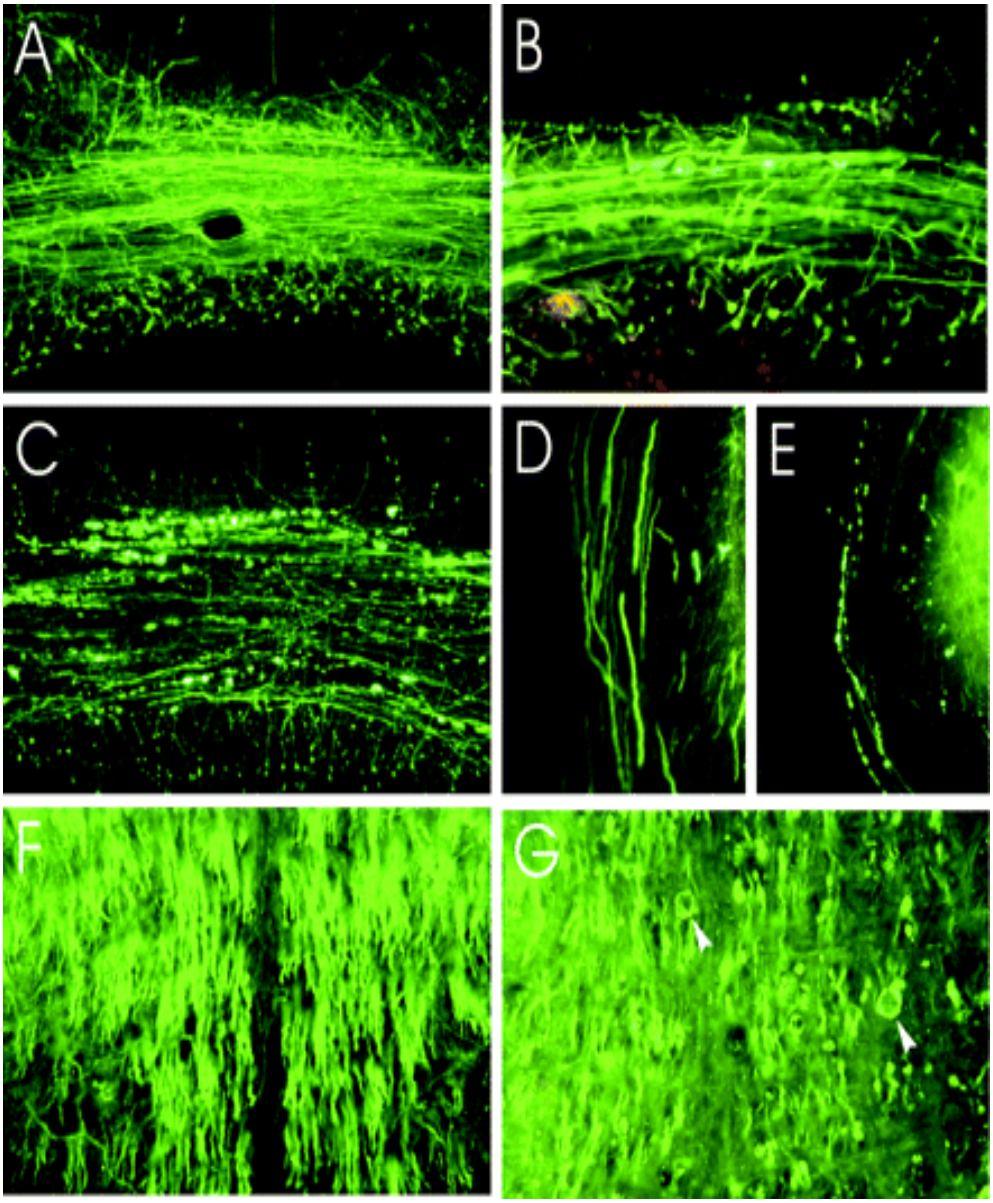

Figure 4: CVS induced neuronal process degeneration in transgenic mice that express yellow fluorescence protein. Mossy fiber axons of mock-infected (A), CVS-infected (B), and moribund (C) mice. Inferior cerebellar peduncle axons of mock-infected (D), and moribund (E) mice. Central tracts in the brainstem in mock-infected mice (F) and CVS-infected moribund mice (G). Distended axonal profile was observed in CVS-infected moribund mice (arrowheads). (reproduced from Scott *et al,* 2008 with permission).

morphological abnormalities were remarkable in moribund mice (Scott *et al.,* 2008) (Figure 4). Vacuolations and swollen mitochondria were also demonstrated in the infected neurons. These swollen mitochondria were localized particularly at the site of the process swellings and beadings suggesting a role for mitochondria in these morphological abnormalities (Scott *et al.,* 2008).

1.8 Oxidative stress:

All cell types, especially neurons of the brain, are vulnerable to oxidative stress (Gandhi and Abramov, 2012). In comparison with other cells, there is a high demand for energy in neuronal cells. Oxygen is consumed in relatively high amounts by neurons to initiate oxidative phosphorylation and produce ATP. Indeed, 20% of the total amount of body oxygen is consumed by the brain (Halliwell *et al,* 2006). Some of the oxygen consumed by neurons during normal physiological aerobic respiration is used to generate reactive species such as hydrogen peroxide, nitric oxide, hydroxyl and superoxide. Reactive oxygen species play a pivotal role in several cellular biochemical activities such as cell signaling, cell adhesion, host defense and regulation of enzyme activities (Dröge, 2001). But accumulation or overproduction of reactive oxygen species (ROS) have undesirable effects on the cells (Freidovich, 1999). Indeed, interaction between different ROS can lead to more devastating outcomes (Huie and Padmaja, 1993). Interaction between superoxide and nitric oxide produces peroxynitrite, an oxidant that can cause severe damage to cellular amino-acids, nucleic acids, and lipid-containing molecules (Huie and Padmaja, 1993). Lipid peroxidation is a common consequence of oxidative stress in which reactive

oxygen species oxidatively damage the lipid-containing components (e.g., arachidonic acid and linoleic acids) and produce 4-hydroxy-2-nonenal (4-HNE), a highly reactive electrophile which can be toxic to the cells (Ferrari, 2000, and Keller *et al.,* 1997). Thus, increased 4-HNE expression is used as a marker for oxidative stress. Imbalance between oxidant and antioxidant systems either due to an increase in ROS production or a defect in antioxidant defense activity leads to ROS accumulation and oxidative stress.

1.8.1 Pro-oxidants and sources of ROS:

Univalent reduction of oxygen generates superoxide whereas bivalent reduction produces hydrogen peroxide. It was shown that plasma membrane, mitochondrial membrane, and endoplasmic reticulum membrane catalyze superoxide production (Chance *et al.,* 1979). Cytosolic (e.g., flavoprotein xanthine oxidase), membrane-bound (e.g., NADPH cytochrome P-450 reductase), and peroxisome enzymes are other enzymatic sources of superoxide and hydrogen peroxide (Fridovich *et al.,* 1970, Brass *et al.,* 1991, and Chance *et al.,* 1979). Non-enzymatic sources involve the metabolism of prostaglandin, catecholamine, and hemoglobin (Misra and Fridovich, 1972, and Cohen and Heikkila, 1974). The immune system may also contribute to ROS production (Babior *et al.,* 1973). Oxidative burst induced by immunocytes (e.g., phagocytes) in order to eliminate bacterial or viral-infected cells largely depends on the ability of these cells to produce high amounts of ROS by plasma membrane NADPH oxidase (Babior *et al.,* 1973).

1.8.2 Antioxidants and scavenging of ROS:

Under normal physiological condition, mitochondrial uncoupling is one way to combat ROS formation by preventing the generation of a very high mitochondrial membrane potential (Sack, 2006). Although generation of high mitochondrial membrane potential by electron transport chain Complexes is required to produce ATP, a very high mitochondrial membrane potential also greatly favors ROS formation (Starkov *et al.,* 2003, and Murphy, 2009). Uncoupling factors such as thyroid hormones and uncoupler proteins are activated when the mitochondrial membrane potential exceeds the desirable limit and, thus, decreases proton pumping across the inner mitochondrial membrane (Terada, 1990). In addition to uncouplers, antioxidant systems are activated in order to eliminate ROS overgeneration and accumulation. Antioxidants either directly scavenge the produced ROS or indirectly inhibit their formation (Gilgun-Sherki *et al.,* 2001). Vitamins (e.g., vitamin E and vitamin C) (Frei, 1994), zinc (Powell, 2000) and glutathione (Shen D *et al.,* 2005) are examples of non-enzymatic antioxidant components. Enzymatic antioxidants include superoxide dismutase, catalase, and glutathione peroxidase (Fang *et al.,* 2002 and Uday *et al.,* 1990). Whereas manganese-superoxide dismutase (Mn-SOD) is found in the mitochondria, copper-zinc superoxide dismutase (Cu-Zn SOD) is located in the cytosolic and extracellular compartments (McCord *et al.,* 1971 and Marklund *et al.,* 1982). The main function of superoxide dismutase is to convert superoxide molecules to hydrogen peroxide and oxygen. This should prevent the release of superoxide into cytoplasm. In addition, it will prevent superoxide-nitric oxide interaction and peroxynitrite formation (Jourd'heuil *et al.,* 1997). Mitochondrial

superoxide dismutase seems to be more important than the other superoxide dismutases. Almost no effect was seen in mice when the cytosolic superoxide dismutase was knocked out (Ho *et al.,* 1997). A similar finding was observed in extracellular superoxide dismutase-knockout mice. However, these mice showed hypersensitivity to hypoxia (Carlsson *et al.,* 1995). In contrast, mitochondrial superoxide dismutase-knockout mice suffered severe cardiomyopathy and serious neuronal degeneration followed by death within a few days (Li *et al.,* 1995). Catalase is found mainly in the peroxisomes. Catalase breaks down hydrogen peroxide and releases oxygen (Mueller *et al.,* 1997). Glutathione peroxidase also reacts with and removes hydrogen peroxide, but no oxygen is released (Brigelius-Floh, 1999, Krishna *et al.,* 2010). Glutathione peroxidase can be detected in both mitochondria and cytoplasm (Meredith and Reed, 1982, and Griffith and Miester, 1985).

1.9 Viral infections associated with oxidative stress:

Several neurotropic and non-neurotropic viral infections are believed to induce oxidative stress either by enhancing ROS generation or by impairing antioxidant dysfunction (Schwarz, 1996). The level of intracellular glutathione, an antioxidant, was reduced in HIV–infected lymphocytes (Buhl *et al.,* 1989). As macrophages modulate the level of glutathione in the lymphocytes (Gmiinder *et al.,* 1990), it was suggested that the viral infection may reduce the glutathione concentration by inducing macrophage dysfunction (Muller *et al.,* 1990). The increased level of ROS in the cells is another reason for the depletion of intracellular glutathione level. A potential mechanism for ROS overproduction is

through the release of cytokines that have a pro-oxidant activity such as tumor necrosis factor (TNF) and interleukin-1 (IL-1) as a response to the infection (Gloenbock *et al.,* 1991, and Klempner *et al.,* 1978). Both the infected cells and the phagocytes are able to promote TNF release. TNF targets the mitochondrial respiration by promoting electron leakage and superoxide production (Schulze-Osthoff, 1992). This action is known to be inhibited by vitamin E, an antioxidant (Schulze-Osthoff, 1992). IL-1 release is stimulated by the activated monocytes (Klempner *et al.,* 1978). As a result, neutrophils secrete lactoferrin, a lysosomal protein that interacts with iron and form lactoferrin-iron complex (Klempner *et al.,* 1978). Lactroferrin-iron complex is sequestered in the reticuendothelial system. If the iron uptake exceeds the cellular iron-binding capacity, iron interacts with superoxide and forms hydroxyl radicals. It was shown that the activity of catalase is increased as HIV disease progresses probably as a compensatory mechanism for glutathione loss (Left *et al.,* 1992). The expression of HIV genes promotes the ROS-induced apoptosis in the T cells (Sandstrom *et al.,* 1993). It was shown that N-acetyl cysteine, an antioxidant, inhibits both the viral replication and its ROS-induced apoptosis (Malorui *et al.,* 1993). In hepatitis B-infected transgenic mice, the level of ROS generation by activated phagocytes was increased (Hegan *et al.,* 1994). Similarly, high levels of superoxide radicals were detected in the resting neutrophils of children with chronic hepatitis B infection, although activated neutrophils did not follow the same trend (Vierucci *et al.,* 1983, and Uehara *et al.,* 1994). The expression of hepatitis B genome in human hepatoma hep 3B cells decreased the activity of superoxide dismutase and catalase

whereas glutathione peroxidase was completely absent (Bannister *et al.,* 1986). It was suggested that oxidative stress plays a role in the carcinogenesis of both hepatitis B and hepatitis C, probably by inducing oxidative damage in the DNA of the infected cells. Woodchuck hepatitis virus and borna virus also induce ROS generation, in particular they prompt nitric oxide production via upregulating nitric oxide synthase (Liu *et al.,* 1991, 1992, and Zheng *et al.,* 1993). Indeed, it was shown that the activity of nitric oxide synthase and the level of nitric oxide in the brain of borna virus-infected rats determine the severity of the viral pathology (Zheng *et al.,* 1993). As mitochondria are well known targets for ROS, mitochondrial respiration of influenza B virus-infected human hepatocytes was assessed in the presence and absence of the activated macrophages (Schwarz *et al.,* 1994). Whereas the mitochondrial respiration was normal in the absence of macrophages, it was significantly inhibited in the presence of macrophages (Schwarz *et al.,* 1994). The addition of vitamin E or monoclonal antibody directed against TNF corrected the respiration inhibition (Schwarz *et al.,* 1994). Therefore, it was concluded that influenza B virus-infected human hepatocytes are sensitive to TNF pro-oxidant activity (Schwarz *et al.,* 1994). The level of several antioxidants like vitamin A and vitamin E were reduced in the lung of influenza A virus-infected mice (Hennet *et al.,* 1992). Another in vivo study of influenza A virus-infected mice showed that the levels of superoxide and hydrogen peroxide were increased in the bronchi alveolar lavage fluid (BALF) and cell-free (BALF), respectively (Buffington *et al.,* 1992). Application of superoxide dismutase conjugated with pyran polymer protected the mice from lethal influenza A-

induced pneumonia (Oda *et al.,* 1989). Noteworthy, oxidative stress plays a critical role in the pathogenesis of several non-infectious neurodegenerative disorders such as Alzheimer's disease, Parkinson's disease and diabetic neuropathy in addition to its critical role in the pathogenesis of infectious diseases.

1.10 Rabies virus-induced oxidative stress:

The morphological abnormalities observed in rabies virus-infected neuronal processes were remarkably similar to these observed in sensory neurons from diabetic rats (Lauria *et al.,* 2003, Zherebitskaya *et al.,* 2009). Oxidative stress plays a crucial role in inducing axonal swellings in cultured neurons derived from diabetic rats (Zherebitskaya *et al.,* 2009). Therefore, the role of oxidative stress in rabies virus infection was investigated. Evidence of oxidative stress were observed in rabies virus-infected mouse dorsal root ganglion (DRG) cultured neurons (Jackson *et al.,* 2010). Rabies virus infection induced axonal swellings in the infected neurons at 48 and 72 hours post-infection (Jackson *et al.,* 2010) (Figure 5). These swellings were labelled by 4-HNE immunostaining, a biomarker for lipid peroxidation (Jackson *et al.,* 2010) (Figure 5). The number of 4-HNE puncta was significantly higher in the infected cells in comparison with their controls. In this model, the axonal outgrowth was dramatically reduced in rabies virus infected neurons (Jackson *et al.,* 2010). Recently, evidence of oxidative stress generation, axonal swelling induction, and axonal outgrowth reduction was also observed in rabies virus-infected rat dorsal root ganglion cultured neurons (Kammouni *et al.,* 2012). Nuclear factor

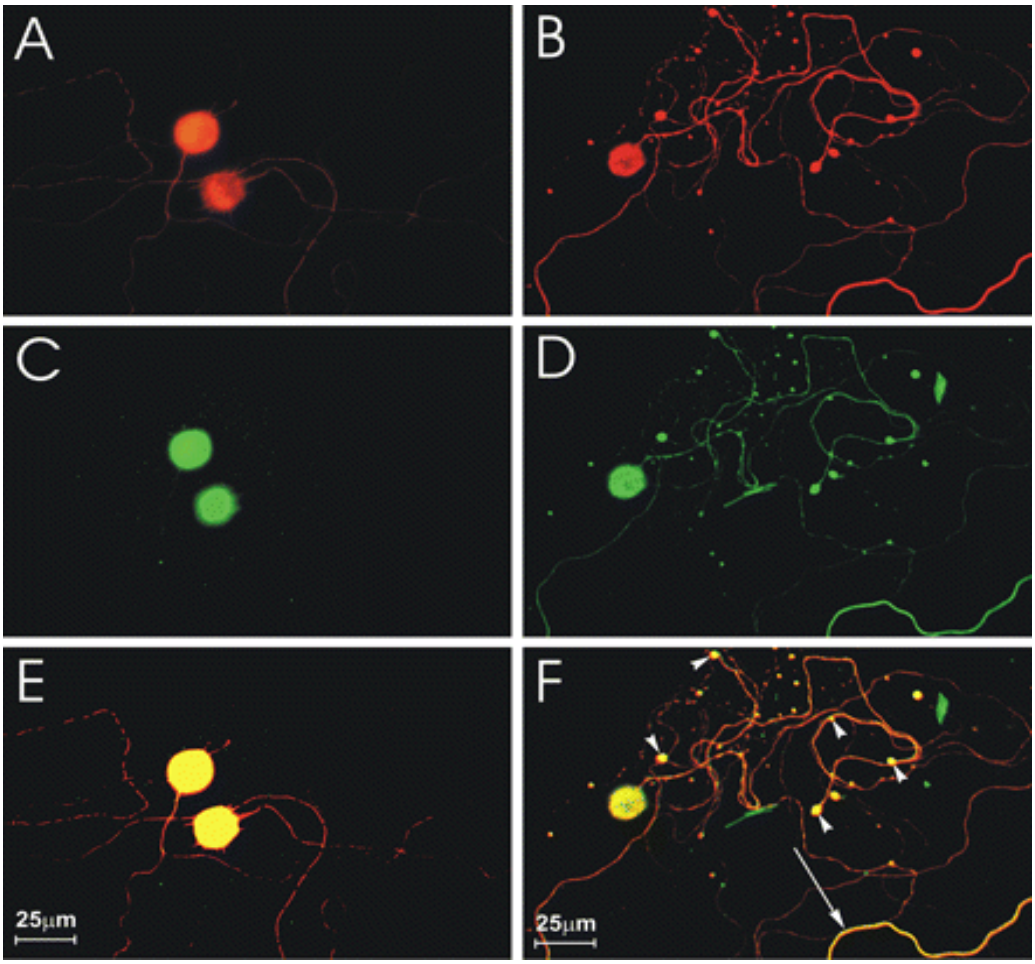

Figure 5: CVS induced axonal swelling in DRG primary neurons. (A, B, and E) mock-infected neurons. (B, D, and F) CVS-infected neurons. A and B were stained with β-tubulin; a marker of neurons. C and D were stained with 4-HNE; a marker of lipid peroxidation. E and F show when both stains were merged. Strong expression was observed in CVS-infected neurons with and without axonal swellings (arrowheads and arrow, respectively). (reproduced from Jackson *et al.,* 2010 with permission).

kappa B (NF-κB) p50 and p65 subunit were overexpressed in CVS-infected neurons as indicated by western blotting analysis (Kammouni *et al.,* 2012). CVS infection in the presence of SN50, a peptide that prevents NF-κB translocation to the nucleus, increased the 4-HNE puncta in the axons of infected neurons (Kammouni *et al.,* 2012). On the other hand, ciliary neurotropic factor, a neurotrophic factor and NF-κB activator, significantly reduced the number of 4-HNE puncta in the infected neurons (Kammouni *et al.,* 2012). Quantitative assessment of NF-kB p50 subunit levels in nuclear and cytoplasm indicated higher nuclear to cytoplasm ratio in CVS-infected cells versus mock-infected neurons at 24 hours post infection, but the nuclear localization of p50 subunit was impaired at 48 and 72 hours post-infection (Kammouni *et al.,* 2012). It was concluded that rabies virus induces oxidative stress in the infected neurons by inhibiting NF-kB activation (Kammouni *et al.,* 2012) although other cellular mechanisms may also be involved.

1.11 Mitochondria:

Mitochondria are significantly involved in modulating numerous cellular functions such as energy production, apoptosis induction, calcium homeostasis, hormone biosynthesis, ROS generation and scavenging (Henze and Martin, 2003). Mitochondria are found in the cytosolic compartment of eukaryotic cells. They are composed of two main compartments: the intermembrane space which is located between the outer and inner membrane and the matrix which is surrounded by the inner site of the inner membrane. Of note, Krebs cycle takes place in the mitochondrial matrix. The inner membrane is folded into cristae in

order to increase the surface area of the inner membrane and enhance ATP production (Henze and Martin, 2003).

1.11.1 Mitochondria as a source of energy:

Mitochondria consume oxygen molecules during aerobic respiration. The production of cellular energy constitutes two pathways: oxidation (electron transport chain) and phosphorylation (Kalckar, 1974). Complex I, NADH-Coenzyme Q oxidoreductase, is the first (Hirst *et al.,* 2005) and largest enzyme in size, approximately 1000 kilo Dalton (Lenaz *et al.,* 2006), in the electron transport chain. It is composed of 39 nuclear-encoded and 7 mitochondrial encoded subunits (Carroll *et al.,* 2003, Chomyn *et al.,* 1985 and 1986). Upon Complex I and NADH interaction, two electrons enter Complex I at its flavin mononucleotide (FMN) site (Ohnishi *et al.,* 1998). As a result, FMN is reduced and four protons are pumped across the mitochondrial inner membrane (Brandt *et al.,* 1997). Complex II, succinate dehydrogenase, is the second enzyme in electron transport chain, and it is also a Krebs cycle enzyme (Cecchini *et al.,* 2003). Its main functions are succinate oxidation and ubiquinone reduction. Noteworthy, no proton pumping takes place at Complex II. Q-cytochrome c oxidoreductase is regarded as Complex III in the electron respiratory chain (Berry *et al.,* 2000). It constitutes 22 proteins equally separated between two major subunits forming a dimer (Iwata *et al.,* 1998). Ubiquinol and cytochrome c are oxidized and reduced, respectively, at Complex III (Berry *et al.,* 2000). In a two step-reaction (Q-cycle), four protons are pumped into the intermembrane space (Trumpower *et al.,* 1990, Hunte *et al.,* 2003). Complex IV or cytochrome c

oxidase is the last enzyme in the electron transport chain (Calhoun *et al.,* 1994). The main function of Complex IV is to oxidize cytochrome c and pass an electron to oxygen releasing water and pumping four protons into the intermembrane space (Yoshikawa *et al.,* 2006). Due to proton pumping through Complex I, III, and IV from the matrix to the intermembrane space, an electrochemical gradient is generated creating the mitochondrial membrane potential (Schultz and Chan 2001, Nicholls, 2004). ATP synthase, which is powered by the mitochondrial membrane potential, completes the oxidative phosphorylation pathway via consuming the proton gradient generated by electron transport chain in order to produce energy in the form of ATPs (Boyer *et al.,* 1997). Three or four protons are consumed to generate one molecule of ATP (Van Walraven *et al.,* 1996, and Yoshida *et al.,* 2001). Figure 6 shows an overview of the oxidative phosphorylation process.

1.11.2 Mitochondria as a source of ROS:

Although ROS can be produced in cells via various pathways, some sources seem to be more significant than others. Mitochondria can be regarded as the major source for ROS. Figure 7 shows an overview of the mitochondrial role in ROS production. Mitochondrial superoxide steady state concentration is 5 to 10 times more than that detected in the nucleus and cytoplasm. Both sub-mitochondrial particles and intact mitochondria contribute to hydrogen peroxide production (Jensen *et al.,* 1966, Hinkle *et al.,* 1967, Chance *et al.,* 1971, Boveris *et al.,* 1972, and Loschen *et al.,* 1975). It was suggested that the whole amount of mitochondrial hydrogen peroxide is due to dismutation of superoxide (Boveris

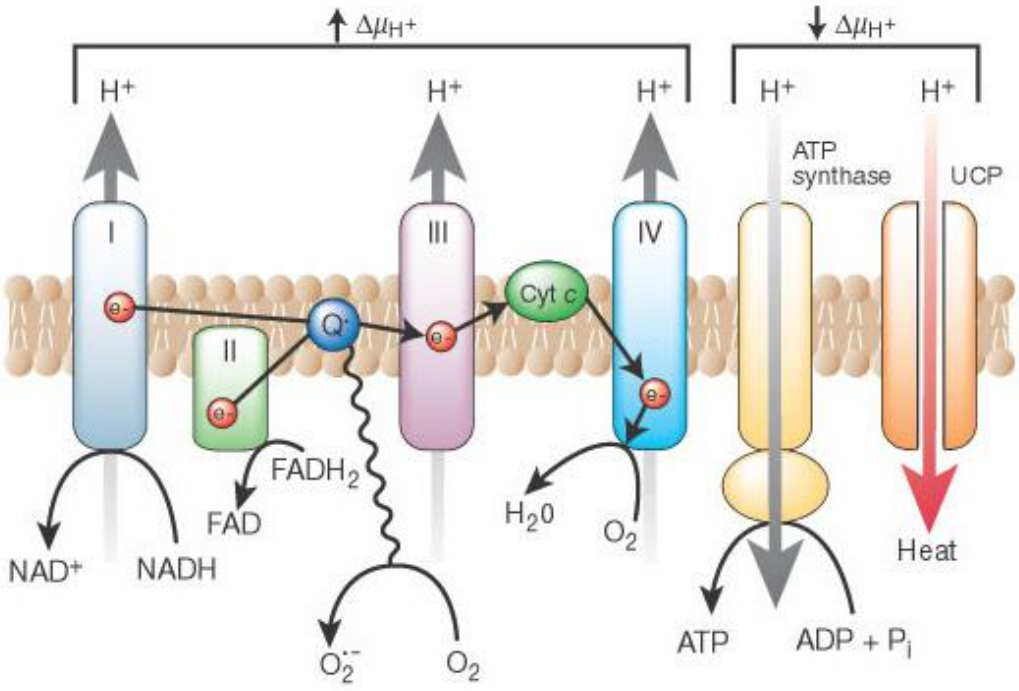

Figure 6: Oxidative phosphorylation process. As the electrons are transported through the electron transport chain Complexes, protons are pumped from the mitochondrial matrix to the intermembrane space generating a high mitochondrial membrane potential. ATP synthase, then, consumes this mitochondrial membrane potential to phosphorylate ADP and produce energy (reproduced from Brownlee, 2001, with permission from Nature Publishing Group www.nature.com).

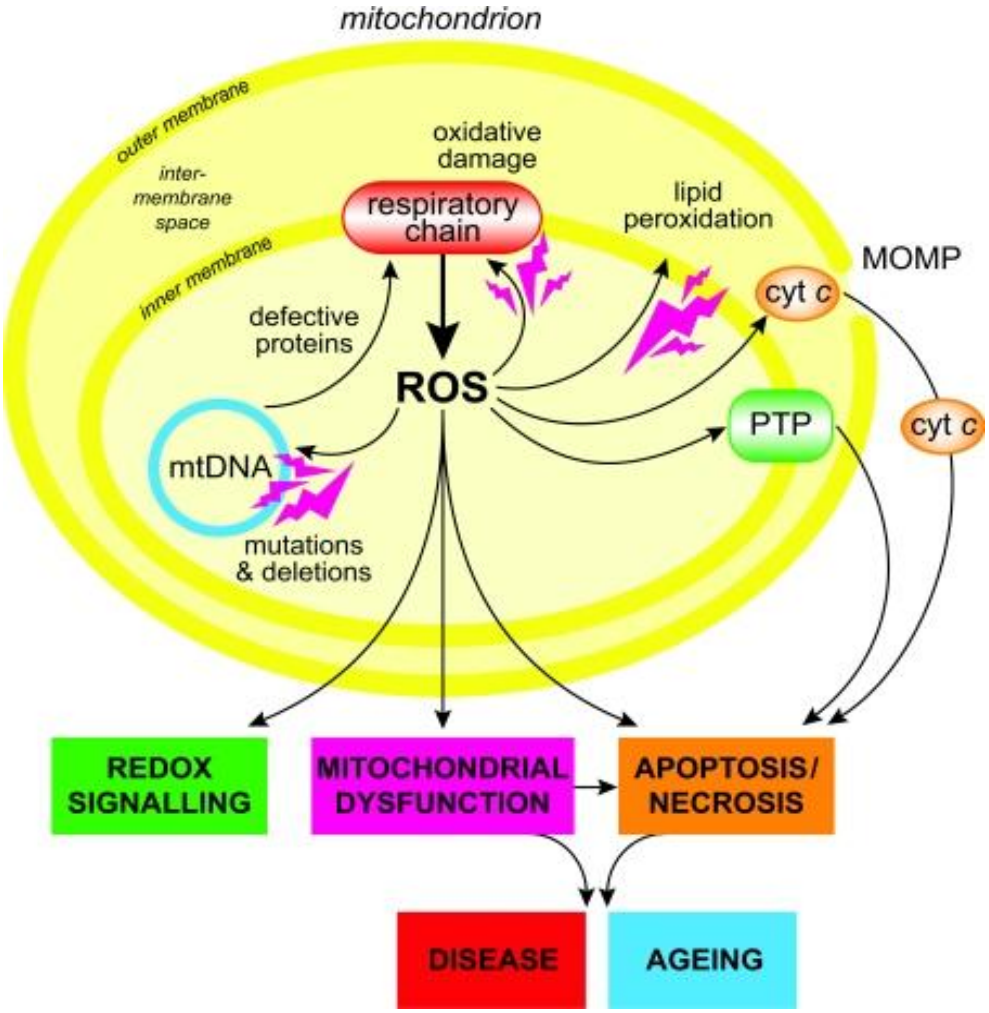

Figure 7: The relationship between mitochondria and ROS production. Mitochondrion is one of the major cellular sources and targets of ROS. In normal physiological condition, ROS are used for redox signaling. In pathological conditions, ROS production is enhanced mainly by electron transport chain Complexes. Mitochondrial DNA is vulnerable to ROS. ROS-induced mutations in mitochondrial DNA lead to mitochondrial dysfunction. Mitochondrial dysfunction leads to more ROS formation and more devastating outcomes (reproduced from Murphy, M. P. "How Mitochondria Produce Reactive Oxygen Species." Biochem J 417, no. 1 (2009): 1-13).

et al., 1975). Within mitochondria themselves, several sites for ROS generation have been identified. Electron transport chain, in particular Complex I and Complex III, can be regarded as the main ROS generators in the mitochondria. Superoxide molecules produced at Complex I are found mainly in the mitochondrial matrix (Brand *et al.,* 2004). The presence of succinate, Complex II substrate, has additive effect on superoxide production at Complex I potentially via reverse electron transport system (Liu *et al.,* 2002). Myxothiozole either increases or decreases superoxide level in the presence of NADH (Complex I-substrate), or succinate (Complex II-substrate), respectively (Giulivi *et al.,* 1995). The level of ROS production was increased in the presence of Complex III-inhibitor, antimycin A. Hence, Complex III was suggested as a site of ROS production (Ohnishi *et al.,* 1980, and Ericinska *et al.,* 1976). Within Complex III, ubisemiquinone and cytochrome-b have been identified as oxygen reactants and, thus, identified as superoxide-producing components (Ohnishi *et al.,* 1980, and Ericinska *et al.,* 1976). When NADH to NAD+ ratio is increased in the cells, Krebs cycle enzyme, in particular α- ketoglutarate dehydrogenase, greatly contribute to ROS production. Figure 8 shows three common modes of ROS production by the mitochondria under normal and abnormal mitochondrial function. Other mitochondrial sources of ROS such as cytochrome P-450 (Bernhardt, 1996) and monoamine oxidase (Pizzinat *et al.,* 1999) have been identified.

1.11.3 Mitochondria as a target for ROS:

Mitochondria are one of the main cellular targets for ROS. Figure 7 shows an overview of the vulnerability of mitochondria to ROS. The number of bases that

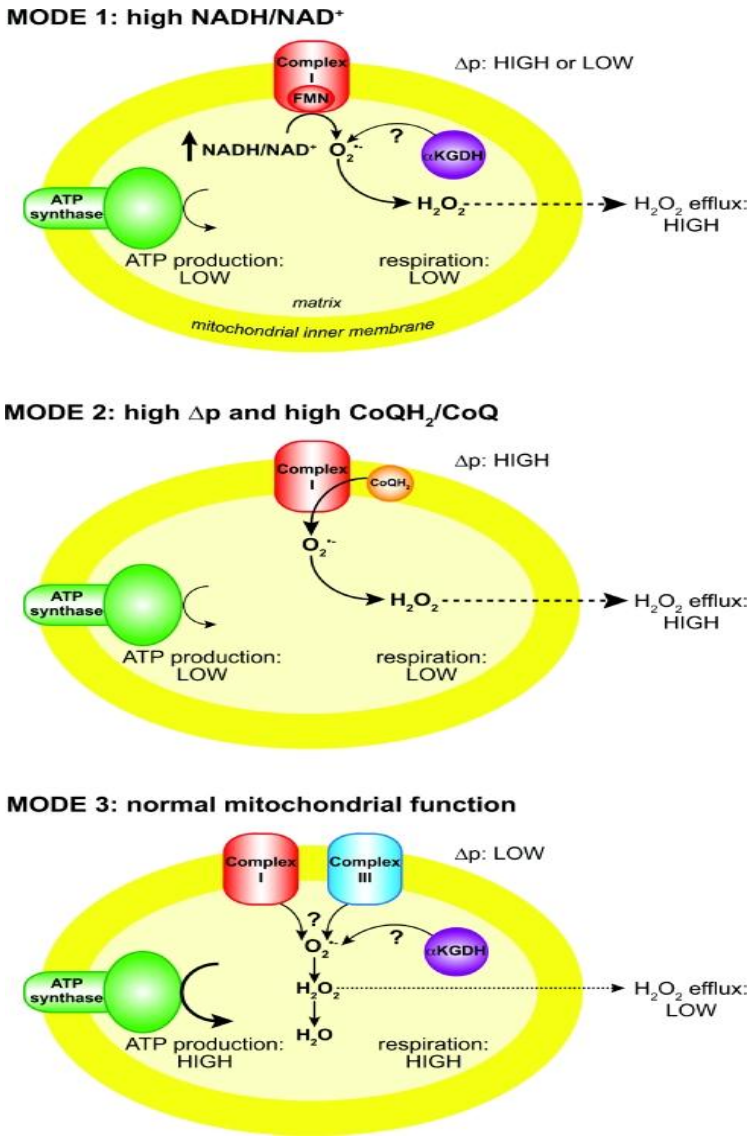

Figure 8: Three common modes for mitochondrial ROS production. Mode1: the increase of NADH to NAD+ ratio, for example, due to a defect in Complex I leads to ROS overproduction at Complex I and α-ketoglutarate dehydrogenase. Mode 2: high mitochondrial membrane potential is associated with low ATP production leading to reverse electron flow and high amount of ROS. Mode 3: under normal physiological condition, mitochondrial produce a low amount of ROS (reproduced from Murphy, M. P. "How Mitochondria Produce Reactive Oxygen Species." Biochem J 417, no. 1 (2009): 1-13)

are oxidatively modified in the mitochondrial DNA is up to 20 higher than it is in nuclear DNA (Brown *et al.,* 1979). Part of this can be explained by the fact that mitochondrial DNA lacks the protective histone that is found around nuclear DNA (Rasmussen *et al.,* 1998). Moreover, mitochondrial DNA is closer to the sites of ROS production than nuclear DNA. In rat liver mitochondria, pyridine nucleotides are lost in the presence of hydrogen peroxides (Birt and Bartley, 1960). Furthermore, calcium release is enhanced and cell cytotoxicity is promoted (Richter and Jörg Schlegel, 1960). It was shown that hydrogen peroxide and nitric oxide alters several mitochondrial parameters such as electron transport chain Complexes and aconitase activities (Raza *et al.,* 2011). In rat liver mitochondria, nitric oxide and peroxynitrite open mitochondrial transition pores and activate calcium efflux (Radi *et al.,* 2002). Modulating the mitochondrial transition pores may lead to pro-apoptotic proteins and promote apoptosis (Radi *et al.,* 2002).

1.12 Rationale, hypothesis, and objectives of this study:

CVS rabies virus strain infection induces oxidative stress in both mouse and rat DRG primary neurons (Jackson *et al.,* 2010, and Kammouni *et al.,* 2012). However, the underlying mechanisms of this process have not been identified. Although several cellular components may induce oxidative stress in the infected cells, mitochondria can be considered as the main source of ROS. Indeed, alteration of mitochondrial functions can enhance ROS production and/or suppress ROS scavenging leading to ROS accumulation and oxidative stress induction in the cells (Murphy, 2009). In addition to the critical role of the

mitochondria in oxidative stress induction, previous findings indicated that rabies virus protein, in particular the matrix protein, is localized to the mitochondria of the infected cells (Gholami *et al*., 2008). These facts led to our hypothesis that rabies virus induces oxidative stress by inducing mitochondrial dysfunction. The purpose of this study is to investigate a linkage between the mitochondrial functions and oxidative stress in rabies virus infected cells. Our objectives include assessment of several mitochondrial parameters in CVS-infected cells and comparing them to mock-infected cells. Four different cell types were initially used in this study: rat DRG primary sensory neurons, nerve growth factor (NGF)-treated PC12 cells, mouse neuroblastoma cells (MNA), and baby hamster kidney clone S13 cell (BHK-S13). The biochemical activity of Krebs cycle enzymes (citrate synthase and malate dehydrogenase) and electron transport chain Complexes (Complex I, Complex II-III, and Complex IV) were assessed. Several states of mitochondrial respiration (leak respiration, coupled respiration, uncoupled respiration, and Complex IV respiration) were also studied. Finally, the effect of the viral infection on the mitochondrial membrane potential, the levels of NAD+, NADH, NADH/NAD+ ratio, intracellular ATP, hydrogen peroxide production were determined.

Materials and methods:

2.1 Virus:

The challenge virus standard-11 strain of fixed rabies virus (CVS), obtained from William H. Wunner (The Wistar Institute, Philadelphia, PA), was used in these studies. Virus propagation was conducted using baby hamster kidney (BHK) (clone C13) cells grown in Dulbecco's modified Eagle medium (DMEM) (11995; Invitrogen, Carlsbad, CA) supplemented with 10% fetal calf serum (B15-001; PAA cell culture company, Etobicoke, Canada) at 37°C in humidified air containing 5% CO_2. Viral titers of stock virus were determined by counting fluorescent foci on mouse neuroblastoma (MNA) cells.

2.2 Cell types and growth condition:

Four different cell types were used in this study: rat DRG primary sensory neurons, nerve growth factor (NGF)-treated PC12 cells, mouse neuroblastoma cells (MNA), and baby hamster kidney clone S13 cell (BHK-S13).

Rat DRG neurons were prepared as described previously (Kammouni *et al.* 2012). Briefly, adult male Sprague Dawley rats (University of Manitoba, Winnipeg, MB, Canada) were killed by decapitation. DRG neurons were dissected after the vertebral column was removed. DRG were treated with 0.125% collagenase type 4 (47C9497; Worthington, Lakewood, NJ) and then with 2.5% trypsin (57H9722; Worthington, Lakewood, NJ) for 45 min at 37°C in order to dissociate the cells. Neonatal calf serum (NCS) was added to a final concentration of 33% to neutralize the collagenase/trypsin. After successive washing with Ham's F12 media (11765-054; Invitrogen) containing 10% fetal

bovine serum, the cells were collected, filtered, and centrifuged at 300 x g for 10 min. The cell pellet were resuspended and centrifuged in Ham's F12 media containing 15% essentially fatty-acid-free bovine serum albumin (BSA) (A9205; Sigma-Aldrich) for 10 minute at 900 X g. 2 ml of Ham's F12 media containing 2 mM L-glutamine and Bottenstein's N2 supplements without insulin were used to resuspend the cell pellet. Bottenstein's N2 supplements contain 0.1 mg/ml transferrin, 20nM progesterone (P8783; Sigma-Aldrich), 100 µM putrescine (P7505; Sigma-Aldrich), 30 nM sodium selenite (S5261; Sigma-Aldrich), and 0.1 mg/ml fatty acid-free BSA (A9205; Sigma-Aldrich). Cells were seeded on six-well plates (Nunclon Surface). Then, cultures were kept for 2 days in N2/F-12 medium at 37°C in humidified air containing 5% CO2 prior to viral adsorption.

PC12 cells were cultivated and differentiated for 3 days in DMEM containing 50 nmol/ml NGF (N2513; Sigma-Aldrich) in the presence of either 1% horse serum (26050-088; Invitrogen) and 0.5% fetal bovine serum or 10% horse serum and 5% fetal bovine serum at 37°C in humidified air containing 5% CO_2 prior to viral adsorption.

MNA cells were cultivated in Minimum Essential Medium Eagle (12-662F; Lonza, Walkersville, MD) containing 1% sodium bicarbonate (17-613E; Lonza), 40mM L-Glutamine (G7513; Sigma-Aldrich), tryptosephosphate broth (T0800; Teknova, Hollister, CA) containing 0.14% tryptose, 0.014% Glucose, 0.035% sodium chloride, 0.0175% sodium phosphate dibasic and 10% fetal calf serum at 37°C in humidified air containing 5% CO_2 prior to viral adsorption.

BHK-S13 cells were cultivated in DMEM containing 10% fetal calf serum at 37°C in humidified air containing 5% CO_2 prior to viral adsorption.

2.3 Viral infection:

Cells were infected with CVS at multiplicity of infection (MOI) of 10 fluorescent foci forming unit per cell. After 1 hr of viral absorption, appropriate and fresh media were added to each cell type.

2.4 Cell viability assay:

The cell viability was determined by trypan blue (17-942E; Lonza) exclusion test. Viable cells are able to exclude the trypan blue staining whereas dead cells retain the dye in their cytoplasm. Seventy two hrs post-infection mock-infected and CVS-infected PC12 cells were stained with trypan blue at 1:1 ratio and the percentage of viable cells was determined.

2.5 Measurement of protein concentration:

The protein concentration was measured in 96 well plate using Bio-Rad DC protein assay kit (500-0116; Bio-Rad, Mississauga, Canada). Cells were lysed in lysis buffer containing 1% NP-40. Then, 5 µl from the sample, 25 µl of alkaline copper tartrate solution (reagent A), 200 µl of dilute folin reagent (reagent B) were added in each well. After 15 min incubation at room temperature, the absorbance was recorded by SpectraMax Plus384 spectrophotometer (Molecular Devices, Sunnyvale, CA) at 750 nm wavelength. The protein concentration was determined from a standard curve prepared by bovine serum albumin (2930; Omnipur, Gibbstown, NJ).

2.6. Western blotting analysis for 4-HNE expression:

Western blotting analysis was performed according to the protocol described previously (Kammouni et al., 2012). At 72 hrs post-infection, CVS- and mock-infected PC12 cells were lysed using ice-cold neurofilament stabilization buffer containing: 0.1 M Pipes, 5 mM MgCl2, 5 mM EGTA, 0.5 % Triton X-100, 20% glycerol, 10 mM NaF, 1 mM PMSF and protease inhibitor cocktail. Protein concentrations were determined. Equal amounts of proteins (5 µg) from CVS and mock-infected PC12 samples were loaded onto 10% SDS-PAGE gel. The proteins were electrotransferred onto a nitrocellulose membrane at 100 V for one hour. Then, it was incubated overnight with rabbit polyclonal antibody anti-extracellular signal-regulated kinase (ERK) (sc-93, Santa Cruz Biotechnology) or rabbit polyclonal anti-HNE Michael adducts (#393207, EMD Millipore, Temecula, CA) (1/1000) followed by incubation with HRP-linked anti-rabbit IgG (Jackson Immunoresearch Laboratories). Western blotting luminol reagent (sc-2048, Santa Cruz Biotechnology) was used for protein detection. Imaging was performed by a BioRad Fluor-S. Densitometeric scan of the blots was detected using Quantity one software. Results are expressed as ratio of scan value of 4-HNE protein to ERK protein.

2.7 Measurement of citrate synthase and malate dehydrogenase activities:

Citrate synthase and malate dehydrogenase activities were measured by spectrophotometric approach in mock-infected and CVS-infected cells at 72 hrs post-infection as previously described with minor modifications (Chowdhury *et al*, 2000, Chowdhury *et al,* 2010, Silverstein and Sulebele, 1970). All measurements were conducted on 96-well plate in a total reaction volume of 100 µl. The assays

were optimized. Therefore, the concentrations of chemicals, the incubation periods, and the assays run time in each assay can be different from those previously reported. The protocols (including the concentration of chemicals, the incubation periods, and the assay run time) used in our studies are fully described below.

2.7.1 Assessment of citrate synthase activity:

2.7.1.1 Principle of the assay:

Measurement of citrate synthase activity was based on the ability of the enzyme to facilitate the formation of citrate in the presence of acetyl-CoA and oxaloacetic acid. The formation of citrate converts 5,5′-Dithiobis(2-nitrobenzoic acid) (DTNB) to 5-thio-2-nitrobenzoic acid (TNB) and, thus, changes its color.

2.7.1.2 Preparation and storage of stock solutions:

1 mM DTNB (D8130; Sigma-Aldrich) stock solution was prepared in 1 M Tris-HCL buffer (pH 8.2). 10 mM Acetyl coenzyme A (acetyl-coA) (A2056; Sigma-Aldrich) stock solution was prepared in distilled water. 10 mM Oxaloacetic acid (O-4126; Sigma-Aldrich) stock solution was prepared in 0.1 M Tris-HCL buffer (pH 8.2). The stock solutions of DTNB, Acetyl-CoA, and oxaloacetic acid were aliquoted in tubes and stored at -20°C.

2.7.1.3 Procedure:

To determine citrate synthase activity, 0.1 mmol/L DTNB and 1-5 µg sample were added in Tris-HCl buffer (pH 8.2) containing 0.05% lauryl maltoside (D4641; Sigma-Aldrich). 0.1 mmol/L acetyl-CoA was added and the absorbance was followed at 412 nm for 5 minutes. Then, the reaction was started by adding

0.05 mmol/L oxaloacetic acid, and citrate synthase activity was monitored for another 5 minutes.

2.7.2 Assessment of malate dehydrogenase activity:

2.7.2.1 Principle of the assay:

Measurement of malate dehydrogenase activity was based on the ability of the enzyme to oxidize β-Nicotinamide adenine dinucleotide (NADH), and convert oxaloacetic acid to malate.

2.7.2.2 Preparation and storage of stock solutions:

1 mM NADH (N8129; Sigma-Aldrich) stock solution was freshly prepared in distilled water and kept on ice. Oxaloacetic acid stock solution was prepared as described above (2.7.1 Assessment of citrate synthase activity).

2.7.2.3 Procedure:

The reaction buffer (100 mM phosphate buffer saline containing 0.05% lauryl maltoside) contained 100 µmol/L NADH, 0.05 mmol/L oxaloacetic acid, 5 µg sample. Then, the reduction in absorbance due to NADH oxidation was monitored at 340 nm for 2 minutes.

2.8 Assessment of electron transport chain (ETC) Complex activities:

The biochemical activities of electron transport chain (ETC) Complex were determined by spectrophotometer approach in mock-infected and CVS-infected cells at 72 hrs post-infection as previously described with minor modifications (Chowdhury *et al*, 2000, Chowdhury *et al,* 2010, and Kiebish *et al,* 2008). All measurements were conducted in 96-well plates in a total reaction volume of 100

µl. The protocols (including the concentration of chemicals, the incubation periods, and the assay runt time) used in our studies are fully described below.

2.8.1 Assessment of Complex I activity:

2.8.1.1 Principle of the assay:

Complex I activity was measured as rotenone-sensitive NADH-cytochrome c reductase activity. The reaction was based on the ability of Complex I, in the presence of NADH, to pass electron to Complex III which, in turn, reduces oxidized cytochrome c. Rotenone, Complex I-specific inhibitor, was added and rotenone-sensitive activity was calculated.

2.8.1.2 Preparation and storage of stock solutions:

10 mM NADH stock solution was freshly prepared as described above (2.7.2 Assessment of malate dehydrogenase activity). 0.1 M Potassium cyanide (KCN) (207810; Sigma-Aldrich) stock solution was freshly prepared in 200 mM potassium phosphate buffer (pH 7.4). 2.5 mM Rotenone was freshly prepared in absolute ethanol (R8875; Sigma-Aldrich). The stock solution of oxidized cytochrome c (C2506; Sigma-Aldrich) was prepared in 10 mM potassium phosphate buffer (pH 7.4), aliquoted in tubes, and stored at -20°C.

2.8.1.3 Procedure:

To determine Complex I activity, samples were subjected to three cycles of freezing and thawing. The reaction buffer contained 20 mmol/L potassium phosphate buffer (pH 7.4), 100 µmol/L NADH, 1 mmol/L KCN, and 1-5 µg sample were pre-incubated for 3 minutes. Then, 100 µmol/L oxidized cytochrome c was

added. The reaction was followed at 550 nm for 5 minutes and for another 5 minutes after adding 25 µmol rotenone.

2.8.2 Assessment of Complex II-III activity:

2.8.2.1 Principle of the assay:

Complex II-III activity was measured as rotenone-sensitive succinate-cytochrome c reductase activity. In the presence of succinate, Complex II passes electron to Complex III which, in turn, reduces oxidized cytochrome c. In order to exclude any contribution from Complex I in this reaction, rotenone, Complex I-specific inhibitors, was added in the reaction mixture.

2.8.2.2 Preparation and storage of stock solutions:

Stock solutions of, oxidized cytochrome c, KCN and rotenone were prepared as described above (2.8.1 Assessment of Complex I activity). 1 M Succinate (Sigma-Aldrich S2378) stock solution was freshly prepared in distilled water.

2.8.2.3 Procedure:

To determine Complex II-III activity, samples were subjected to three freeze-thaw cycles. 50 mmol succinate, 1 mmol/L KCN, 25 µmol/L rotenone, and 1-5 µg sample were pre-incubated in 20 mM potassium phosphate buffer containing 0.01% BSA for 3 minutes. 100 µmol/L oxidized cytochrome c was added, and the increase in absorbance was followed at 550 nm for 5 minutes.

2.8.3 Assessment of Complex IV activity:

2.8.3.1 Principle of the assay:

Complex Ⅳ activity was measured as cytochrome c oxidase activity. The assay was based on the ability of Complex Ⅳ to oxidize the reduced cytochrome c.

3.8.3.2 Preparation of stock solution:

The stock solution of reduced cytochrome c was kindly prepared by Dr. Subir Roy Chowdhury. The stock solution was aliquoted in tubes and stored at -20°C.

2.8.3.3 Procedure:

To determine Complex Ⅳ activity, 1-5 µg samples were pre-incubated in 20 mM potassium phosphate buffer containing 0.05% lauryl maltoside for 10 minutes. Then, 40 µmol/L of reduced cytochrome c was added. The oxidation rate of the reduced cytochrome c was measured for 5 minutes.

2.9 Mitochondrial respiration assay:

Mitochondrial respiration in CVS-infected and mock-infected PC12 cells were assessed using OROBOROS Oxygraph-2k (OROBOROS instruments GmbH, Innsbruck, Austria) as previously described (Chowdhury *et al,* 2010).

2.9.1 Preparation and storage of stock solutions:

5 mg/ml digitonin (D-180-250; Gold Biotechnology, St. Louis, MO), 1 M puryvate (P2256; Sigma-Aldrich), 1 M ascorbate (A7631; Sigma-Aldrich), and 0.1 M N,N,N′,N′-Tetramethyl-p-phenylenediamine dihydrochloride (TMPD) (T3134; Sigma-Aldrich) stock solutions were freshly prepared in distilled water. 1 M malate stock solution was prepared by Dr. Subir Roy Chowdhury. 0.5 M adenosine 5′-diphosphate monopotassium salt dehydrate (ADP) (Sigma-Aldrich;

A5285) stock solution was prepared in distilled water containing 6.8% potassium hydroxide (KOH). The ADP stock solution was aliqouted in tubes and stored at –80°C. 50 mM FCCP (ab120081; Abcam) stock solution was prepared in absolute ethanol, aliqouted in tubes, and stored at –80°C. 2 mM antimycin A (A8674; Sigma-Aldrich) and 5 mM oligomycin (O4876; Sigma-Aldrich) stock solutions were prepared in absolute ethanol, aliqouted in tubes, and stored at –20°C. 0.1 M KCN was freshly prepared in 200 mM potassium phosphate buffer (pH 7.4).

2.9.2 Principle and procedure:

At 72 hrs post-infection, the cells were harvested and washed with phosphate buffer saline. The cells were counted and $2x10^6$ cells were added to each chamber of OROBOROS Oxygraph-2k in a total volume of 2 ml. The respiration media contained 80 mmol/l potassium chloride (KCl), 10 mmol/l Tris-HCl (T5941; Sigma-Aldrich), 3 mmol/l MgCl2 (M-33-500; Fisher Scientific, Fair Lawn, NJ), 1 mmol/l EDTA (BP120-500; Fisher Scientific), 5 mmol/l potassium phosphate (pH 7.4). Because whole cell lysates rather than isolated mitochondria were used, digitonin was added after addition of the cells for permeabilization. Digitonin permeabilizes the plasma membrane of the cells whereas the mitochondrial membrane remains intact. 10 mmol/l pyruvate and 5 mmol/l malate (M7397; Sigma-Aldrich) were added in order to start the basal respiration. This step was followed by the addition of 2 mmol/l ADP to start the coupled respiration. After inhibiting the coupled respiration with 1 µmol/l oligomycin, an ATP synthase inhibitor, the coupled respiration was measured as oligomycin-sensitive respiration whereas oligomycin-insensitive respiration determined the

leak respiration of the cells. Addition of oligomycin blocks reverse proton pumping through ATP synthase. FCCP was titrated and 0.25 µmol/l was found to induce maximum uncoupling of the mitochondria. FCCP catalyzes the proton transfer to the matrix and, thus, abolishes the mitochondrial membrane potential. 0.25 µmol/l FCCP was added to initiate the uncoupled respiration followed by the addition of 1 µg/ml antimycin A. Uncoupled respiration was calculated as an antimyicn-sensitive FCCP-induce respiration. Then, Complex IV respiration was induced by the addition of 5 mmol/l ascorbate and 0.5 mmol/l TMPD. 0.25 mmol/l of KCN, a Complex IV-specific inhibitor, was added and Complex IV respiration rate was measured as a KCN-sensitive ascorbate and TMPD-induced respiration. The rate of oxygen consumption was determined using OROBOROS DatLab software.

2.10 Measurement of NAD+, NADH, NADH/NAD+ ratio:

2.10.1 Principle of the assay:

NAD+ and NADH levels were determined by EnzyChromTM NAD+/NADH Assay Kit (ECND-100; Bioassay System, Hayward, CA) in mock-infected and CVS-infected PC12 cells at 72 hr post infection. The reaction was based on the ability of NADH to reduce tetrazolium dye (MTT) through alcohol dehydrogenase-based reaction.

2.10.2 Procedure:

According to the manufacturer's instructions, $1x10^5$ cells from mock-infected and CVS-infected groups were incubated with either 100 µl NAD+ or NADH buffer for NAD+ or NADH extraction, respectively. Samples were heated

at 60°C for 5 min before adding 20 µl assay buffer. Then, the extracts were neutralized by adding 100 µl of the opposite extraction buffer. After 5 min centrifugation, 40 µl of the supernatant were used for each assay. 80 µl of the working solution containing 50 µL assay Buffer, 1 µL enzyme, 10 µL 1v% Ethanol, 14 µL phenazine methosulfate (PMS) and 14 µL MTT was added to each sample and incubated for 15 min. The reduction of MTT color was measured at 565nm. NAD+ and NADH concentration were determined from a standard curve prepared using the standard solution provided with the kit. Then, NADH/NAD+ ratio was calculated.

2.11 Detection of ATP levels:

2.11.1 Principle of the assay:

The ATP levels were determined using ATP Colorimetric/Fluorometric Assay Kit (K354-100; Biovision, Mountain View, CA) in mock-infected and CVS-infected PC12 and MNA cells at 72 hr post infection. This assay was based on glycerol phosphorylation and the level of ATP can be detected by both colorimetric and fluorometric methods.

2.11.2 Procedure:

According to the manufacturer's instructions, 100 µl of ATP extraction buffer were added to $1X10^6$ cells from mock-infected and CVS-infected samples. Then, samples were homogenized in perchloric acid followed by a neutralization step using deproteinizing sample preparation kit (K808-200; Biovision). After 2 min centrifugation, supernatants were collected and used for the assay. 50 µl of reaction mix containing 44 µl ATP assay buffer, 2 µl ATP probe, 2 µl ATP

converter, and 2 µl developer mix were added to each sample. After 30 minute incubation in dark, optical densities were read at 570 nm using SpectraMax Plus384 spectrophotometer. The intracellular ATP level was determined from a standard curve prepared using the ATP standard solution provided with the kit.

2.12 Assessment of mitochondrial membrane potential:

2.12.1 Principle of the assay:

The mitochondrial membrane potentials were determined using tetramethylrhodamine ethyl ester (TMRE) Mitochondrial Membrane Potential Assay Kit (113852; Abcam, Toronto, Canada) in mock-infected and CVS-infected PC12 and MNA cells at 72 hr post infection. This kit is based on the ability of TMRE, a positively-charged dye, to stain actively respiring mitochondria, negatively-charged organelles. While depolarized or inactive mitochondria fail to retain TMRE, hyperpolarized or active respiring mitochondria are able to sequester TMRE. Fluorescence intensity distinguishes between depolarized, normal, and hyperpolarized mitochondria. TMRE is the least toxic dye among the most widely used ones (e.g., Rhodamine 123). Redistribution of the dye across the plasma membrane is quite fast. It can function in both matrix quench and matrix non-quench modes although TMRE is a common choice for the non-quench mode. Quench mode occurs when the concentration of the dye in the matrix reaches a certain threshold where further dye accumulation does not affect the intensity of fluorescent signal. Depolarization of mitochondria in quench mode leads to a transient increase in the whole cell fluorescent signal due to the dye redistribution across the plasma membrane. In non-quench mode, the dye

concentration accumulated in the matrix should be adequately below the threshold concentration. In this mode, depolarization of the mitochondria is mirrored by a decrease in whole cell fluorescent signal. Quench mode is usually applied to determine a rapid change in the mitochondrial membrane potential whereas non-quench is applied to assess pre-existing values.

2.12.2 Optimization and validation of the assay:

In this study, the dye functions in non-quench mode and TMRE was titrated (5-100 nM) to determine the lowest concentration that gave a reasonable signal. 25 nM was chosen as the optimum concentration. Carbonylcyanide p-trifluoromethoxyphenylhydrazone (FCCP) is a mitochondrial uncoupler that specifically collapses the mitochondrial membrane potential by facilitating proton transfer into the mitochondrial matrix. Hence, FCCP was used to induce mitochondrial depolarization. The lack of increase in whole cell fluorescent signal after the addition of 1 µM FCCP further confirms that the dye functions in non-quench mode.

2.12.3 Procedure:

At 72 hrs post-infection, $2X10^5$ cells of mock-infected and CVS-infected samples were loaded with 25 nM TMRE, and incubated for 30 minutes in the dark at 37°C. Just before washing out TMRE-containing media, 1 µM FCCP, mitochondrial uncoupler, was added to some samples. FCCP-treated cells were used as controls in this experiment. The media was then washed out in order to eliminate background interference. Using fluorescence microplate reader, the fluorescence intensity was determined at excitation 549 nm and emission 575nm.

2.13 Assessment of hydrogen peroxide production:

The rate of hydrogen peroxide production was determined in MNA cells at 72 hrs post-infection using the Amplex Red Hydrogen Peroxide/Peroxidase Assay kit (Invitrogen A22188).

2.13.1 Principle:

The assay is based on the ability of Amplex Red reagent (10-acetyl-3,7-dihydroxyphenoxazine) in the presence of horseradish peroxidase (HPR) to detect the rate of H_2O_2 production from the cells.

2.13.2 Procedure:

At 72 hrs post-infection, 1 X 10^4 cells of mock-infected and CVS-infected cells were added per well of 96-well plate. The cells were allowed to attach for 2 hrs at 37°C in humidified air containing 5% CO2. Media was removed and 50 µl of 1X reaction buffer containing digitonin and 10 mmol/l succinate were added to each well. Then, 50 µl of working solution containing 100 µM Amplex Red reagent and 0.2 U/ml HRP was added to each well. The reaction was followed for 2 hrs at excitation/emission 530/590 nm using a fluorescence microplate reader.

2.14 Statistical analysis:

Standard two-tailed Student's t-test was used to determine the significance of the difference between the means of mock-infected and CVS-infected cells. The difference was indicated as statistically significant when $p < 0.05$.

3. Results:

3.1 PC12 cells viability assay:

No significant difference in the cell viability was observed between mock-infected and CVS-infected cells at 72 hrs post infection. The percentage of viable cells was 99.8 ± 0.2% in mock-infected cells versus 99.5 ± 0.3% in CVS-infected cells (p=0.410). Results were obtained from 3 independent experiments performed in duplicate, and expressed as mean ± the standard error of the mean (SEM).

3.2 Western blotting analysis for 4-HNE expression in PC12 cells:

In comparison with mock-infected cells, CVS infection significantly increased 4-HNE expression by approximately 2-fold (p=0.003) at 72 hrs post-infection (Figure 9). Results were obtained from duplicate samples from one experiment, and, are expressed as mean ± SEM.

3.3 Krebs cycle enzyme activities:

3.3.1 Citrate synthase activity:

No significant difference was found in the activities of citrate synthase enzyme between mock infected and CVS-infected DRG (p=0.690), PC12 (p=0.465), MNA (p=0.963), and BHK-S13 (p=0.307) cells (Figure 10). For DRG, results were obtained from duplicate samples from one experiment. For PC12, MNA, and BHK-S13, results were obtained from duplicate samples from 2 or 3 independent experiments. Results are expressed as mean ± SEM.

3.3.2 Malate dehydrogenase activity:

No significant difference was found in the activities of malate dehydrogenase enzyme between mock infected and CVS-infected PC12 (p=0.119), MNA (p=0.366), and BHK-S13 (p=0.217) cells (Figure 11). Results were obtained from duplicate samples from 2 or 3 independent experiments. Results are expressed as mean ± SEM.

3.4 Electron transport chain Complex activities:

3.4.1 Complex I activity:

Complex I activity was significantly upregulated in all types of CVS-infected cells. In comparison with mock-infected cells, the activity in CVS-infected DRG neurons, PC12, MNA, and BHK-S13 cells was increased by 34.6% (p=0.009), 38.8% (p=0.042), 64.4% (p=0.001), and 75.0% (p=0.0001), respectively (Figure 12). For DRG, results were obtained from duplicate samples from one experiment. For PC12, MNA, and BHK-S13, results were obtained from duplicate samples from 2 or 3 independent experiments. Results are expressed as mean ± SEM.

3.4.2 Complex II-III activity:

Measurement of Complex II-III activity did not reveal a significant difference between mock-infected and CVS-infected DRG (p=0.212), PC12 (p=0.142), MNA (P=0.093), and BHK-S13 (p=0.203) cells (Figure 13). For DRG, results were obtained from duplicate samples from one experiment. For PC12, MNA, and BHK-S13, results were obtained from duplicate or triplicate samples from 2 or 3 independent experiments. Results are expressed as mean ± SEM.

3.4.3 Complex IV activity:

Complex IV activity was significantly increased in all type of CVS-infected cells. The activity was increased by 29.2% (p=0.004) in DRG neurons, 29.3% (p=0.004) in PC12, 33.8% (p=0.017) in MNA, and 43.7% (p=0.007) in BHK-S13 cells (Figure 14). For DRG, results were obtained from duplicate samples from one experiment. For PC12, MNA, and BHK-S13, results were obtained from duplicate or triplicate samples from 2 or 3 independent experiments. Results are expressed as mean ± SEM.

3.5 Mitochondrial respiration:

Several respiratory states have been assessed in mock-infected and CVS-infected PC12 cells (Figure 15). The leak respiration and OXPHOS capacity were not different in mock and CVS-infected cells (p=0.847 and p=0.868, respectively). On the other hand, both ETC capacity and Complex IV respiration were significantly enhanced by 33.4% (p=0.018) and 49.1% (p=0.027), respectively, in the CVS-infected cells in comparison with mock-infected cells (Figure 16). Results were obtained from duplicate samples from 3 independent samples, and are expressed as mean ± SEM.

3.6 NAD+ levels, NADH levels, and NADH/NAD+ ratios:

At 72 hrs post-infection, CVS infection did not significantly affect the NAD+ level (p=0.901) (Figure 17a). The NADH level was significantly higher by 42.6% (p=0.043) in CVS infected PC12 cells than in mock-infected cells (Figure 17b). NADH/NAD+ ratio in CVS-infected cells was increased by 36.8% (p=0.018) in comparison with mock-infected cells (Figure 17c). Results were obtained from

duplicate samples from 3 independent experiments, and are expressed as mean ± SEM.

3.7 Intracellular ATP levels:

The intracellular ATP levels of CVS-infected cells were significantly lower than the intracellular ATP level in mock-infected cells at 72 hrs post-infection. In CVS-infected PC12 cells, the ATP level was lower by 26.7% (p=0.0022), whereas it was decreased by 36.5% (p=0.0004) in CVS-infected MNA cells (Figure 18). Results were obtained from duplicate or triplicate samples from 3 independent experiments, and are expressed as mean ± SEM.

3.8 Mitochondrial membrane potential:

The mitochondrial membrane potential was significantly enhanced in CVS-infected cells in comparison with mock-infected cells at 72 hrs post-infection. In comparison with mock-infected cells, the mitochondrial membrane potential was enhanced by 27.9% (p=0.0.033) and 42.9% (p=0.009) in CVS-infected PC12 and MNA cells, respectively. In the presence of FCCP, no significant change was observed in CVS-infected PC12 (p=0.189) and MNA (p=0.459) cells (Figure 19). Results were obtained from duplicate or triplicate samples from 3 independent experiments, and are expressed as mean ± SEM.

3.9 Hydrogen peroxide production:

The rate of succinate driven-hydrogen peroxide production was increased in CVS-infected cells by 51.4% (p=0.0167) in comparison with mock-infected cells (Figure 20). Results were obtained from duplicate samples from 2 independent experiments and are expressed as mean ± SEM.

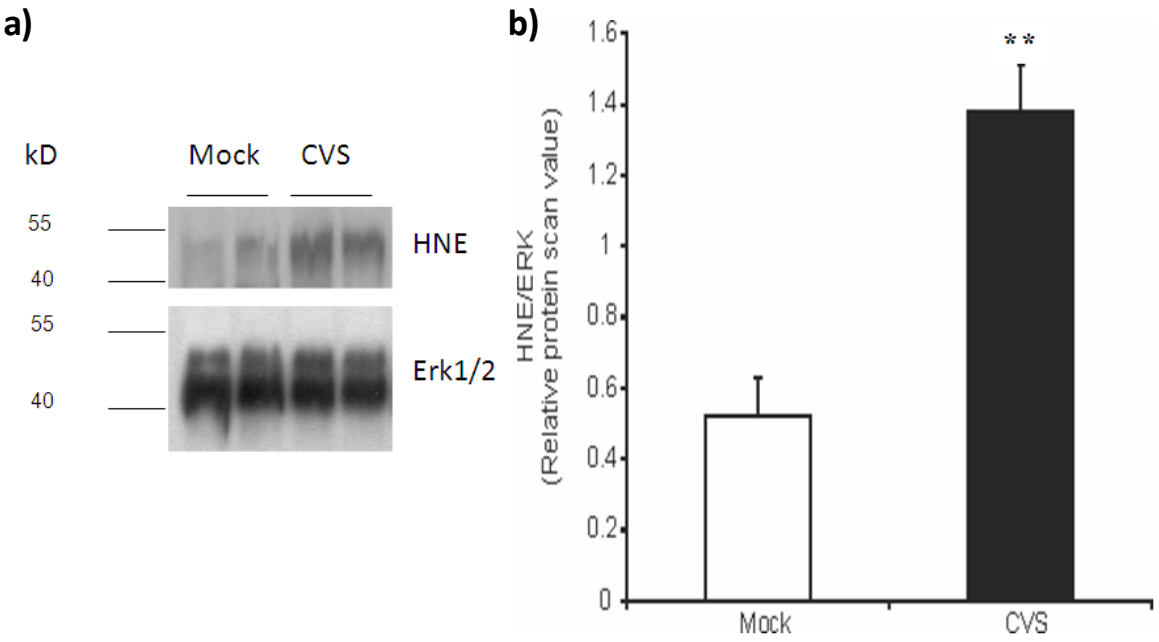

Figure 9: Enhanced 4-HNE expression in CVS-infected PC12 cells at 72 hrs post-infection. a) Western blot of mock-infected and CVS-infected PC12 cells at 72 hrs post-infection. Cell protein lysates were loaded on 10% SDS-PAGE gel. b) Relative scan value show approximately 3-fold increase in 4-HNE expression (P=0.003) in CVS-infected cells versus mock-infected cells. Results were obtained from duplicate samples from one experiment, and, are expressed as mean ± SEM (from Kammouni and Jackson with permission).

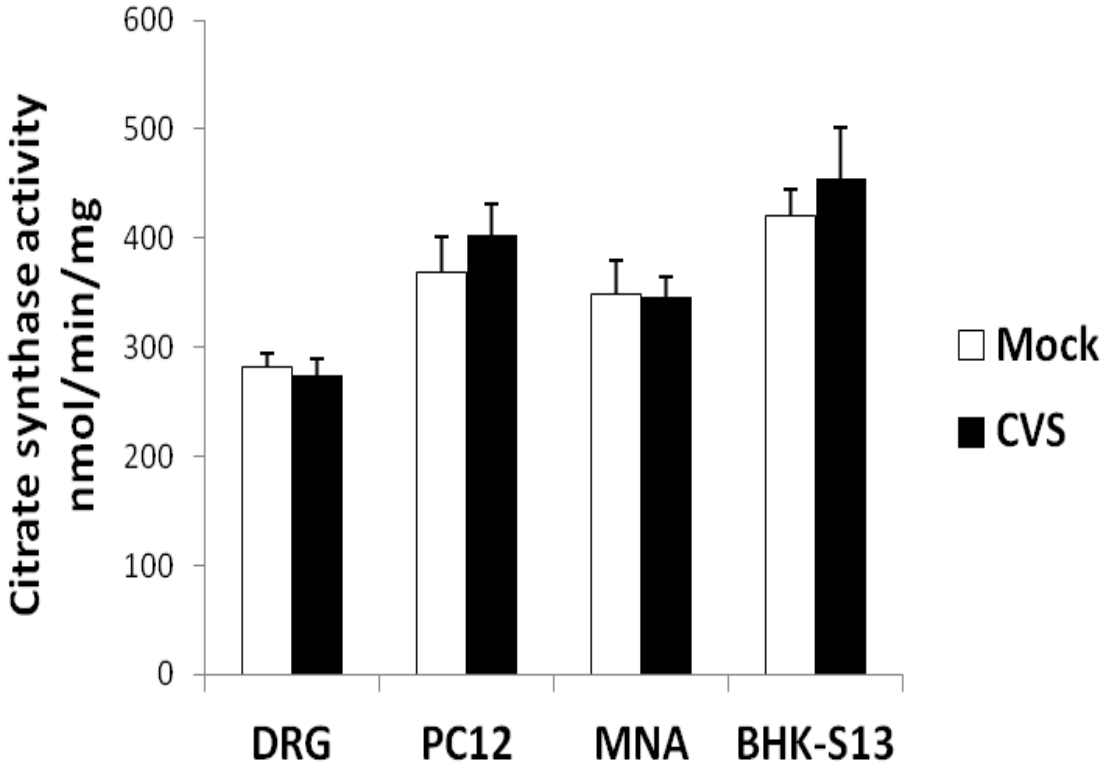

Figure 10: CVS infection did not alter citrate synthase activity at 72 hrs post-infection. No significant difference was observed in CVS-infected DRG (p=0.690), PC12 (p=0.465), MNA (p=0.963), and BHK-S13 (p=0.307) in comparison with mock-infected controls. For DRG, results were obtained from duplicate samples from one experiment. For PC12, MNA, and BHK-S13, results were obtained from duplicate samples from 2 or 3 independent experiments. Results are expressed as mean ± SEM.

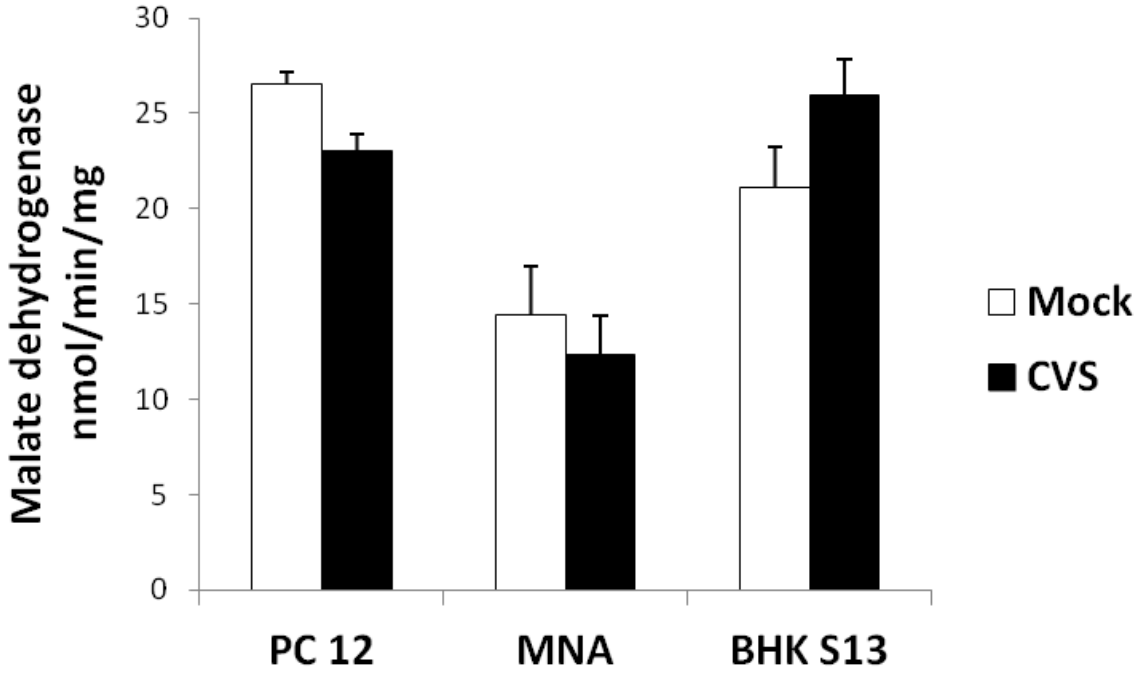

Figure 11: CVS did not affect malate dehydrogenase activity at 72 hrs post-infection. No significant difference was observed in CVS-infected PC12 (p=0.119), MNA (p=0.366), and BHK-S13 (p=0.217) in comparison with mock-infected controls. Results were obtained from duplicate samples from 2 or 3 independent experiments. Results are expressed as mean ± SEM.

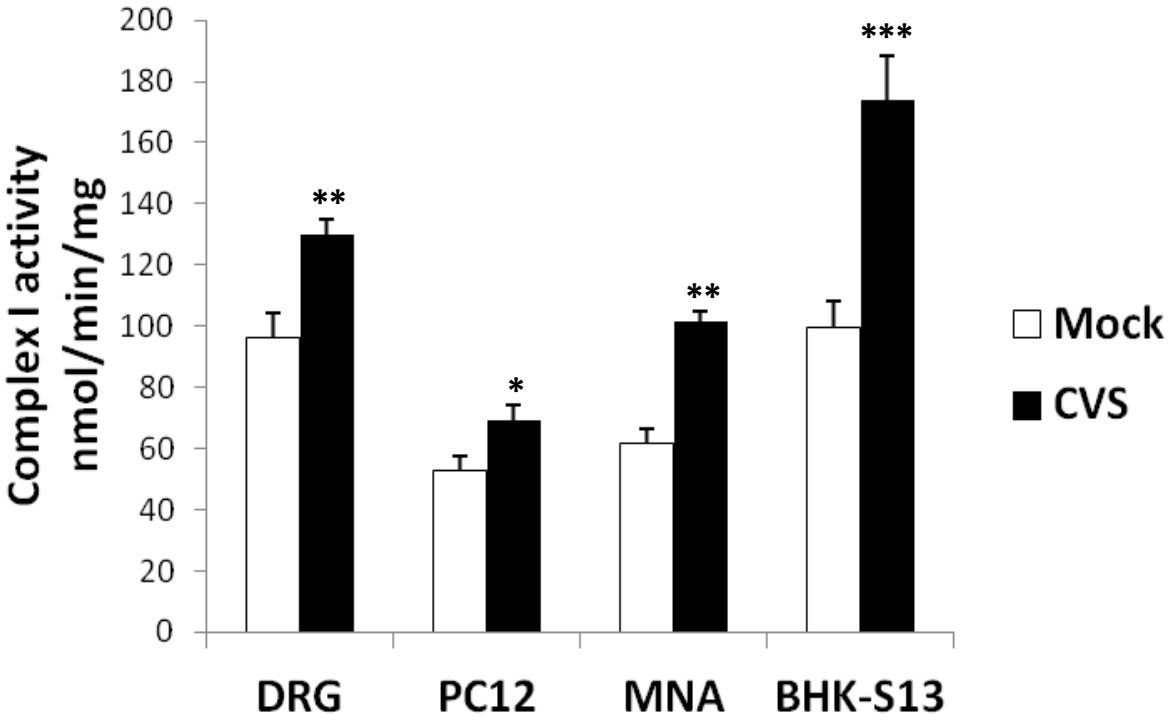

Figure 12: CVS infection upregulated Complex I activity at 72 hrs post-infection. In comparison with mock-infected cells, the activity in CVS-infected DRG neurons, PC12, MNA, and BHK-S13 cells was increased by 34.6% (p=0.009), 38.8% (p=0.042), 64.4% (p=0.001), and 75.0% (p=0.0001), respectively. For DRG, results were obtained from duplicate samples from one experiment. For PC12, MNA, and BHK-S13, results were obtained from duplicate samples from 2 or 3 independent experiments. Results are expressed as mean ± SEM. (* means $p < 0.05$, ** means $p < 0.01$, *** means $p < 0.001$).

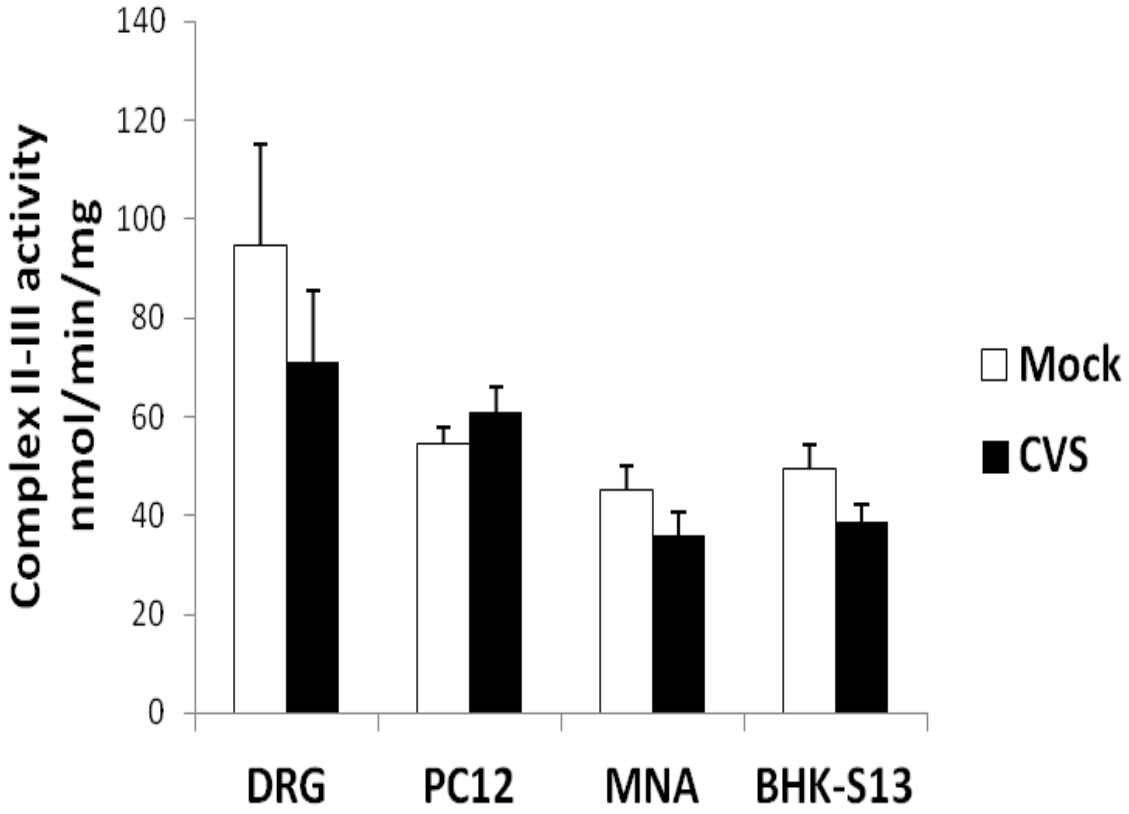

Figure 13: CVS infection did not change Complex II-III activity. No significant difference was observed in CVS-infected DRG (p=0.212), PC12 (p=0.142), MNA (p=0.093), and BHK-S13 (p=0.203) in comparison with mock-infected controls. For DRG, results were obtained from duplicate samples from one experiment. For PC12, MNA, and BHK-S13, results were obtained from duplicate or triplicate samples from 2 or 3 independent experiments. Results are expressed as mean ± SEM.

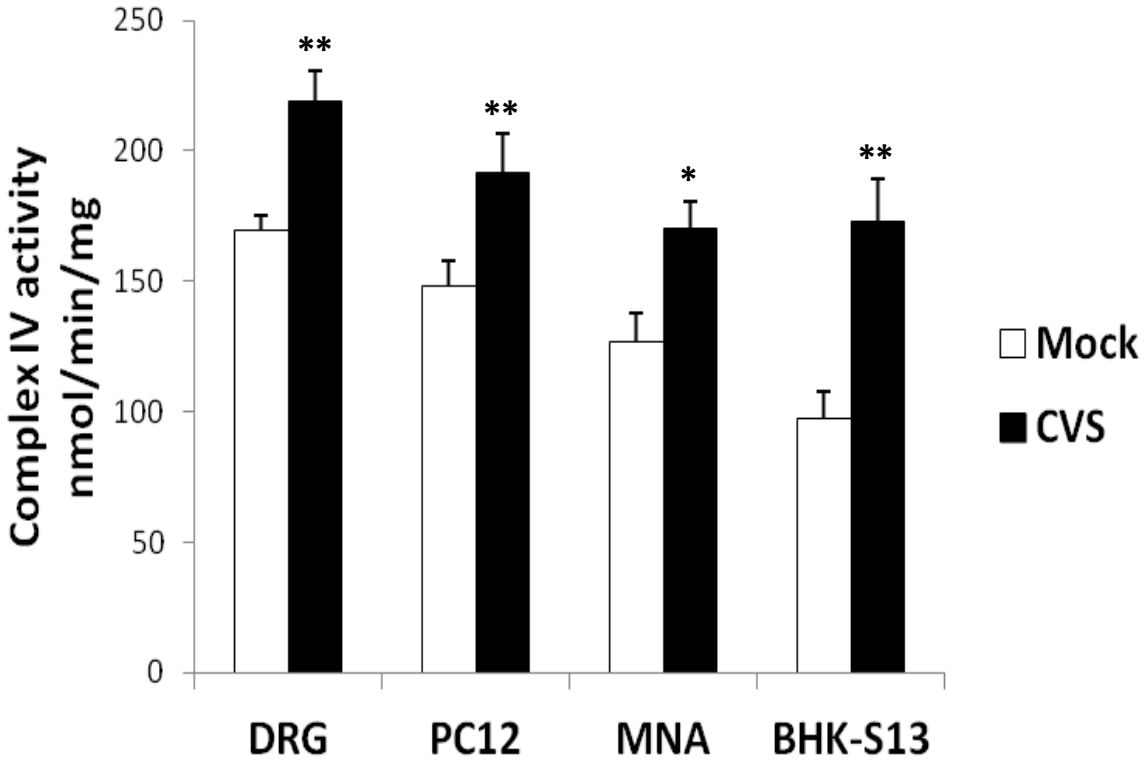

Figure 14: CVS infection upregulated Complex IV activity. In comparison with mock infected cells, the activity was increased by 29.2% (p=0.004) in DRG neurons, 29.3% (p=0.004) in PC12, 33.8% (p=0.017) in MNA, and 43.7% (p=0.007) in BHK-S13 cells. For DRG, results were obtained from duplicate samples from one experiment. For PC12, MNA, and BHK-S13, results were obtained from duplicate or triplicate samples from 2 or 3 independent experiments. Results are expressed as mean ± SEM. (* means $p < 0.05$, ** means $p < 0.01$)

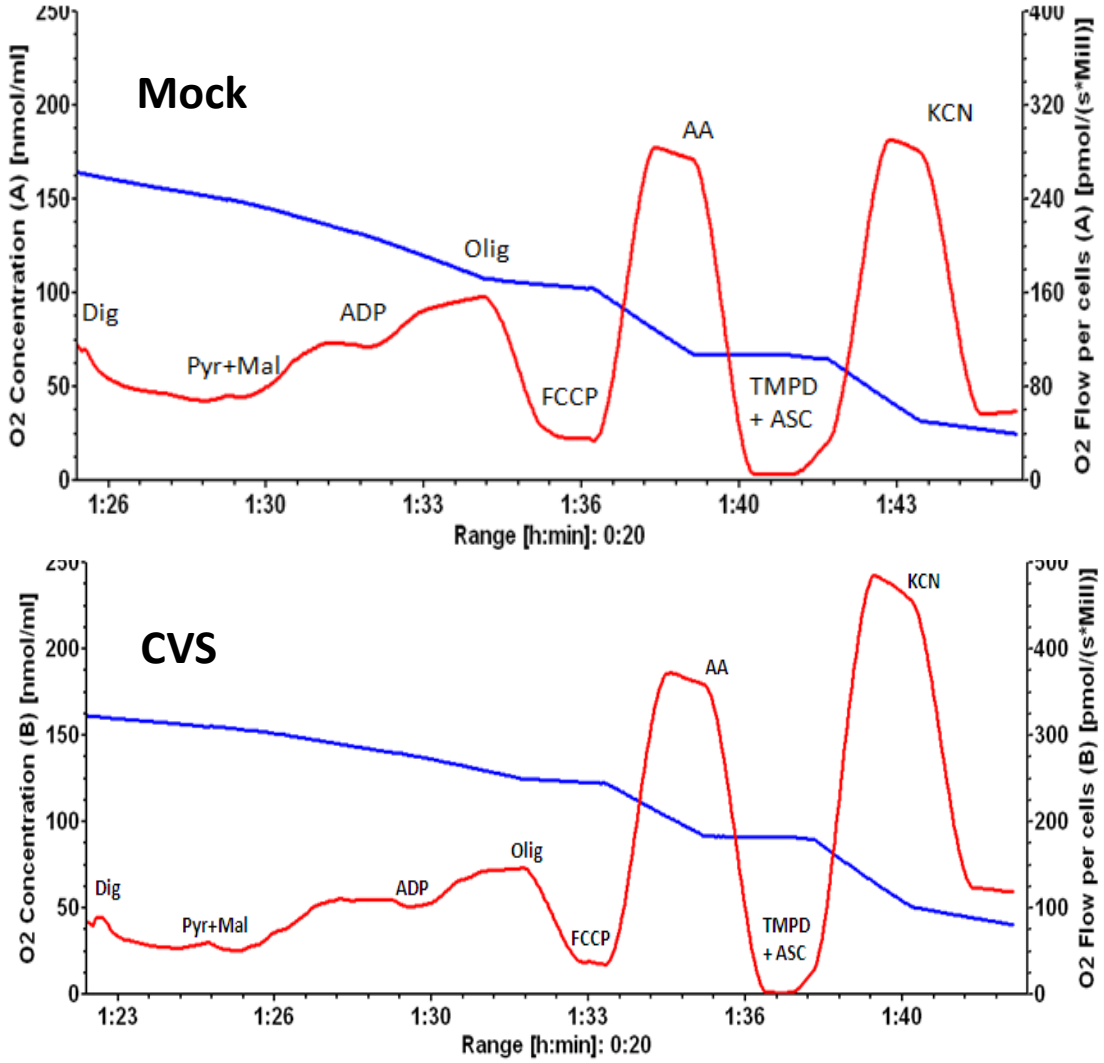

Figure 15: Mitochondrial respiration of Mock-infected and CVS-infected PC12 cells at 72 hrs post-infection. Several substrates and inhibitors were added as indicated in order to assess various mitochondrial respiration states. Blue lines show the oxygen level in the chamber of electrode and expressed in nmol/ml. Red lines show oxygen flow per million cells (pmol O_2/(s*Mill) cell). Digitonin (Dig) was added to induce permeabilization in the cells. Pyruvate (Pyr), malate (Mal), and adenosine diphosphate (ADP) were added to initiate coupled respiration. Then, oligomycin (Olig) was added to inhibit the phosphorylation system. Oxidative phosphorylation capacity was measured as oligomycin-sensitive coupled respiration. Oligomycin-insensitive respiration represented the leak respiration. FCCP was added to initiate uncoupled respiration. Antimycin A (AA) was added to inhibit the uncoupled respiration. Electron transport chain capacity was determined as Antimycin A-sensitive uncoupled-respiration. Complex IV respiration was induced by Ascorbate (Asc) and (TMPD). KCN was added to inhibit Complex IV respiration. Complex IV rate was determined as KCN-sensitive ascorbate + TMPD-induced respiration.

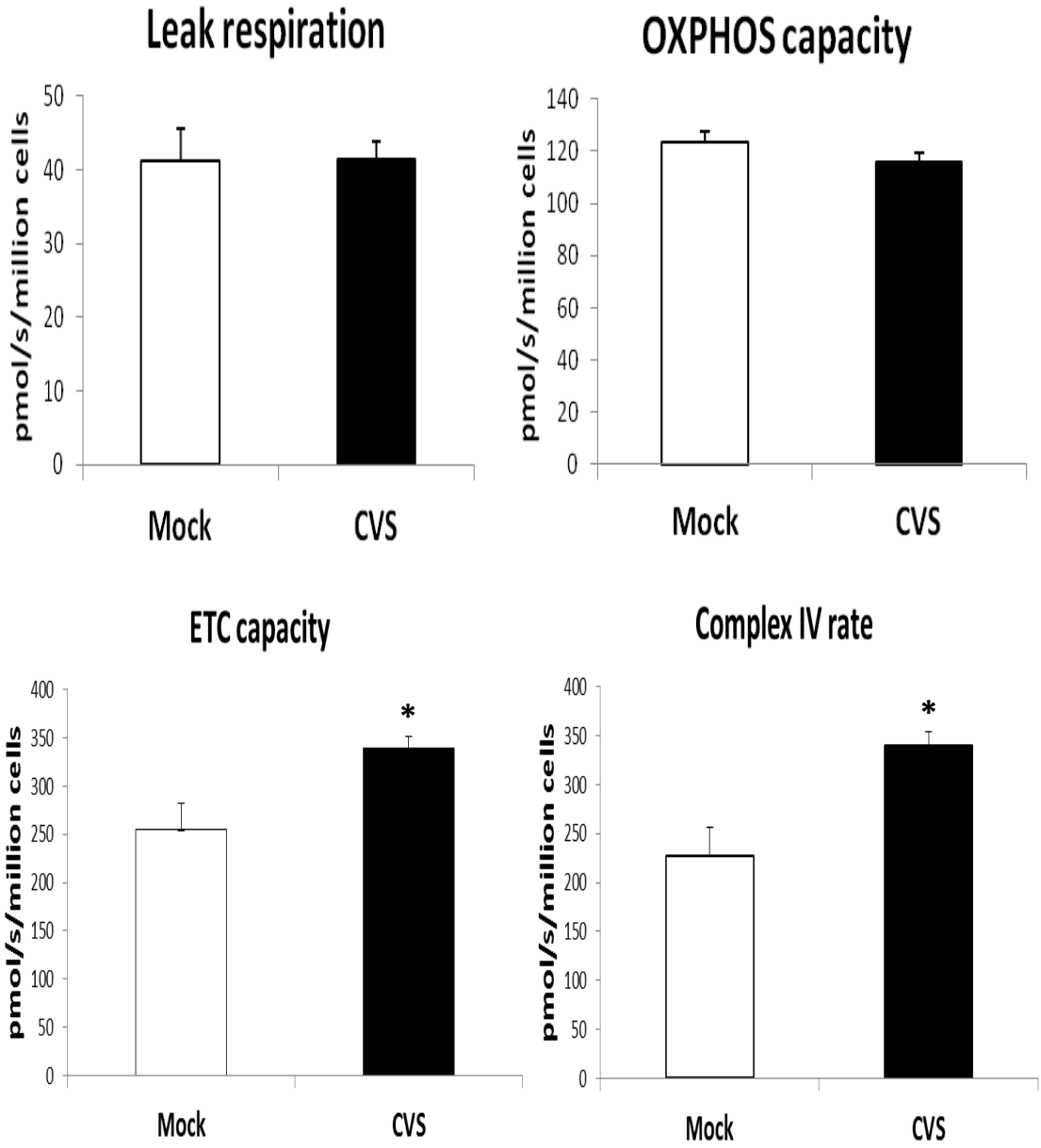

Figure 16: CVS infection enhanced ETC capacity and Complex IV respiration in PC12 cells at 72 hrs post-infection. No significant changes were observed in leak respiration ($p=0.847$) and OXPHOS capacity ($p=0.868$) in CVS-infected cells. ETC capacity was enhanced by 33.4% ($p=0.018$) and Complex IV respiration rate was increased by 49% ($p=0.027$). Results were obtained from duplicate samples from 3 independent samples, and are expressed as mean ± SEM. (* means $p < 0.05$).

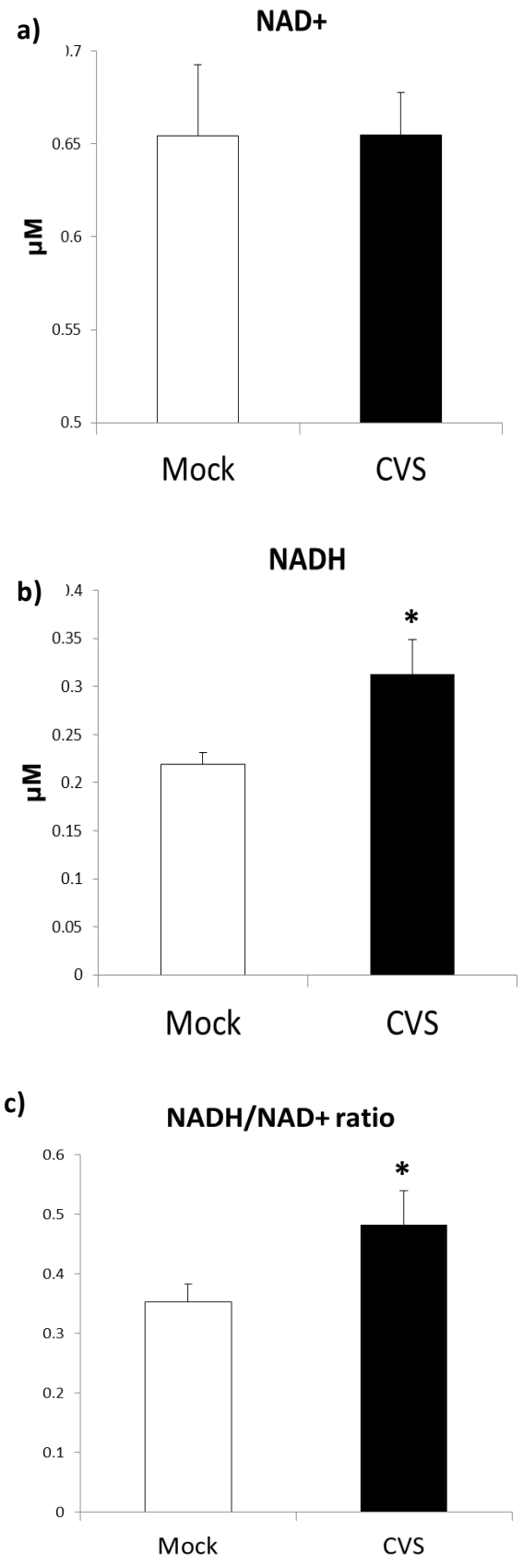

Figure 17: Increased NADH levels, and NADH/NAD+ ratio in CVS-infected PC12 cells. a) There was no significant difference in the NAD+ level (p= 0.901) in mock-infected versus CVS-infected cells at 72 hrs post-infection. B) NADH level was significantly increased by 42.6% (p= 0.043) in CVS-infected cells versus mock-infected cells at 72 hrs post-infection. C) NADH/NAD+ ratio was was significantly increased by 36.0% (p=0.018) in CVS-infected cells versus mock-infected cells at 72 hrs post-infection. Results were obtained from duplicate samples from 3 independent experiments, and are expressed as mean ± SEM. (* means $p < 0.05$).

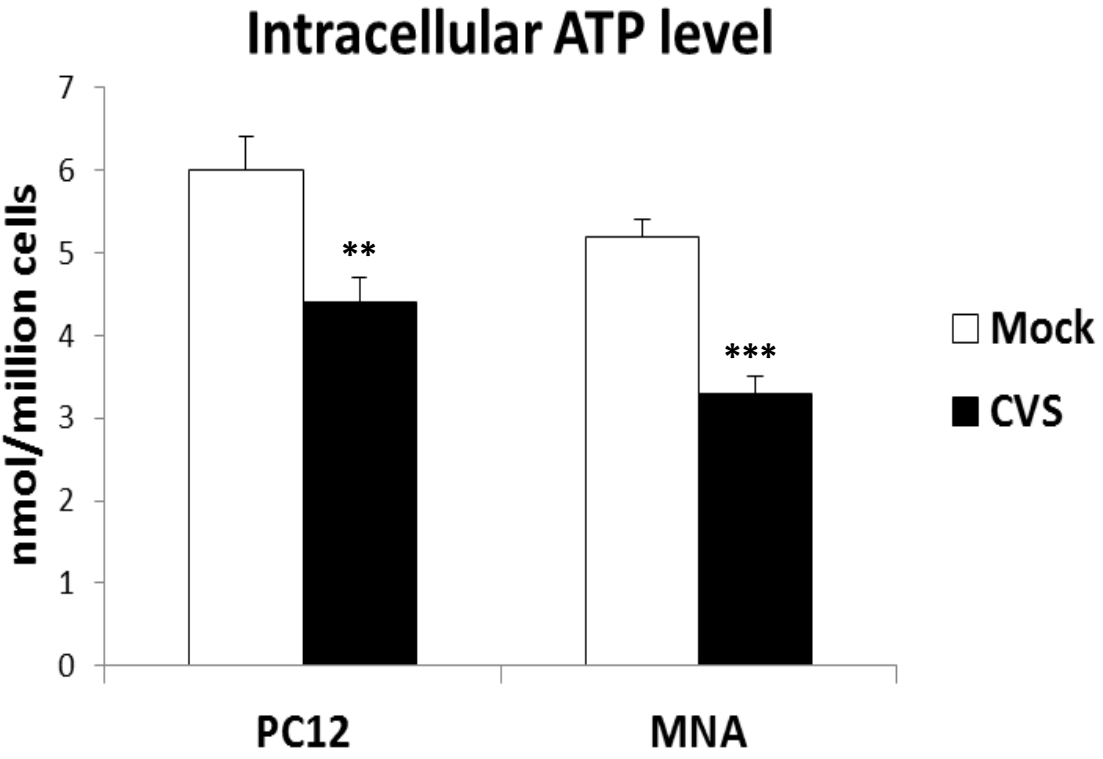

Figure 18: Reduced level of intracellular ATP in CVS-infected cells at 72 hrs post-infection. Intracellular ATP level was significantly reduced in CVS-infected PC12 and MNA cells by 26.7% (p=0.0022) and 36.5% (p=0.0004), respectively versus mock-infected cells. Results were obtained from duplicate or triplicate samples from 3 independent experiments, and are expressed as mean ± SEM. (** means $p < 0.01$, *** means $p < 0.001$)

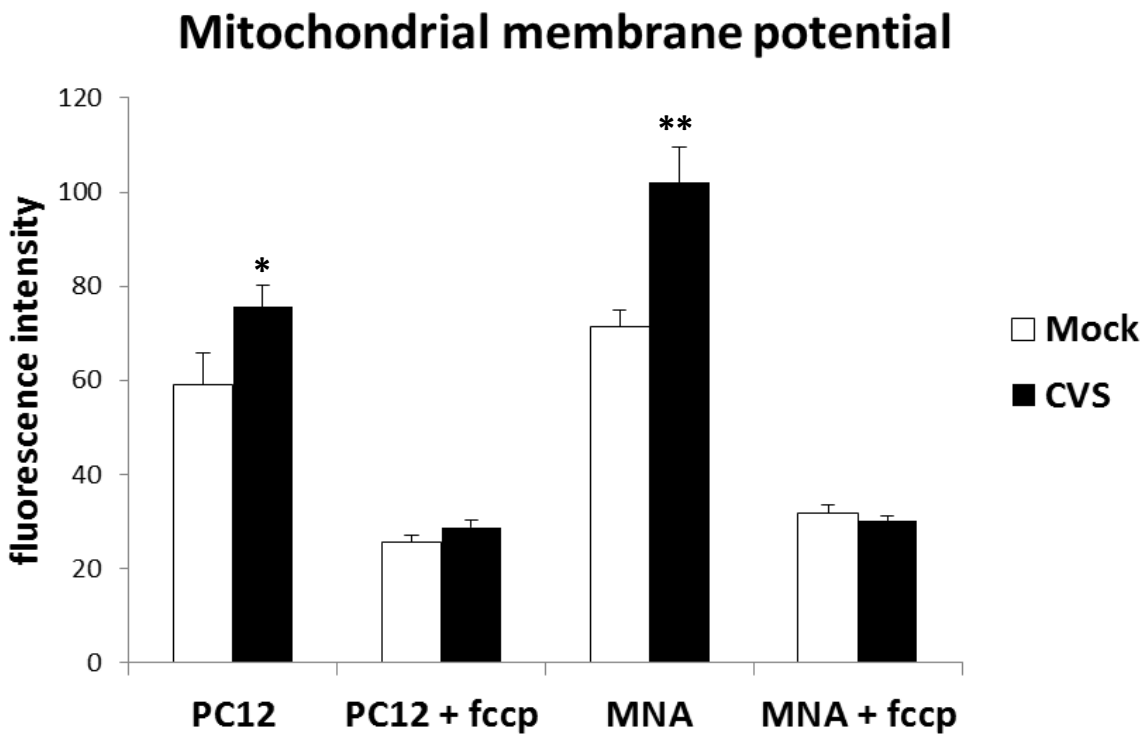

Figure 19: Increased mitochondrial membrane potential in CVS-infected cells at 72 hrs post-infection. CVS infection induced mitochondrial membrane potential in the infected PC12 and MNA cells versus mock-infected cells by 27.9% (p=0.0.033) and 42.9% (p=0.009), respectively. Results were obtained from duplicate or triplicate samples from 3 independent experiments, and are expressed as mean ± SEM. (* means $p < 0.05$, ** means $p < 0.01$)

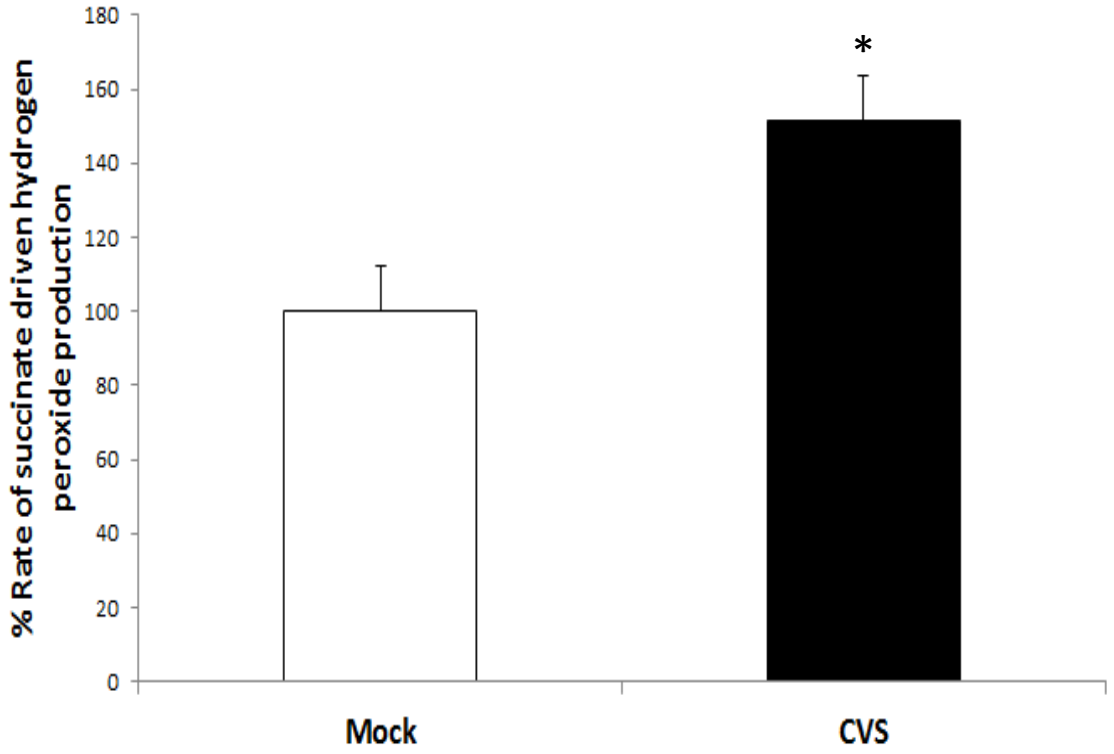

Figure 20: Increased succinate-driven hydrogen peroxide production in CVS-infected MNA cells at 72 hrs post-infection. Hydrogen peroxide production was significantly higher in CVS-infected cells by 51.4% ($p=0.0167$) versus mock-infected cells. Results were obtained from duplicate samples from 2 independent experiments, and are expressed as percentage of rate relative to that for mock-infected cells. (* means $p < 0.05$)

4. Discussion:

The mechanisms by which rabies virus infection induces neurodegeneration remain elusive. Accumulating evidence suggests that rabies virus induces neuronal dysfunction in the infected cells. Jackson *et al. (*2010) and Kammouni *et al.* (2012) demonstrated that CVS infection induced axonal swellings associated with 4-HNE staining in adult rodent DRG primary neurons. 4-HNE is a toxic component produced by lipid peroxidation, a downstream process of oxidative stress. Quantitative analysis indicated that adducts of 4-HNE expression were significantly enhanced in CVS-infected DRG neurons versus mock-infected controls. Therefore, it was concluded that oxidative stress plays a critical role in CVS-induced morphological abnormalities in the neuronal processes. Here we show that 4-HNE expression was also enhanced in CVS-infected PC12 in comparison with mock-infected cells. The role of mitochondria in inducing oxidative stress in a variety of infectious and non-infectious neurological disorders is well recognized (Uttar et al., 2009, Schwarz, 1996). Several sites within mitochondria have been identified as ROS generators (Murphy, 2009). Mitochondrial DNA, which plays an important role in the synthesis of numerous mitochondrial and non-mitochondrial proteins, is believed to be vulnerable to ROS (Murphy, 2009). Moreover, the exogenous treatment of DRG primary neurons with 4-HNE greatly alters several mitochondrial parameters (Akude et al, 2010). In CVS-infected DRG neurons, active respiring mitochondria were localized at the sites of 4-HNE-labelled axonal swelling (Jackson *et al.,* 2010). Accumulation of swollen mitochondria at the site of axonal

swellings was also observed in CVS-infected axons of transgenic mice that express yellow fluorescence protein (Scott *et al.,* 2008). Here we have investigated the effects of rabies virus infection on several mitochondrial parameters, and have linked these alterations to the oxidative stress induction.

Four different cell types: DRG, NGF-treated PC12, MNA, and BHK-S13 cells (primary neurons, differentiated neuronal cell lines, non-differentiated neuronal cell lines, and non-neuronal cell lines, respectively) were initially studied. The susceptibility of these cells to rabies virus infection is variable. Approximately 29-52% of PC12 and DRG neurons were infected at 72 hr post-infection whereas up to 100% of BHK and MNA cells are infected by 24 hr post-infection (Jackson *et al.,* 2010 and Thoulouze *et al.,* 1998). This variability has been explained, at least in part, by the expression of neuronal cell adhesion molecule (NCAM), which acts as a rabies virus receptor, on these cells (Thoulouze *et al.,* 1998). CVS infection did not affect the viability of PC12 cells as determined by trypan blue exclusion test. Similar findings were previously observed in CVS-infected mouse DRG primary neurons, and MNA cells (Jackson *et al.,* 2010 and Gholami *et al.,* 2008).

The Krebs cycle is one of the most important mitochondrial pathways. The protein structure of Krebs cycle enzymes involves both nuclear-encoded and mitochondrial-encoded subunits. It was shown that the presence of ROS, in particular superoxide anions, inhibits the activity of citrate synthase and induces mitochondrial swelling in isolated mitochondria from rat brain (Galindo *et al.,* 2003). Similarly, oxidative stress downregulates the activity of several Krebs

cycle enzymes (i.e., citrate synthase, malate dehydrogenase, and aconitase) in myocardial tissues (Sharma *et al.,* 2007). Hence, we evaluated the effect of CVS infection on citrate synthase and malate dehydrogenase activities. In our studies, citrate synthase and malate dehydrogenase activities remained normal in all types of CVS-infected cells at 72 hrs post-infection. Krebs cycle enzyme activities in particular and mitochondrial function as a whole can be affected by the presence of superoxide anions, which are membrane-impermeable components, in the mitochondrial matrix. Yet, overexpression of antioxidant enzymes can prevent such damage. Kammouni *et al. (*2012) showed that the expression of mitochondrial superoxide dismutase is increased in CVS-infected DRG neurons. This antioxidant enzyme dismutates superoxide to hydrogen peroxide, a membrane-permeable component that can diffuse through mitochondrial membranes to the cell cytoplasm and, thereby, not affect the Krebs cycle enzymes. Therefore, the normal activities of citrate synthase and malate dehydrogenase in CVS-infected cells can be explained, at least in part, by the overexpression of superoxide dismutase.

The ETC is another important pathway that takes place in the mitochondria. Different sites within ETC Complexes have been reported to be involved in ROS production. Complex I and III are considered the main ROS generators (Murphy, 2009). ETC respiration capacity and its Complex, in particular Complex I and Complex IV, activities were upregulated in all types of CVS-infected cells. The increase in Complex I activity correlated with the susceptibility of the cells to rabies virus infection. It was previously shown that

rabies virus matrix protein is localized to the mitochondria. However, the viral matrix protein does not directly interact with Complex IV (Gholami *et al*., 2008). As the increase in Complex I activity correlated with the susceptibility of the cells to rabies virus infection, Complex I can be considered as a potential direct target for rabies virus. The level of NADH, which is a Complex I substrate, was also increased in the CVS-infected cells. NADH is important for the function of apoptosis inducing factor (AIF), which a NADH oxidase that is believed to be crucial for the activity of Complex I (Modjtahedi et al., 2006). Complex I is one of the main sites of ROS generation. It was previously shown that hydrogen peroxide production directly correlates with the concentration of Complex I (Kussmaul and Hirst, 2006). Interestingly, ROS overproduction was reported in association with both increased and decreased activity of Complex I (Li *et al.,* 2003, and Lee *et al.,* 2011). In addition, ROS production at Complex I is believed to occur during both forward and reverse electron flow (Selivanov *et al.,* 2011). Therefore, Complex I can be an important source for ROS in rabies virus-infected cells.

The activities of Complex II-III were normal in all types of CVS-infected cells. Consistent with our findings, Nakamichi *et al.,* 2004 observed that only attenuated rabies virus strain (HEP), but not CVS, significantly inhibited the succinate dehydrogenase (Complex II) activity in murine neuroblastoma cells. Similarly, normal to only a slight decrease in Complex II activity was observed in CVS-infected infected murine B (A20) and T (EL4) cells (Nakamichi *et al.,* 2004). In contrast, hyperactivity of Complex II was observed in CVS-infected

macrophages (RAW264) whereas the activity remained normal in HEP-infected macrophages (Nakamichi *et al.,* 2004).

Complex Ⅳ activity was up-regulated in all types of CVS-infected-cells. However, this increase did not correlate with the susceptibility of the cells to the infection which suggests an indirect viral effect. Gholami *et al.,* (2008) showed a very modest, albeit statistically insignificant increase, in Complex Ⅳ activity in human epithelial carcinoma (Hela) cells infected with wild-type rabies virus (dog isolate from Thailand) at 24 and 48 hrs post-infection (Gholami *et al.,* 2008). Hence, this modest increase in Complex Ⅳ activity might be important after taking into consideration the fact that only 10% of Hela cells were susceptible to CVS infection at 24 hrs post-infection, although the susceptibility of Hela cells to wild-type rabies virus infection were not assessed and might be different (Thoulouze *et al.,* 1998). About 200% increase in Complex Ⅳ was detected in the same cells after transfection with rabies virus matrix protein (Gholami *et al.,* 2008). Furthermore, replacement of amino acid residue 77 and 81 of Mokola virus, a rabies-related virus, matrix protein with that from dog isolate rabies virus resulted in more than 250% increase in Complex Ⅳ activity (Gholami *et al.,* 2008). The increased Complex Ⅳ activity may play a role in apoptosis prevention in CVS-infected cells. Mokola virus, which comprises several conserved regions of gene sequence and protein structure with rabies virus, significantly inhibited Complex Ⅳ activity in human epithelial cells leading to apoptosis. The decreased activity of Complex Ⅳ resulted in release of the cytochrome c from mitochondria. As a consequence, apoptosomes were formed, and caspases were activated

which eventually led to apoptosis (Gholami *et al.,* 2008). Interestingly, the ratios of mitochondrial to cytoplasmic cytochrome c in rabies virus infected and rabies virus matrix protein-transfected cells were not only higher than that in Mokola virus-infected and Mokola virus matrix- transfected cells, but they were even higher than the ratio of mitochondrial to cytoplasmic cytochrome c in non-infected cells (Gholami *et al.,* 2008). Therefore, CVS-infected cells may avoid apoptosis by increasing the activity of Complex IV and sequestering cytochrome c in the mitochondria (Gholami *et al.,* 2008).

We evaluated the effect of CVS infection on the mitochondrial membrane potential, and found that the mitochondrial membrane potential was significantly increased in infected cells versus mock-infected cells. The increased proton pumping through hyperactive Complex I and IV in association with normal proton leakage can explain this finding. Furthermore, the increased NADH level in the infected cells may further contribute to maintain a high mitochondrial membrane potential via inhibiting mitochondrial permeability transition (MPT) pore and stimulating voltage-dependent anion channels closure (Zoratti and Szabò, 1995). There is evidence that mitochondria swellings are associated with increased mitochondrial membrane potential (Garlid and Paucek, 2003). Thus, the increase in the mitochondrial membrane potential may be responsible for the swollen mitochondria that was previously observed in rabies virus-infected transgenic mice. However, others have reported mitochondrial swellings in the presence of normal or even low mitochondrial membrane potential (Scott *et al.,* 2008, Gao *et al.,* 2001, and Lyamzaev *et al.,* 2004). Generation of a high mitochondrial

membrane potential is required for ATP production in the cells. However, it also favors mitochondrial ROS formation via several pathways (Murphy, 2009).

Interestingly, the enhanced capacity of ETC in the infected cells was accompanied by a reduction in the intracellular level of ATP. This reduction is likely due to an increase in ATP hydrolysis rather than a defect in ATP synthesis. Inhibition of ATP synthase activity and oxidative phosphorylation dyscoupling are two common mechanisms that lead to a decrease in ATP production. We have observed normal oxidative phosphorylation capacity suggesting a normal ATP synthase activity, although direct assessment of ATP synthase expression and activity would be more informative. Azzu *et al.,* (2008) indicated that 4-HNE expression in the presence of high mitochondrial membrane potential dyscouples oxidation and phosphorylation. During mitochondrial dyscoupling ATP production is decreased due to high proton leakage from the mitochondria. However, we have observed normal proton leakage which may exclude this hypothesis. In addition to the above-mentioned mechanism, interaction between CVS and adenine nucleotide translocator (ANT) is another potential mechanism for inhibition of ATP synthesis. ANT is crucial for ADP/ATP exchange and, thus, for ATP synthesis (Halestrap and Brenner, 2003). Several viruses (e.g., HIV, cytomegalovirus (CMV), and hepatitis B virus (HBV)) directly bind and affect ANT (Chang *et al.,* 2006, Goldmacher, 2002, and Bergametti *et al.,* 1999). HIV Vpr interacts with ANT and enhances its opening whereas CMV and HBV inhibit its opening. In both cases, this may suppress ATP synthesis (Chang *et al.,* 2006, Goldmacher, 2002, and Bergametti *et al.,* 1999). Opening of ANT diminishes the

high mitochondrial membrane potential and inhibits ATP synthesis. Closure of ANT may affect ATP synthesis by impairing the ADP translocation from cytoplasm to the mitochondria, and the ATP translocation from the mitochondria to the cytoplasm (Halestrap and Brenner, 2003). Increased ATP hydrolysis can be due to the viral replication. Vesicular stomatitis virus (VSV) is another rhabdovirus that shares with rabies virus a very similar structure, genome, and replication cycle. It was shown that VSV utilizes the cellular ATP in order to complete its replication cycle (Beckes *et al.,* 1987). Another hypothesis that may explain reduced ATP levels in rabies virus-infected cells is the presence of ROS. It was shown that the presence of hydrogen peroxide reduced the cellular ATP level in both dose- and time-dependent manners (Teepker *et al.,* 2007). Regardless of the underlying mechanism, the reduction of intracellular ATP level may explain the reduction of axonal outgrowth that was previously observed in rabies virus-infected DRG neurons (Jackson *et al.,* 2010). The depletion of ATP level may affect the function of motor proteins (e.g., dynein and kinesin) which play a critical role in mediating normal mitochondrial transportation (Chang *et al.,* 2006). Normal mitochondrial trafficking is believed to be important during neuronal development (Chang *et al.,* 2006). HIV soluble viral protein R (Vpr), which is present in the cerebrospinal fluid (CSF) of HIV-infected individuals with neurological symptoms, directly interacts with adenine nucleotide translocator (ANT) in the mitochondrial inner membrane, and enhances its opening (Kitayama *et al.,* 2008). As a consequence, ATP synthesis is inhibited, mitochondrial transportation is interfered, and axonal outgrowth is reduced (Kitayama *et al.,*

2008). Aggregation of mitochondria was previously observed in rabies virus-infected DRG neurons which may suggest abnormality in the transportation of the mitochondria (Jackson *et al.,* 2010). Therefore, we propose that rabies virus infection may reduce the axonal outgrowth by decreasing the level of ATP and impairing the trafficking of the mitochondria. Also, the enhanced ETC capacity in the infected cells can be a compensatory mechanism driven by the mitochondria in order to meet the cellular energy demand.

The NADH to NAD+ ratio is a redox system believed to be crucial in determining the cellular redox state that is significantly involved in mediating several biological functions such as energy metabolism, oxidation, antioxidation, and cell fate (Ying, 2008). We have observed an increase in the NADH level and the NADH to NAD+ ratio in infected cells indicating alteration of the cellular redox state. The increase of NADH level can be due to reverse electron flow, which is a significant source for ROS production, from Complex III to Complex I which converts NAD+ to NADH (Murphy, 2009). Alteration in the redox state may affect several biochemical reactions within the cell (Ying, 2008). NADH can promote the release of ferrous iron leading to “reductive stress” (Jaeschke *et al.,* 1992). In addition, oxidizing NADH by xanthine oxidase/xanthine dehydrogenase can enhance ROS generation (Zhang et al., 1998). α-ketoglutarate dehydrogenase is another source for NADH-dependent ROS generation (Starkov et al., 2004). It was shown that NADH inhibits the activity of adenine monophosphate-activated protein kinase (AMPK) (Rafaeloff-Phail *et al.*, 2004). Downregulation of AMPK resulted in suppression of neurite outgrowth in sensory neurons from diabetic

rats (Roy Chowdhury et al., 2012). Hence, reduction of axonal outgrowth in CVS-infected neurons can be due to the presence of high NADH and the downregulation of AMPK. Sirtuin (SIRT) expression is also regulated by NADH/NAD+ ratio. Gambini *et al.,* (2011) indicated that the increase in NADH to NAD+ ratio upregulated the expression of SIRT mRNA and protein. It is well-known that the upregulation of SIRT family enhances mitochondrial biogenesis. For instance, SIRT3 expression is an important regulator for all ETC Complexes (I, II, III, IV, and V). Physical interaction between SIRT3 and a Complex I subunit (NDUFA9) has been identified (Ahn *et al.,* 2008). Treatment of mitochondria with exogenous SIRT3 increased Complex I activity by increasing the deactykation of several proteins (Ahn *et al*., 2008). In SIRT3-deficient or knockdown models, the activities of these Complexes were decreased probably due to increased acetylation of the Complexes (Ahn *et al.* 2008, Bao *et al.* 2010, Kim *et al.* 2010, and Cimen *et al.* 2010). Hence, the hyperactivity of ETC Complexes in CVS-infected cells can be due to a high NADH to NAD+ ratio, overexpression of SIRT, and increased deacetylation of Complexes' proteins.

The alteration of cellular redox state, induction of high mitochondrial membrane potential, and reduction of intracellular ATP level provide a conductive environment for mitochondrial ROS production (Murphy, 2009). Here we show that hydrogen peroxide production was significantly higher in CVS-infected cells versus mock-infected cells in the presence of succinate. Succinate accelerates ATP-dependent reverse electron flow through Complex I to NAD+ which leads to high NADH/NAD+ ratio and ROS overproduction (Selivanov et al., 2011). The

mechanisms by which reverse electron transport increases ROS generation remain unclear. However, it is known that ROS production mainly occurs at Complex I (Selivanov et al., 2011). Also, this process is believed to be inhibited in the presence of Complex I inhibitors (e.g., rotenone) and mitochondrial uncouplers (e.g., FCCP) (Miwa and Brand, 2003). We postulate that CVS infection induces reverse electron transport-driven hydrogen peroxide overgeneration which leads to oxidative stress. Production of hydrogen peroxide through reverse electron transport was previously suggested under normal physiological conditions in which differentiated muscles produce high amounts of hydrogen peroxide at hyperactive Complex I (Lee *et al.,* 2011). Alteration of redox state in the differentiated muscle was observed as indicated by a high NADH/NAD+ ratio. Addition of rotenone, which is a Complex I-inhibitor, not only decreased the NADH/NAD+ ratio, but also inhibited hydrogen peroxide production in differentiated muscles (Lee *et al.,* 2011).

Here we show that rabies virus infection induces hydrogen peroxide production. It was shown that rabies virus infection induces nitric oxide production (Hooper *et al.,* 1995, and Nakamichi *et al.,* 2004). Although the presence of nitric oxide, superoxide, and hydrogen peroxide can cause harm to cells, interaction between these components can lead to more devastating outcomes. For instance, interaction of nitric oxide with superoxide leads to peroxynitrite formation. Also, singlet oxygen can be formed by interaction of hydrogen peroxide with nitric oxide or superoxide. The generation of this deadly

mixture of radical and non-radical ROS can explain the rabies virus-induced neuronal degeneration.

Given the evidence that oxidative stress and mitochondrial dysfunction are crucial in rabies virus-induced neuronal degeneration, therapeutic approaches protecting mitochondria from oxidative damage may be effective strategies to prevent rabies virus-induced neuronal dysfunction. Unfortunately, there is no current effective therapy for oxidative stress and mitochondrial dysfunction. The neuroprotection efficiency of conventional antioxidants (i.e., Vitamin E, Vitamin C, creatine, and coenzyme Q10) has been studied in several neurodegenerative disorders. Unfortunately, they showed no consistent benefits in clinical trials, in part, due to the difficulty of delivering them to the mitochondria (Szeto, 2006). To overcome this problem, “mitochondria-targeted” antioxidants were developed and their efficiency *in vivo* was assessed (Adlam et al., 2005, Szeto, 2006, and Xun et al., 2012). These antioxidants, which specifically target the mitochondria, showed promising results in preventing mitochondrial destruction, improving mitochondrial functions, and enhancing cell survival in mice with cardiovascular or neurodegenerative diseases (Adlam et al., 2005, and Xun et al., 2012). The mitochondrial-targeted antioxidants can be considered as a potential therapeutic approach to rabies virus infection.

5. Conclusions:

Rabies virus induced several alterations in mitochondrial functions in a variety of cultured cells. The ETC Complex activities, in particular Complex I and IV, were increased. The increase in Complex I activity was positively correlated with the susceptibility of the cells to the infection indicating a direct effect of the virus on this Complex. Hyperactivity of Complex I was associated with increase in NADH level, a Complex I-substrate. The increase in Complex IV activity was not correlated to the susceptibility of the cells to the infection. The enhanced ETC capacity in the infected cells is likely due to the reduction of the intracellular ATP level and/or the alteration of the cellular redox state as indicated by a high NADH/NAD+ ratio. Regardless, a high mitochondrial membrane potential was generated in the mitochondria of the infected cells due to high proton pumping, tight coupling and normal proton leakage. Several sites within mitochondria may enhance ROS generation in the presence of high mitochondrial membrane potential, high NADH/NAD+ ratio, and low ATP level. Hydrogen peroxide production was significantly higher in rabies virus-infected cells probably due to reverse electron transport. We conclude that rabies virus induces mitochondrial dysfunction, enhances ROS generation, and induces oxidative stress which eventually leads to neuronal degeneration and death of the host.

6. Future directions:

We have observed that rabies virus altered several mitochondrial parameters providing a conductive environment (high mitochondrial membrane potential, tight mitochondrial coupling, high NADH to NAD+ ratio, and low ATP level) for ROS over-generation (Murphy, 2009). The next step will be to identify the mitochondrial sites for ROS production. Due to increased production of hydrogen peroxide in CVS-infected cells in the presence of succinate, we postulate that rabies virus induces mitochondrial ROS overproduction at Complex I by accelerating reverse electron transport (Murphy, 2009). During reverse electron flow, the main electron leakage site is at the ubiquinone binding site of Complex I. Addition of rotenone, Complex I-inhibitor, dramatically reduces ROS production during reverse electron transport. In contrast, addition of succinate further induces reverse electron flow and, thereby, enhances ROS production (Liu *et al.,* 2002). It was also shown that reverse electron flow-driven ROS production is highly sensitive to mitochondrial membrane potential-diminishing agent (i.e., uncouplers). By studying ROS production on the mitochondrial preparations in the presence or absence of several ETC substrates and inhibitors, we will be able to confirm this hypothesis and probably identify other sources for ROS production. In case of positive results, the next step will be to determine the viral component that is responsible for induction of mitochondrial dysfunction. It was shown that matrix protein of dog isolate rabies virus is localized to the mitochondria of Hela cells (Gholami et al., 2008). Hence, matrix protein might be the first viral protein to be considered.

7. References:

Adlam, V. J., J. C. Harrison, C. M. Porteous, A. M. James, R. A. Smith, M. P. Murphy and I. A. Sammut. "Targeting an Antioxidant to Mitochondria Decreases Cardiac Ischemia-Reperfusion Injury." FASEB J 19, no. 9 (2005): 1088-95.

Advisory Committee on Immunization Practices (ACIP). "Human Rabies Prevention--United States, 1999. Recommendations of the Advisory Committee on Immunization Practices (Acip)." MMWR Recomm Rep 48, no. RR-1 (1999): 1-21.

Ahn, B. H., H. S. Kim, S. Song, I. H. Lee, J. Liu, A. Vassilopoulos, C. X. Deng and T. Finkel. "A Role for the Mitochondrial Deacetylase Sirt3 in Regulating Energy Homeostasis." Proc Natl Acad Sci U S A 105, no. 38 (2008): 14447-52.

Azzu, V., N. Parker and M. D. Brand. "High Membrane Potential Promotes Alkenal-Induced Mitochondrial Uncoupling and Influences Adenine Nucleotide Translocase Conformation." Biochem J 413, no. 2 (2008): 323-32.

Babior, B. M., R. S. Kipnes and J. T. Curnutte. "Biological Defense Mechanisms. The Production by Leukocytes of Superoxide, a Potential Bactericidal Agent." J Clin Invest 52, no. 3 (1973): 741-4.

Bannister, W. H., G. Federici, J. K. Heath and J. V. Bannister. "Antioxidant Systems in Tumour Cells: The Levels of Antioxidant Enzymes, Ferritin, and Total Iron in a Human Hepatoma Cell Line." Free Radic Res Commun 1, no. 6 (1986): 361-7.

Bao, J., I. Scott, Z. Lu, L. Pang, C. C. Dimond, D. Gius and M. N. Sack. "Sirt3 Is Regulated by Nutrient Excess and Modulates Hepatic Susceptibility to Lipotoxicity." Free Radic Biol Med 49, no. 7 (2010): 1230-7.

Beck, A. M. and B. A. Jones. "Unreported Dog Bites in Children." Public Health Rep 100, no. 3 (1985): 315-21.

Beckes, J. D., A. A. Haller and J. Perrault. "Differential Effect of Atp Concentration on Synthesis of Vesicular Stomatitis Virus Leader Rnas and Mrnas." J Virol 61, no. 11 (1987): 3470-8.

Bergametti, F., S. Prigent, B. Luber, A. Benoit, P. Tiollais, A. Sarasin and C. Transy. "The Proapoptotic Effect of Hepatitis B Virus Hbx Protein Correlates with Its Transactivation Activity in Stably Transfected Cell Lines." Oncogene 18, no. 18 (1999): 2860-71.

Bernhardt, R. "Cytochrome P450: Structure, Function, and Generation of Reactive Oxygen Species." Rev Physiol Biochem Pharmacol 127, (1996): 137-221.

Berry, E. A., M. Guergova-Kuras, L. S. Huang and A. R. Crofts. "Structure and Function of Cytochrome Bc Complexes." Annu Rev Biochem 69, (2000): 1005-75.

Bhabak, K. P. and G. Mugesh. "Functional Mimics of Glutathione Peroxidase: Bioinspired Synthetic Antioxidants." Acc Chem Res 43, no. 11 (2010): 1408-19.

Birt, L. M. and W. Bartley. "The Behaviour of Pyridine Nucleotides of Mitochondria in a 'Saline Medium'." Biochem J 76, (1960): 328-41.

Blanton, J. D., D. Palmer, J. Dyer and C. E. Rupprecht. "Rabies Surveillance in the United States During 2010." J Am Vet Med Assoc 239, no. 6 (2011): 773-83.

Bourhy, H., N. Tordo, M. Lafon and P. Sureau. "Complete Cloning and Molecular Organization of a Rabies-Related Virus, Mokola Virus." J Gen Virol 70 (Pt 8), (1989): 2063-74.

Boveris, A. "Mitochondrial Production of Superoxide Radical and Hydrogen Peroxide." Adv Exp Med Biol 78, (1977): 67-82.

Boveris, A. and E. Cadenas. "Mitochondrial Production of Superoxide Anions and Its Relationship to the Antimycin Insensitive Respiration." FEBS Lett 54, no. 3 (1975): 311-4.

Boveris, A., N. Oshino and B. Chance. "The Cellular Production of Hydrogen Peroxide." Biochem J 128, no. 3 (1972): 617-30.

Boyer, P. D. "The Atp Synthase--a Splendid Molecular Machine." Annu Rev Biochem 66, (1997): 717-49.

Brandt, U. "Proton-Translocation by Membrane-Bound Nadh:Ubiquinone-Oxidoreductase (Complex I) through Redox-Gated Ligand Conduction." Biochim Biophys Acta 1318, no. 1-2 (1997): 79-91.

Brass, C. A., J. Narciso and J. L. Gollan. "Enhanced Activity of the Free Radical Producing Enzyme Xanthine Oxidase in Hypoxic Rat Liver. Regulation and Pathophysiologic Significance." J Clin Invest 87, no. 2 (1991): 424-31.

Brigelius-Flohe, R. "Tissue-Specific Functions of Individual Glutathione Peroxidases." Free Radic Biol Med 27, no. 9-10 (1999): 951-65.

Brown, W. M., M. George, Jr. and A. C. Wilson. "Rapid Evolution of Animal Mitochondrial DNA." Proc Natl Acad Sci U S A 76, no. 4 (1979): 1967-71.

Brownlee, M. "Biochemistry and Molecular Cell Biology of Diabetic Complications." Nature 414, no. 6865 (2001): 813-20.

Brzozka, K., S. Finke and K. K. Conzelmann. "Identification of the Rabies Virus Alpha/Beta Interferon Antagonist: Phosphoprotein P Interferes with Phosphorylation of Interferon Regulatory Factor 3." J Virol 79, no. 12 (2005): 7673-81.

Buffinton, G. D., S. Christen, E. Peterhans and R. Stocker. "Oxidative Stress in Lungs of Mice Infected with Influenza a Virus." Free Radic Res Commun 16, no. 2 (1992): 99-110.

Buhl, R., H. A. Jaffe, K. J. Holroyd, F. B. Wells, A. Mastrangeli, C. Saltini, A. M. Cantin and R. G. Crystal. "Systemic Glutathione Deficiency in Symptom-Free Hiv-Seropositive Individuals." Lancet 2, no. 8675 (1989): 1294-8.

Calhoun, M. W., J. W. Thomas and R. B. Gennis. "The Cytochrome Oxidase Superfamily of Redox-Driven Proton Pumps." Trends Biochem Sci 19, no. 8 (1994): 325-30.

Carlsson, L. M., J. Jonsson, T. Edlund and S. L. Marklund. "Mice Lacking Extracellular Superoxide Dismutase Are More Sensitive to Hyperoxia." Proc Natl Acad Sci U S A 92, no. 14 (1995): 6264-8.

Carroll, J., I. M. Fearnley, R. J. Shannon, J. Hirst and J. E. Walker. "Analysis of the Subunit Composition of Complex I from Bovine Heart Mitochondria." Mol Cell Proteomics 2, no. 2 (2003): 117-26.

Castellanos, J. E., D. R. Castaneda, A. E. Velandia and H. Hurtado. "Partial Inhibition of the in Vitro Infection of Adult Mouse Dorsal Root Ganglion Neurons by Rabies Virus Using Nicotinic Antagonists." Neurosci Lett 229, no. 3 (1997): 198-200.

Ceccaldi, P. E., M. P. Fillion, A. Ermine, H. Tsiang and G. Fillion. "Rabies Virus Selectively Alters 5-Ht1 Receptor Subtypes in Rat Brain." Eur J Pharmacol 245, no. 2 (1993): 129-38.

Cecchini, G. "Function and Structure of Complex Ii of the Respiratory Chain." Annu Rev Biochem 72, (2003): 77-109.

Centre for Disease Control and Prevention. "Human-to-Human Transmission of Rabies Via Corneal Transplantation—France." MMWR Morb Mortal Wkly Rep. 29, (1980):25-26.

Centre for Disease Control and Prevention. "Human-to-Human Transmission of Rabies Via Corneal Transplant--Thailand." MMWR Morb Mortal Wkly Rep 30, no. 37 (1981): 473-4.

Centre for Disease Control and Prevention. "Human Rabies--Rwanda." MMWR Morb Mortal Wkly Rep 31, no. 10 (1982): 135.

Centre for Disease Control and Prevention. "Human Rabies--Kenya." MMWR Morb Mortal Wkly Rep 32, no. 38 (1983): 494-5.

Centres for Disease Control and Prevention. "Compendium of animal rabies prevention and control, 2005: National associate of state public health Veterinarians, Inc. (NASPHV) ." MMWR Recomm Rep. 53 (2005): 586-589.

Chance, B., H. Sies and A. Boveris. "Hydroperoxide Metabolism in Mammalian Organs." Physiol Rev 59, no. 3 (1979): 527-605.

Chang, D. T. and I. J. Reynolds. "Mitochondrial Trafficking and Morphology in Healthy and Injured Neurons." Prog Neurobiol 80, no. 5 (2006): 241-68.

Charlton, K. M., S. Nadin-Davis, G. A. Casey and A. I. Wandeler. "The Long Incubation Period in Rabies: Delayed Progression of Infection in Muscle at the Site of Exposure." Acta Neuropathol 94, no. 1 (1997): 73-7.

Childs, J. and L, Real. "Epidemiology." In *Rabies*. Jackson AC, Wunner WH (2nd ed). Academic Press (2007):123–199.

Chenik, M., M. Schnell, K. K. Conzelmann and D. Blondel. "Mapping the Interacting Domains between the Rabies Virus Polymerase and Phosphoprotein." J Virol 72, no. 3 (1998): 1925-30.

Chomyn, A., M. W. Cleeter, C. I. Ragan, M. Riley, R. F. Doolittle and G. Attardi. "Urf6, Last Unidentified Reading Frame of Human Mtdna, Codes for an Nadh Dehydrogenase Subunit." Science 234, no. 4776 (1986): 614-8.

Chomyn, A., P. Mariottini, M. W. Cleeter, C. I. Ragan, A. Matsuno-Yagi, Y. Hatefi, R. F. Doolittle and G. Attardi. "Six Unidentified Reading Frames of Human Mitochondrial DNA Encode Components of the Respiratory-Chain Nadh Dehydrogenase." Nature 314, no. 6012 (1985): 592-7.

Chowdhury, S. K., Z. Drahota, D. Floryk, P. Calda and J. Houstek. "Activities of Mitochondrial Oxidative Phosphorylation Enzymes in Cultured Amniocytes." Clin Chim Acta 298, no. 1-2 (2000): 157-73.

Chowdhury, S. K., E. Zherebitskaya, D. R. Smith, E. Akude, S. Chattopadhyay, C. G. Jolivalt, N. A. Calcutt and P. Fernyhough. "Mitochondrial Respiratory Chain Dysfunction in Dorsal Root Ganglia of Streptozotocin-Induced Diabetic Rats and Its Correction by Insulin Treatment." Diabetes 59, no. 4 (2010): 1082-91.

Cimen, H., M. J. Han, Y. Yang, Q. Tong, H. Koc and E. C. Koc. "Regulation of Succinate Dehydrogenase Activity by Sirt3 in Mammalian Mitochondria." Biochemistry 49, no. 2 (2010): 304-11.

Cleaveland, S., E. M. Fevre, M. Kaare and P. G. Coleman. "Estimating Human Rabies Mortality in the United Republic of Tanzania from Dog Bite Injuries." Bull World Health Organ 80, no. 4 (2002): 304-10.

Cohen, G. and R. E. Heikkila. "The Generation of Hydrogen Peroxide, Superoxide Radical, and Hydroxyl Radical by 6-Hydroxydopamine, Dialuric Acid, and Related Cytotoxic Agents." J Biol Chem 249, no. 8 (1974): 2447-52.

Colonno, R. J. and A. K. Banerjee. "Complete Nucleotide Sequence of the Leader Rna Synthesized in Vitro by Vesicular Stomatitis Virus." Cell 15, no. 1 (1978): 93-101.

Conzelmann, K. K. and M. Schnell. "Rescue of Synthetic Genomic Rna Analogs of Rabies Virus by Plasmid-Encoded Proteins." J Virol 68, no. 2 (1994): 713-9.

Davies, M. J. "The Oxidative Environment and Protein Damage." Biochim Biophys Acta 1703, no. 2 (2005): 93-109.

Dhingra, V., X. Li, Y. Liu and Z. F. Fu. "Proteomic Profiling Reveals That Rabies Virus Infection Results in Differential Expression of Host Proteins Involved in Ion Homeostasis and Synaptic Physiology in the Central Nervous System." J Neurovirol 13, no. 2 (2007): 107-17.

Droge, W. "Free Radicals in the Physiological Control of Cell Function." Physiol Rev 82, no. 1 (2002): 47-95.

Eng, T. R., D. B. Fishbein, H. E. Talamante, D. B. Hall, G. F. Chavez, J. G. Dobbins, F. J. Muro, J. L. Bustos, M. de los Angeles Ricardy, A. Munguia and et al. "Urban Epizootic of Rabies in Mexico: Epidemiology and Impact of Animal Bite Injuries." Bull World Health Organ 71, no. 5 (1993): 615-24.

Erecinska, M. and D. F. Wilson. "The Effect of Antimycin a on Cytochromes B561, B566, and Their Relationship to Ubiquinone and the Iron-Sulfer Centers S-1 (+N-2) and S-3." Arch Biochem Biophys 174, no. 1 (1976): 143-57.

Etessami, R., K. K. Conzelmann, B. Fadai-Ghotbi, B. Natelson, H. Tsiang and P. E. Ceccaldi. "Spread and Pathogenic Characteristics of a G-Deficient Rabies

Virus Recombinant: An in Vitro and in Vivo Study." J Gen Virol 81, no. Pt 9 (2000): 2147-53.

Faber, M., R. Pulmanausahakul, S. S. Hodawadekar, S. Spitsin, J. P. McGettigan, M. J. Schnell and B. Dietzschold. "Overexpression of the Rabies Virus Glycoprotein Results in Enhancement of Apoptosis and Antiviral Immune Response." J Virol 76, no. 7 (2002): 3374-81.

Fang, Y. Z., S. Yang and G. Wu. "Free Radicals, Antioxidants, and Nutrition." Nutrition 18, no. 10 (2002): 872-9.

Faul, E. J., C. N. Wanjalla, J. P. McGettigan and M. J. Schnell. "Interferon-Beta Expressed by a Rabies Virus-Based Hiv-1 Vaccine Vector Serves as a Molecular Adjuvant and Decreases Pathogenicity." Virology 382, no. 2 (2008): 226-38.

Fekadu, M. "Rabies in Ethiopia." Am J Epidemiol 115, no. 2 (1982): 266-73.

Fekadu, M., T. Endeshaw, W. Alemu, Y. Bogale, T. Teshager and J. G. Olson. "Possible Human-to-Human Transmission of Rabies in Ethiopia." Ethiop Med J 34, no. 2 (1996): 123-7.

Ferrari, C. K. B. "Free radicals, lipid peroxidation and antioxidants in apoptosis: implications in cancer, cardiovascular and neurological diseases". *Biologia* **55**, (2000):581-590.

Finke, S. and K. K. Conzelmann. "Dissociation of Rabies Virus Matrix Protein Functions in Regulation of Viral Rna Synthesis and Virus Assembly." J Virol 77, no. 22 (2003): 12074-82.

Frei, B. "Reactive Oxygen Species and Antioxidant Vitamins: Mechanisms of Action." Am J Med 97, no. 3A (1994): 5S-13S; discussion 22S-28S.

Fridovich, I. "Quantitative Aspects of the Production of Superoxide Anion Radical by Milk Xanthine Oxidase." J Biol Chem 245, no. 16 (1970): 4053-7.

Fridovich, I. "Fundamental Aspects of Reactive Oxygen Species, or What's the Matter with Oxygen?" Ann N Y Acad Sci 893, (1999): 13-8.

Galindo, M. F., J. Jordan, C. Gonzalez-Garcia and V. Cena. "Reactive Oxygen Species Induce Swelling and Cytochrome C Release but Not Transmembrane Depolarization in Isolated Rat Brain Mitochondria." Br J Pharmacol 139, no. 4 (2003): 797-804.

Gambini, J., M. C. Gomez-Cabrera, C. Borras, S. L. Valles, R. Lopez-Grueso, V. E. Martinez-Bello, D. Herranz, F. V. Pallardo, J. A. Tresguerres, M. Serrano and

J. Vina. "Free [Nadh]/[Nad(+)] Regulates Sirtuin Expression." Arch Biochem Biophys 512, no. 1 (2011): 24-9.

Gandhi, S. and A. Y. Abramov. "Mechanism of Oxidative Stress in Neurodegeneration." Oxid Med Cell Longev 2012, (2012): 428010.

Gao, W., Y. Pu, K. Q. Luo and D. C. Chang. "Temporal Relationship between Cytochrome C Release and Mitochondrial Swelling During Uv-Induced Apoptosis in Living Hela Cells." J Cell Sci 114, no. Pt 15 (2001): 2855-62.

Garlid, K. D. and P. Paucek. "Mitochondrial Potassium Transport: The K(+) Cycle." Biochim Biophys Acta 1606, no. 1-3 (2003): 23-41.

Gholami, A., R. Kassis, E. Real, O. Delmas, S. Guadagnini, F. Larrous, D. Obach, M. C. Prevost, Y. Jacob and H. Bourhy. "Mitochondrial Dysfunction in Lyssavirus-Induced Apoptosis." J Virol 82, no. 10 (2008): 4774-84.

Gilgun-Sherki, Y., E. Melamed and D. Offen. "Oxidative Stress Induced-Neurodegenerative Diseases: The Need for Antioxidants That Penetrate the Blood Brain Barrier." Neuropharmacology 40, no. 8 (2001): 959-75.

Girotti, A. W. and T. Kriska. "Role of Lipid Hydroperoxides in Photo-Oxidative Stress Signaling." Antioxid Redox Signal 6, no. 2 (2004): 301-10.

Giulivi, C., A. Boveris and E. Cadenas. "Hydroxyl Radical Generation During Mitochondrial Electron Transfer and the Formation of 8-Hydroxydesoxyguanosine in Mitochondrial DNA." Arch Biochem Biophys 316, no. 2 (1995): 909-16.

Gmunder, H., H. P. Eck, B. Benninghoff, S. Roth and W. Droge. "Macrophages Regulate Intracellular Glutathione Levels of Lymphocytes. Evidence for an Immunoregulatory Role of Cysteine." Cell Immunol 129, no. 1 (1990): 32-46.

Gode, G. R. and N. K. Bhide. "Two Rabies Deaths after Corneal Grafts from One Donor." Lancet 2, no. 8614 (1988): 791.

Goldmacher, V. S. "Vmia, a Viral Inhibitor of Apoptosis Targeting Mitochondria." Biochimie 84, no. 2-3 (2002): 177-85.

Golenbock, D. T., R. Y. Hampton, N. Qureshi, K. Takayama and C. R. Raetz. "Lipid a-Like Molecules That Antagonize the Effects of Endotoxins on Human Monocytes." J Biol Chem 266, no. 29 (1991): 19490-8.

Griffith, O. W. and A. Meister. "Origin and Turnover of Mitochondrial Glutathione." Proc Natl Acad Sci U S A 82, no. 14 (1985): 4668-72.

Hagen, T. M., S. Huang, J. Curnutte, P. Fowler, V. Martinez, C. M. Wehr, B. N. Ames and F. V. Chisari. "Extensive Oxidative DNA Damage in Hepatocytes of Transgenic Mice with Chronic Active Hepatitis Destined to Develop Hepatocellular Carcinoma." Proc Natl Acad Sci U S A 91, no. 26 (1994): 12808-12.

Halestrap, A. P. and C. Brenner. "The Adenine Nucleotide Translocase: A Central Component of the Mitochondrial Permeability Transition Pore and Key Player in Cell Death." Curr Med Chem 10, no. 16 (2003): 1507-25.

Halliwell, B. "Oxidative Stress and Neurodegeneration: Where Are We Now?" J Neurochem 97, no. 6 (2006): 1634-58.

Held, J. R., E. S. Tierkel and J. H. Steele. "Rabies in Man and Animals in the United States, 1946-65." Public Health Rep 82, no. 11 (1967): 1009-18.

Hemachudha, T., S. Wacharapluesadee, E. Mitrabhakdi, H. Wilde, K. Morimoto and R. A. Lewis. "Pathophysiology of Human Paralytic Rabies." J Neurovirol 11, no. 1 (2005): 93-100.

Hennet, T., E. Peterhans and R. Stocker. "Alterations in Antioxidant Defences in Lung and Liver of Mice Infected with Influenza a Virus." J Gen Virol 73 (Pt 1), (1992): 39-46.

Henze, K. and W. Martin. "Evolutionary Biology: Essence of Mitochondria." Nature 426, no. 6963 (2003): 127-8.

Hinkle, P. C., R. A. Butow, E. Racker and B. Chance. "Partial Resolution of the Enzymes Catalyzing Oxidative Phosphorylation. Xv. Reverse Electron Transfer in the Flavin-Cytochrome Beta Region of the Respiratory Chain of Beef Heart Submitochondrial Particles." J Biol Chem 242, no. 22 (1967): 5169-73.

Hirst, J. "Energy Transduction by Respiratory Complex I--an Evaluation of Current Knowledge." Biochem Soc Trans 33, no. Pt 3 (2005): 525-9.

Ho, Y. S., M. Gargano, J. Cao, R. T. Bronson, I. Heimler and R. J. Hutz. "Reduced Fertility in Female Mice Lacking Copper-Zinc Superoxide Dismutase." J Biol Chem 273, no. 13 (1998): 7765-9.

Homola, V. "World Breifing Europe: Germany: rabies after transplant." The New York times. February 18, 2005 Friday. Late Edition- Final, 6. New York: New York times Inc.

Hooper, D. C., S. T. Ohnishi, R. Kean, Y. Numagami, B. Dietzschold and H. Koprowski. "Local Nitric Oxide Production in Viral and Autoimmune Diseases of

the Central Nervous System." Proc Natl Acad Sci U S A 92, no. 12 (1995): 5312-6.

Hornung, V., J. Ellegast, S. Kim, K. Brzozka, A. Jung, H. Kato, H. Poeck, S. Akira, K. K. Conzelmann, M. Schlee, S. Endres and G. Hartmann. "5'-Triphosphate Rna Is the Ligand for Rig-I." Science 314, no. 5801 (2006): 994-7.

Houff, S. A., R. C. Burton, R. W. Wilson, T. E. Henson, W. T. London, G. M. Baer, L. J. Anderson, W. G. Winkler, D. L. Madden and J. L. Sever. "Human-to-Human Transmission of Rabies Virus by Corneal Transplant." N Engl J Med 300, no. 11 (1979): 603-4.

Huie, R. E. and S. Padmaja. "The Reaction of No with Superoxide." Free Radic Res Commun 18, no. 4 (1993): 195-9.

Hunte, C., H. Palsdottir and B. L. Trumpower. "Protonmotive Pathways and Mechanisms in the Cytochrome Bc1 Complex." FEBS Lett 545, no. 1 (2003): 39-46.

Iseni, F., A. Barge, F. Baudin, D. Blondel and R. W. Ruigrok. "Characterization of Rabies Virus Nucleocapsids and Recombinant Nucleocapsid-Like Structures." J Gen Virol 79 (Pt 12), (1998): 2909-19.

Iwasaki Y, and M, Tobita. "Pathology." In *Rabies*. Jackson AC, Wunner WH (eds). Academic Press: San Diego, 2nd eds (2007):283–306.

Iwata, M., S. Komori, T. Unno, N. Minamoto and H. Ohashi. "Modification of Membrane Currents in Mouse Neuroblastoma Cells Following Infection with Rabies Virus." Br J Pharmacol 126, no. 8 (1999): 1691-8.

Iwata, S., J. W. Lee, K. Okada, J. K. Lee, M. Iwata, B. Rasmussen, T. A. Link, S. Ramaswamy and B. K. Jap. "Complete Structure of the 11-Subunit Bovine Mitochondrial Cytochrome Bc1 Complex." Science 281, no. 5373 (1998): 64-71.

Jackson, A. C. "Pathogenesis." In *Rabies*. Jackson AC, Wunner WH (eds). Academic Press: San Diego, 2nd eds (2007): 245–282.

Jackson, A. C. "Rabies." Neurol Clin 26, no. 3 (2008): 717-26, ix.

Jackson, A. C. Rabies pathogenesis update. Rev Pan-Amaz Saude 1, no. 1 (2010): 167-172.

Jackson, A. C. "Therapy of Human Rabies." Adv Virus Res 79, (2011): 365-75.

Jackson, A. C., W. Kammouni, E. Zherebitskaya and P. Fernyhough. "Role of Oxidative Stress in Rabies Virus Infection of Adult Mouse Dorsal Root Ganglion Neurons." J Virol 84, no. 9 (2010): 4697-705.

Jackson, A. C., E. Randle, G. Lawrance and J. P. Rossiter. "Neuronal Apoptosis Does Not Play an Important Role in Human Rabies Encephalitis." J Neurovirol 14, no. 5 (2008): 368-75.

Jackson, A. C. and J. P. Rossiter. "Apoptosis Plays an Important Role in Experimental Rabies Virus Infection." J Virol 71, no. 7 (1997): 5603-7.

Jacob, Y., H. Badrane, P. E. Ceccaldi and N. Tordo. "Cytoplasmic Dynein Lc8 Interacts with Lyssavirus Phosphoprotein." J Virol 74, no. 21 (2000): 10217-22.

Jaeschke, H., C. Kleinwaechter and A. Wendel. "Nadh-Dependent Reductive Stress and Ferritin-Bound Iron in Allyl Alcohol-Induced Lipid Peroxidation in Vivo: The Protective Effect of Vitamin E." Chem Biol Interact 81, no. 1-2 (1992): 57-68.

Jensen, P. K. "Antimycin-Insensitive Oxidation of Succinate and Reduced Nicotinamide-Adenine Dinucleotide in Electron-Transport Particles. I. Ph Dependency and Hydrogen Peroxide Formation." Biochim Biophys Acta 122, no. 2 (1966): 157-66.

Jourd'heuil, D., D. Kang and M. B. Grisham. "Interactions between Superoxide and Nitric Oxide: Implications in DNA Damage and Mutagenesis." Front Biosci 2, (1997): d189-96.

Kalckar, H. M. "Origins of the Concept Oxidative Phosphorylation." Mol Cell Biochem 5, no. 1-2 (1974): 55-63.

Kammouni, W., L. Hasan, A. Saleh, H. Wood, P. Fernyhough and A. C. Jackson. "Role of Nuclear Factor-Kappab in Oxidative Stress Associated with Rabies Virus Infection of Adult Rat Dorsal Root Ganglion Neurons." J Virol 86, no. 15 (2012): 8139-46.

Keller, J. N., Z. Pang, J. W. Geddes, J. G. Begley, A. Germeyer, G. Waeg and M. P. Mattson. "Impairment of Glucose and Glutamate Transport and Induction of Mitochondrial Oxidative Stress and Dysfunction in Synaptosomes by Amyloid Beta-Peptide: Role of the Lipid Peroxidation Product 4-Hydroxynonenal." J Neurochem 69, no. 1 (1997): 273-84.

Kelly, R. M. and P. L. Strick. "Rabies as a Transneuronal Tracer of Circuits in the Central Nervous System." J Neurosci Methods 103, no. 1 (2000): 63-71.

Kiebish, M. A., X. Han, H. Cheng, J. H. Chuang and T. N. Seyfried. "Cardiolipin and Electron Transport Chain Abnormalities in Mouse Brain Tumor Mitochondria:

Lipidomic Evidence Supporting the Warburg Theory of Cancer." J Lipid Res 49, no. 12 (2008): 2545-56.

Kim, S. C., R. Sprung, Y. Chen, Y. Xu, H. Ball, J. Pei, T. Cheng, Y. Kho, H. Xiao, L. Xiao, N. V. Grishin, M. White, X. J. Yang and Y. Zhao. "Substrate and Functional Diversity of Lysine Acetylation Revealed by a Proteomics Survey." Mol Cell 23, no. 4 (2006): 607-18.

Kitayama, H., Y. Miura, Y. Ando, S. Hoshino, Y. Ishizaka and Y. Koyanagi. "Human Immunodeficiency Virus Type 1 Vpr Inhibits Axonal Outgrowth through Induction of Mitochondrial Dysfunction." J Virol 82, no. 5 (2008): 2528-42.

Klempner, M. S., C. A. Dinarello and J. I. Gallin. "Human Leukocytic Pyrogen Induces Release of Specific Granule Contents from Human Neutrophils." J Clin Invest 61, no. 5 (1978): 1330-6.

Klingen, Y., K. K. Conzelmann and S. Finke. "Double-Labeled Rabies Virus: Live Tracking of Enveloped Virus Transport." J Virol 82, no. 1 (2008): 237-45.

Knobel, D. L., S. Cleaveland, P. G. Coleman, E. M. Fevre, M. I. Meltzer, M. E. Miranda, A. Shaw, J. Zinsstag and F. X. Meslin. "Re-Evaluating the Burden of Rabies in Africa and Asia." Bull World Health Organ 83, no. 5 (2005): 360-8.

Koschel, K. and P. Munzel. "Inhibition of Opiate Receptor-Mediated Signal Transmission by Rabies Virus in Persistently Infected Ng-108-15 Mouse Neuroblastoma-Rat Glioma Hybrid Cells." Proc Natl Acad Sci U S A 81, no. 3 (1984): 950-4.

Krebs, J. W., A. M. Mondul, C. E. Rupprecht and J. E. Childs. "Rabies Surveillance in the United States During 2000." J Am Vet Med Assoc 219, no. 12 (2001): 1687-99.

Kucera, P., M. Dolivo, P. Coulon and A. Flamand. "Pathways of the Early Propagation of Virulent and Avirulent Rabies Strains from the Eye to the Brain." J Virol 55, no. 1 (1985): 158-62.

Kussmaul, L. and J. Hirst. "The Mechanism of Superoxide Production by Nadh:Ubiquinone Oxidoreductase (Complex I) from Bovine Heart Mitochondria." Proc Natl Acad Sci U S A 103, no. 20 (2006): 7607-12.

Ladogana, A., E. Bouzamondo, M. Pocchiari and H. Tsiang. "Modification of Tritiated Gamma-Amino-N-Butyric Acid Transport in Rabies Virus-Infected Primary Cortical Cultures." J Gen Virol 75 (Pt 3), (1994): 623-7.

Lahaye, X., A. Vidy, C. Pomier, L. Obiang, F. Harper, Y. Gaudin and D. Blondel. "Functional Characterization of Negri Bodies (Nbs) in Rabies Virus-Infected

Cells: Evidence That Nbs Are Sites of Viral Transcription and Replication." J Virol 83, no. 16 (2009): 7948-58.

Langevin, C., H. Jaaro, S. Bressanelli, M. Fainzilber and C. Tuffereau. "Rabies Virus Glycoprotein (Rvg) Is a Trimeric Ligand for the N-Terminal Cysteine-Rich Domain of the Mammalian P75 Neurotrophin Receptor." J Biol Chem 277, no. 40 (2002): 37655-62.

Lauria, G., M. Morbin, R. Lombardi, M. Borgna, G. Mazzoleni, A. Sghirlanzoni and D. Pareyson. "Axonal Swellings Predict the Degeneration of Epidermal Nerve Fibers in Painful Neuropathies." Neurology 61, no. 5 (2003): 631-6.

Le Mercier, P., Y. Jacob and N. Tordo. "The Complete Mokola Virus Genome Sequence: Structure of the Rna-Dependent Rna Polymerase." J Gen Virol 78 (Pt 7), (1997): 1571-6.

Lee, S., E. Tak, J. Lee, M. A. Rashid, M. P. Murphy, J. Ha and S. S. Kim. "Mitochondrial H2o2 Generated from Electron Transport Chain Complex I Stimulates Muscle Differentiation." Cell Res 21, no. 5 (2011): 817-34.

Leff, J. A., M. A. Oppegard, T. J. Curiel, K. S. Brown, R. T. Schooley and J. E. Repine. "Progressive Increases in Serum Catalase Activity in Advancing Human Immunodeficiency Virus Infection." Free Radic Biol Med 13, no. 2 (1992): 143-9.

Lenaz, G., R. Fato, M. L. Genova, C. Bergamini, C. Bianchi and A. Biondi. "Mitochondrial Complex I: Structural and Functional Aspects." Biochim Biophys Acta 1757, no. 9-10 (2006): 1406-20.

Lentz, T. L., T. G. Burrage, A. L. Smith, J. Crick and G. H. Tignor. "Is the Acetylcholine Receptor a Rabies Virus Receptor?" Science 215, no. 4529 (1982): 182-4.

Lentz, T. L., E. Hawrot and P. T. Wilson. "Synthetic Peptides Corresponding to Sequences of Snake Venom Neurotoxins and Rabies Virus Glycoprotein Bind to the Nicotinic Acetylcholine Receptor." Proteins 2, no. 4 (1987): 298-307.

Leppert, M., L. Rittenhouse, J. Perrault, D. F. Summers and D. Kolakofsky. "Plus and Minus Strand Leader Rnas in Negative Strand Virus-Infected Cells." Cell 18, no. 3 (1979): 735-47.

Li, N., K. Ragheb, G. Lawler, J. Sturgis, B. Rajwa, J. A. Melendez and J. P. Robinson. "Mitochondrial Complex I Inhibitor Rotenone Induces Apoptosis through Enhancing Mitochondrial Reactive Oxygen Species Production." J Biol Chem 278, no. 10 (2003): 8516-25.

Li, X. Q., L. Sarmento and Z. F. Fu. "Degeneration of Neuronal Processes after Infection with Pathogenic, but Not Attenuated, Rabies Viruses." J Virol 79, no. 15 (2005): 10063-8.

Li, Y., T. T. Huang, E. J. Carlson, S. Melov, P. C. Ursell, J. L. Olson, L. J. Noble, M. P. Yoshimura, C. Berger, P. H. Chan, D. C. Wallace and C. J. Epstein. "Dilated Cardiomyopathy and Neonatal Lethality in Mutant Mice Lacking Manganese Superoxide Dismutase." Nat Genet 11, no. 4 (1995): 376-81.

Liu, P., J. Yang, X. Wu and Z. F. Fu. "Interactions Amongst Rabies Virus Nucleoprotein, Phosphoprotein and Genomic Rna in Virus-Infected and Transfected Cells." J Gen Virol 85, no. Pt 12 (2004): 3725-34.

Liu, R. H., B. Baldwin, B. C. Tennant and J. H. Hotchkiss. "Elevated Formation of Nitrate and N-Nitrosodimethylamine in Woodchucks (Marmota Monax) Associated with Chronic Woodchuck Hepatitis Virus Infection." Cancer Res 51, no. 15 (1991): 3925-9.

Liu, R. H., J. R. Jacob, B. C. Tennant and J. H. Hotchkiss. "Nitrite and Nitrosamine Synthesis by Hepatocytes Isolated from Normal Woodchucks (Marmota Monax) and Woodchucks Chronically Infected with Woodchuck Hepatitis Virus." Cancer Res 52, no. 15 (1992): 4139-43.

Loschen, G. and A. Azzi. "On the Formation of Hydrogen Peroxide and Oxygen Radicals in Heart Mitochondria." Recent Adv Stud Cardiac Struct Metab 7, (1975): 3-12.

Lyamzaev, K. G., D. S. Izyumov, A. V. Avetisyan, F. Yang, O. Y. Pletjushkina and B. V. Chernyak. "Inhibition of Mitochondrial Bioenergetics: The Effects on Structure of Mitochondria in the Cell and on Apoptosis." Acta Biochim Pol 51, no. 2 (2004): 553-62.

Maier, T., A. Schwarting, D. Mauer, R. S. Ross, A. Martens, V. Kliem, J. Wahl, M. Panning, S. Baumgarte, T. Muller, S. Pfefferle, H. Ebel, J. Schmidt, K. Tenner-Racz, P. Racz, M. Schmid, M. Struber, B. Wolters, D. Gotthardt, F. Bitz, L. Frisch, N. Pfeiffer, H. Fickenscher, P. Sauer, C. E. Rupprecht, M. Roggendorf, A. Haverich, P. Galle, J. Hoyer and C. Drosten. "Management and Outcomes after Multiple Corneal and Solid Organ Transplantations from a Donor Infected with Rabies Virus." Clin Infect Dis 50, no. 8 (2010): 1112-9.

Malgaroli, A., L. Vallar and V. Zimarino. "Protein Homeostasis in Neurons and Its Pathological Alterations." Curr Opin Neurobiol 16, no. 3 (2006): 270-4.

Malorni, W., R. Rivabene, M. T. Santini and G. Donelli. "N-Acetylcysteine Inhibits Apoptosis and Decreases Viral Particles in Hiv-Chronically Infected U937 Cells." FEBS Lett 327, no. 1 (1993): 75-8.

Marklund, S. L. "Human Copper-Containing Superoxide Dismutase of High Molecular Weight." Proc Natl Acad Sci U S A 79, no. 24 (1982): 7634-8.

Marston, D. A., L. M. McElhinney, N. Johnson, T. Muller, K. K. Conzelmann, N. Tordo and A. R. Fooks. "Comparative Analysis of the Full Genome Sequence of European Bat Lyssavirus Type 1 and Type 2 with Other Lyssaviruses and Evidence for a Conserved Transcription Termination and Polyadenylation Motif in the G-L 3' Non-Translated Region." J Gen Virol 88, no. Pt 4 (2007): 1302-14.

Masters, P. S. and A. K. Banerjee. "Complex Formation with Vesicular Stomatitis Virus Phosphoprotein Ns Prevents Binding of Nucleocapsid Protein N to Nonspecific Rna." J Virol 62, no. 8 (1988): 2658-64.

Masters, P. S. and A. K. Banerjee. "Resolution of Multiple Complexes of Phosphoprotein Ns with Nucleocapsid Protein N of Vesicular Stomatitis Virus." J Virol 62, no. 8 (1988): 2651-7.

Matsumoto, S. "Electron Microscopy of Nerve Cells Infected with Street Rabies Virus." Virology 17, (1962): 198-202.

Mavrakis, M., F. Iseni, C. Mazza, G. Schoehn, C. Ebel, M. Gentzel, T. Franz and R. W. Ruigrok. "Isolation and Characterisation of the Rabies Virus N Degrees-P Complex Produced in Insect Cells." Virology 305, no. 2 (2003): 406-14.

Mavrakis, M., S. Mehouas, E. Real, F. Iseni, D. Blondel, N. Tordo and R. W. Ruigrok. "Rabies Virus Chaperone: Identification of the Phosphoprotein Peptide That Keeps Nucleoprotein Soluble and Free from Non-Specific Rna." Virology 349, no. 2 (2006): 422-9.

McCord, J. M., B. B. Keele, Jr. and I. Fridovich. "An Enzyme-Based Theory of Obligate Anaerobiosis: The Physiological Function of Superoxide Dismutase." Proc Natl Acad Sci U S A 68, no. 5 (1971): 1024-7.

McGettigan, J. P., H. D. Foley, I. M. Belyakov, J. A. Berzofsky, R. J. Pomerantz and M. J. Schnell. "Rabies Virus-Based Vectors Expressing Human Immunodeficiency Virus Type 1 (Hiv-1) Envelope Protein Induce a Strong, Cross-Reactive Cytotoxic T-Lymphocyte Response against Envelope Proteins from Different Hiv-1 Isolates." J Virol 75, no. 9 (2001): 4430-4.

Mebatsion, T., M. Konig and K. K. Conzelmann. "Budding of Rabies Virus Particles in the Absence of the Spike Glycoprotein." Cell 84, no. 6 (1996): 941-51.

Mebatsion, T., F. Weiland and K. K. Conzelmann. "Matrix Protein of Rabies Virus Is Responsible for the Assembly and Budding of Bullet-Shaped Particles and

Interacts with the Transmembrane Spike Glycoprotein G." J Virol 73, no. 1 (1999): 242-50.

Menager, P., P. Roux, F. Megret, J. P. Bourgeois, A. M. Le Sourd, A. Danckaert, M. Lafage, C. Prehaud and M. Lafon. "Toll-Like Receptor 3 (Tlr3) Plays a Major Role in the Formation of Rabies Virus Negri Bodies." PLoS Pathog 5, no. 2 (2009): e1000315.

Meredith, M. J. and D. J. Reed. "Status of the Mitochondrial Pool of Glutathione in the Isolated Hepatocyte." J Biol Chem 257, no. 7 (1982): 3747-53.

Misra, H. P. and I. Fridovich. "The Role of Superoxide Anion in the Autoxidation of Epinephrine and a Simple Assay for Superoxide Dismutase." J Biol Chem 247, no. 10 (1972): 3170-5.

Miwa, S. and M. D. Brand. "Mitochondrial Matrix Reactive Oxygen Species Production Is Very Sensitive to Mild Uncoupling." Biochem Soc Trans 31, no. Pt 6 (2003): 1300-1.

Modjtahedi, N., F. Giordanetto, F. Madeo and G. Kroemer. "Apoptosis-Inducing Factor: Vital and Lethal." Trends Cell Biol 16, no. 5 (2006): 264-72.

Mori, I., Y. Nishiyama, T. Yokochi and Y. Kimura. "Virus-Induced Neuronal Apoptosis as Pathological and Protective Responses of the Host." Rev Med Virol 14, no. 4 (2004): 209-16.

Mueller, S., H. D. Riedel and W. Stremmel. "Direct Evidence for Catalase as the Predominant H2o2 -Removing Enzyme in Human Erythrocytes." Blood 90, no. 12 (1997): 4973-8.

Muller, F., H. Rollag and S. S. Froland. "Reduced Oxidative Burst Responses in Monocytes and Monocyte-Derived Macrophages from Hiv-Infected Subjects." Clin Exp Immunol 82, no. 1 (1990): 10-5.

Murphy, M. P. "How Mitochondria Produce Reactive Oxygen Species." Biochem J 417, no. 1 (2009): 1-13.

Nakamichi, K., S. Inoue, T. Takasaki, K. Morimoto and I. Kurane. "Rabies Virus Stimulates Nitric Oxide Production and Cxc Chemokine Ligand 10 Expression in Macrophages through Activation of Extracellular Signal-Regulated Kinases 1 and 2." J Virol 78, no. 17 (2004): 9376-88.

Nicholls, D. G. "Mitochondrial Dysfunction and Glutamate Excitotoxicity Studied in Primary Neuronal Cultures." Curr Mol Med 4, no. 2 (2004): 149-77.

Noah, D. L., C. L. Drenzek, J. S. Smith, J. W. Krebs, L. Orciari, J. Shaddock, D. Sanderlin, S. Whitfield, M. Fekadu, J. G. Olson, C. E. Rupprecht and J. E. Childs. "Epidemiology of Human Rabies in the United States, 1980 to 1996." Ann Intern Med 128, no. 11 (1998): 922-30.

Oda, T., T. Akaike, T. Hamamoto, F. Suzuki, T. Hirano and H. Maeda. "Oxygen Radicals in Influenza-Induced Pathogenesis and Treatment with Pyran Polymer-Conjugated Sod." Science 244, no. 4907 (1989): 974-6.

Ogino, T. and A. K. Banerjee. "Unconventional Mechanism of Mrna Capping by the Rna-Dependent Rna Polymerase of Vesicular Stomatitis Virus." Mol Cell 25, no. 1 (2007): 85-97.

Ohnishi, T., V. D. Sled, T. Yano, T. Yagi, D. S. Burbaev and A. D. Vinogradov. "Structure-Function Studies of Iron-Sulfur Clusters and Semiquinones in the Nadh-Q Oxidoreductase Segment of the Respiratory Chain." Biochim Biophys Acta 1365, no. 1-2 (1998): 301-8.

Ohnishi, T. and B. L. Trumpower. "Differential Effects of Antimycin on Ubisemiquinone Bound in Different Environments in Isolated Succinate . Cytochrome C Reductase Complex." J Biol Chem 255, no. 8 (1980): 3278-84.

Pizzinat, N., N. Copin, C. Vindis, A. Parini and C. Cambon. "Reactive Oxygen Species Production by Monoamine Oxidases in Intact Cells." Naunyn Schmiedebergs Arch Pharmacol 359, no. 5 (1999): 428-31.

Powell, S. R. "The Antioxidant Properties of Zinc." J Nutr 130, no. 5S Suppl (2000): 1447S-54S.

Prehaud, C., S. Lay, B. Dietzschold and M. Lafon. "Glycoprotein of Nonpathogenic Rabies Viruses Is a Key Determinant of Human Cell Apoptosis." J Virol 77, no. 19 (2003): 10537-47.

Prosniak, M., D. C. Hooper, B. Dietzschold and H. Koprowski. "Effect of Rabies Virus Infection on Gene Expression in Mouse Brain." Proc Natl Acad Sci U S A 98, no. 5 (2001): 2758-63.

Radi, R., A. Cassina and R. Hodara. "Nitric Oxide and Peroxynitrite Interactions with Mitochondria." Biol Chem 383, no. 3-4 (2002): 401-9.

Rafaeloff-Phail, R., L. Ding, L. Conner, W. K. Yeh, D. McClure, H. Guo, K. Emerson and H. Brooks. "Biochemical Regulation of Mammalian Amp-Activated Protein Kinase Activity by Nad and Nadh." J Biol Chem 279, no. 51 (2004): 52934-9.

Rasmussen L. J., and K. K. Singh. "Genetic integrity of the mitochondrial genome." In: Singh KK (ed). Mitochondrial DNA Mutations in Aging, Disease, and Cancer. New York, NY: Springer, (1998):115–127

Raux, H., A. Flamand and D. Blondel. "Interaction of the Rabies Virus P Protein with the Lc8 Dynein Light Chain." J Virol 74, no. 21 (2000): 10212-6.

Raza, H., S. K. Prabu, A. John and N. G. Avadhani. "Impaired Mitochondrial Respiratory Functions and Oxidative Stress in Streptozotocin-Induced Diabetic Rats." Int J Mol Sci 12, no. 5 (2011): 3133-47.

Roy, A., T. W. Phares, H. Koprowski and D. C. Hooper. "Failure to Open the Blood-Brain Barrier and Deliver Immune Effectors to Central Nervous System Tissues Leads to the Lethal Outcome of Silver-Haired Bat Rabies Virus Infection." J Virol 81, no. 3 (2007): 1110-8.

Roy Chowdhury, S. K., D. R. Smith, A. Saleh, J. Schapansky, A. Marquez, S. Gomes, E. Akude, D. Morrow, N. A. Calcutt and P. Fernyhough. "Impaired Adenosine Monophosphate-Activated Protein Kinase Signalling in Dorsal Root Ganglia Neurons Is Linked to Mitochondrial Dysfunction and Peripheral Neuropathy in Diabetes." Brain 135, no. Pt 6 (2012): 1751-66.

Sack, M. N. "Mitochondrial Depolarization and the Role of Uncoupling Proteins in Ischemia Tolerance." Cardiovasc Res 72, no. 2 (2006): 210-9.

Sandstrom, P. A., B. Roberts, T. M. Folks and T. M. Buttke. "Hiv Gene Expression Enhances T Cell Susceptibility to Hydrogen Peroxide-Induced Apoptosis." AIDS Res Hum Retroviruses 9, no. 11 (1993): 1107-13.

Schnell, M. J., J. P. McGettigan, C. Wirblich and A. Papaneri. "The Cell Biology of Rabies Virus: Using Stealth to Reach the Brain." Nat Rev Microbiol 8, no. 1 (2010): 51-61.

Schultz, B. E. and S. I. Chan. "Structures and Proton-Pumping Strategies of Mitochondrial Respiratory Enzymes." Annu Rev Biophys Biomol Struct 30, (2001): 23-65.

Schulze-Osthoff, K., A. C. Bakker, B. Vanhaesebroeck, R. Beyaert, W. A. Jacob and W. Fiers. "Cytotoxic Activity of Tumor Necrosis Factor Is Mediated by Early Damage of Mitochondrial Functions. Evidence for the Involvement of Mitochondrial Radical Generation." J Biol Chem 267, no. 8 (1992): 5317-23.

Schwarz, K. B. "Oxidative Stress During Viral Infection: A Review." Free Radic Biol Med 21, no. 5 (1996): 641-9.

Schwarz, K. B., T. M. Zieber, S. Sharma, M. G. Clemens and P. Seligman. "Activated Thp-1 Cells Depress Mitochondrial Respiration in Hep G2 Cells Infected with Influenza B Virus." Mol Cell Probes 8, no. 5 (1994): 345-51.

Scott, C. A., J. P. Rossiter, R. D. Andrew and A. C. Jackson. "Structural Abnormalities in Neurons Are Sufficient to Explain the Clinical Disease and Fatal Outcome of Experimental Rabies in Yellow Fluorescent Protein-Expressing Transgenic Mice." J Virol 82, no. 1 (2008): 513-21.

Selivanov, V. A., T. V. Votyakova, V. N. Pivtoraiko, J. Zeak, T. Sukhomlin, M. Trucco, J. Roca and M. Cascante. "Reactive Oxygen Species Production by Forward and Reverse Electron Fluxes in the Mitochondrial Respiratory Chain." PLoS Comput Biol 7, no. 3 (2011): e1001115.

Sharma, A. B., J. Sun, L. L. Howard, A. G. Williams, Jr. and R. T. Mallet. "Oxidative Stress Reversibly Inactivates Myocardial Enzymes During Cardiac Arrest." Am J Physiol Heart Circ Physiol 292, no. 1 (2007): H198-206.

Shen, D., T. P. Dalton, D. W. Nebert and H. G. Shertzer. "Glutathione Redox State Regulates Mitochondrial Reactive Oxygen Production." J Biol Chem 280, no. 27 (2005): 25305-12.

Silverstein, E. and G. Sulebele. "Modulation of Heart Muscle Mitochondrial Malate Dehydrogenase Activity. I. Activation and Inhibition by P-Mercuribenzoate." Biochemistry 9, no. 2 (1970): 274-82.

Sipahioglu, U. and S. Alpaut. "[Transplacental Rabies in Humans]." Mikrobiyol Bul 19, no. 2 (1985): 95-9.

Smith, J. S., D. B. Fishbein, C. E. Rupprecht and K. Clark. "Unexplained Rabies in Three Immigrants in the United States. A Virologic Investigation." N Engl J Med 324, no. 4 (1991): 205-11.

Srinivasan, A., E. C. Burton, M. J. Kuehnert, C. Rupprecht, W. L. Sutker, T. G. Ksiazek, C. D. Paddock, J. Guarner, W. J. Shieh, C. Goldsmith, C. A. Hanlon, J. Zoretic, B. Fischbach, M. Niezgoda, W. H. El-Feky, L. Orciari, E. Q. Sanchez, A. Likos, G. B. Klintmalm, D. Cardo, J. LeDuc, M. E. Chamberland, D. B. Jernigan and S. R. Zaki. "Transmission of Rabies Virus from an Organ Donor to Four Transplant Recipients." N Engl J Med 352, no. 11 (2005): 1103-11.

Starkov, A. A. and G. Fiskum. "Regulation of Brain Mitochondrial H2o2 Production by Membrane Potential and Nad(P)H Redox State." J Neurochem 86, no. 5 (2003): 1101-7.

Starkov, A. A., G. Fiskum, C. Chinopoulos, B. J. Lorenzo, S. E. Browne, M. S. Patel and M. F. Beal. "Mitochondrial Alpha-Ketoglutarate Dehydrogenase

Complex Generates Reactive Oxygen Species." J Neurosci 24, no. 36 (2004): 7779-88

Superti, F., M. Derer and H. Tsiang. "Mechanism of Rabies Virus Entry into Cer Cells." J Gen Virol 65 (Pt 4), (1984): 781-9.

Superti, F., B. Hauttecoeur, M. J. Morelec, P. Goldoni, B. Bizzini and H. Tsiang. "Involvement of Gangliosides in Rabies Virus Infection." J Gen Virol 67 (Pt 1), (1986): 47-56.

Tang, Y., O. Rampin, F. Giuliano and G. Ugolini. "Spinal and Brain Circuits to Motoneurons of the Bulbospongiosus Muscle: Retrograde Transneuronal Tracing with Rabies Virus." J Comp Neurol 414, no. 2 (1999): 167-92.

Teepker, M., N. Anthes, S. Fischer, J. C. Krieg and H. Vedder. "Effects of Oxidative Challenge and Calcium on Atp-Levels in Neuronal Cells." Neurotoxicology 28, no. 1 (2007): 19-26.

Terada, H. "Uncouplers of Oxidative Phosphorylation." Environ Health Perspect 87, (1990): 213-8.

Theerasurakarn, S. and S. Ubol. "Apoptosis Induction in Brain During the Fixed Strain of Rabies Virus Infection Correlates with Onset and Severity of Illness." J Neurovirol 4, no. 4 (1998): 407-14.

Thomas, D., W. W. Newcomb, J. C. Brown, J. S. Wall, J. F. Hainfeld, B. L. Trus and A. C. Steven. "Mass and Molecular Composition of Vesicular Stomatitis Virus: A Scanning Transmission Electron Microscopy Analysis." J Virol 54, no. 2 (1985): 598-607.

Thoulouze, M. I., M. Lafage, J. A. Montano-Hirose and M. Lafon. "Rabies Virus Infects Mouse and Human Lymphocytes and Induces Apoptosis." J Virol 71, no. 10 (1997): 7372-80.

Thoulouze, M. I., M. Lafage, M. Schachner, U. Hartmann, H. Cremer and M. Lafon. "The Neural Cell Adhesion Molecule Is a Receptor for Rabies Virus." J Virol 72, no. 9 (1998): 7181-90.

Tordo, N., O. Poch, A. Ermine and G. Keith. "Primary Structure of Leader Rna and Nucleoprotein Genes of the Rabies Genome: Segmented Homology with Vsv." Nucleic Acids Res 14, no. 6 (1986a): 2671-83.

Tordo, N., O. Poch, A. Ermine, G. Keith and F. Rougeon. "Walking Along the Rabies Genome: Is the Large G-L Intergenic Region a Remnant Gene?" Proc Natl Acad Sci U S A 83, no. 11 (1986b): 3914-8.

Tordo, N., and O. Poch. Strong and weak transcription signals within the rabies genome. Virus Res 11, (1988a): 30–32.

Tordo, N., and O. Poch. "Structure of rabies virus." In ‘‘Rabies’’ (J. B. Campbell and K. M. Charlton, eds.), (1988b):25–45. Rabies. Kluwer Academic Publishers, Boston.

Toriumi, H. and A. Kawai. "Association of Rabies Virus Nominal Phosphoprotein (P) with Viral Nucleocapsid (Nc) Is Enhanced by Phosphorylation of the Viral Nucleoprotein (N)." Microbiol Immunol 48, no. 5 (2004): 399-409.

Trumpower, B. L. "The Protonmotive Q Cycle. Energy Transduction by Coupling of Proton Translocation to Electron Transfer by the Cytochrome Bc1 Complex." J Biol Chem 265, no. 20 (1990): 11409-12.

Tsiang, H. "Neuronal Function Impairment in Rabies-Infected Rat Brain." J Gen Virol 61 (Pt 2), (1982): 277-81.

Tsiang, H., P. E. Ceccaldi and E. Lycke. "Rabies Virus Infection and Transport in Human Sensory Dorsal Root Ganglia Neurons." J Gen Virol 72 (Pt 5), (1991): 1191-4.

Tuffereau, C., J. Benejean, D. Blondel, B. Kieffer and A. Flamand. "Low-Affinity Nerve-Growth Factor Receptor (P75ntr) Can Serve as a Receptor for Rabies Virus." EMBO J 17, no. 24 (1998): 7250-9.

Tuffereau, C., H. Leblois, J. Benejean, P. Coulon, F. Lafay and A. Flamand. "Arginine or Lysine in Position 333 of Era and Cvs Glycoprotein Is Necessary for Rabies Virulence in Adult Mice." Virology 172, no. 1 (1989): 206-12.

Uday, B., Dipak, D., and B. K. Ranajit. "Reactive oxygen species: Oxidative damage and pathogenesis." Curr Sci **77,** (1990): 658-666.

Uehara, M. and N. Sato. "Impaired Ability of Neutrophils to Produce Oxygen-Derived Free Radicals in Patients with Chronic Liver Disease and Hepatocellular Carcinoma." Hepatology 20, no. 2 (1994): 326-30.

Uttara, B., A. V. Singh, P. Zamboni and R. T. Mahajan. "Oxidative Stress and Neurodegenerative Diseases: A Review of Upstream and Downstream Antioxidant Therapeutic Options." Curr Neuropharmacol 7, no. 1 (2009): 65-74.

Van Walraven, H. S., H. Strotmann, O. Schwarz and B. Rumberg. "The H+/Atp Coupling Ratio of the Atp Synthase from Thiol-Modulated Chloroplasts and Two Cyanobacterial Strains Is Four." FEBS Lett 379, no. 3 (1996): 309-13.

Vidy, A., M. Chelbi-Alix and D. Blondel. "Rabies Virus P Protein Interacts with Stat1 and Inhibits Interferon Signal Transduction Pathways." J Virol 79, no. 22 (2005): 14411-20.

Vierucci, A., M. De Martino, E. Graziani, M. E. Rossi, W. T. London and B. S. Blumberg. "A Mechanism for Liver Cell Injury in Viral Hepatitis: Effects of Hepatitis B Virus on Neutrophil Function in Vitro and in Children with Chronic Active Hepatitis." Pediatr Res 17, no. 10 (1983): 814-20.

World Health Organization. "World survey of rabies No.31: for the year 1995." Geneva: World Health Organization (1997): 1-29.

World Health Organization. "World survey of rabies No.32: For the year 1996." Geneva: World Health Organization. (1998): 1-27.

World Health Organization. "World survey of rabies No.33 For the year of 1997." Geneva: World Health Organization (1999): 1-29.

World Health Organization Expert Consultation on Rabies. "Who Expert Consultation on Rabies." World Health Organ Tech Rep Ser 931, (2005): 1-88, back cover.

Wu, X., X. Gong, H. D. Foley, M. J. Schnell and Z. F. Fu. "Both Viral Transcription and Replication Are Reduced When the Rabies Virus Nucleoprotein Is Not Phosphorylated." J Virol 76, no. 9 (2002): 4153-61.

Xun, Z., S. Rivera-Sanchez, S. Ayala-Pena, J. Lim, H. Budworth, E. M. Skoda, P. D. Robbins, L. J. Niedernhofer, P. Wipf and C. T. McMurray. "Targeting of Xjb-5-131 to Mitochondria Suppresses Oxidative DNA Damage and Motor Decline in a Mouse Model of Huntington's Disease." Cell Rep, (2012).

Ying, W. "Nad+/Nadh and Nadp+/Nadph in Cellular Functions and Cell Death: Regulation and Biological Consequences." Antioxid Redox Signal 10, no. 2 (2008): 179-206.

Yoshida, M., E. Muneyuki and T. Hisabori. "Atp Synthase--a Marvellous Rotary Engine of the Cell." Nat Rev Mol Cell Biol 2, no. 9 (2001): 669-77.

Yoshikawa, S., K. Muramoto, K. Shinzawa-Itoh, H. Aoyama, T. Tsukihara, K. Shimokata, Y. Katayama and H. Shimada. "Proton Pumping Mechanism of Bovine Heart Cytochrome C Oxidase." Biochim Biophys Acta 1757, no. 9-10 (2006): 1110-6.

Zhang, Z., D. R. Blake, C. R. Stevens, J. M. Kanczler, P. G. Winyard, M. C. Symons, M. Benboubetra and R. Harrison. "A Reappraisal of Xanthine

Dehydrogenase and Oxidase in Hypoxic Reperfusion Injury: The Role of Nadh as an Electron Donor." Free Radic Res 28, no. 2 (1998): 151-64.

Zheng, Y. M., M. K. Schafer, E. Weihe, H. Sheng, S. Corisdeo, Z. F. Fu, H. Koprowski and B. Dietzschold. "Severity of Neurological Signs and Degree of Inflammatory Lesions in the Brains of Rats with Borna Disease Correlate with the Induction of Nitric Oxide Synthase." J Virol 67, no. 10 (1993): 5786-91.

Zherebitskaya, E., E. Akude, D. R. Smith and P. Fernyhough. "Development of Selective Axonopathy in Adult Sensory Neurons Isolated from Diabetic Rats: Role of Glucose-Induced Oxidative Stress." Diabetes 58, no. 6 (2009): 1356-64.

Zoratti, M. and I. Szabo. "The Mitochondrial Permeability Transition." Biochim Biophys Acta 1241, no. 2 (1995): 139-76.